Active Vision Strategies in Predation

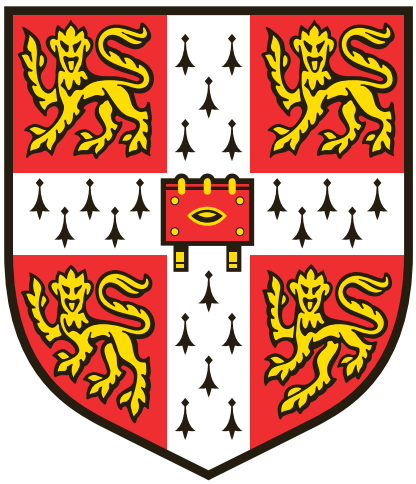

Sergio Rossoni

Department of Zoology – Clare College
University of Cambridge

This thesis is submitted for the degree of
Doctor of Philosophy

March 2021

To my father Enrico,

Who broke my heart by passing away
before he could see this work completed.
I proudly dedicate this thesis to you.

A mio padre Enrico,

Che mi ha spezzato il cuore andandosene
prima di poter vedere questo lavoro concluso.
Dedico questa tesi a te con orgoglio.

Fà balà l'öcc.

Declaration

This thesis is the result of my own work and includes nothing which is the outcome of work done in collaboration, except as specified in the text.

It is not substantially the same as any that I have submitted, or, is being concurrently submitted for a degree, diploma or other qualification at the University of Cambridge or any other University or similar institution except as specified in the text. I further state that no substantial part of my thesis has already been submitted, or, is being concurrently submitted for any such degree, diploma or other qualification at the University of Cambridge or any other University or similar institution except as specified in the text.

It does not exceed the word limit prescribed by the Degree Committee of the Faculty of Biology (60,000 words, exclusive of tables, footnotes, bibliography, and appendices).

Sergio Rossoni

Active Vision Strategies in Predation

Sergio Rossoni

Summary

Visual predation requires precise and accurate behaviour, for which many predators have evolved excellent visual skills. However, an animal's visual abilities are greatly affected by how it moves its eyes, known as active vision. Insects have immobile eyes but can direct their gaze by moving their heads and bodies. This thesis examines three predatory insects with different predatory strategies, to understand the extent to which active vision can be used in predation.

The first experimental chapter considers the African praying mantid, *Sphodromantis lineola*. Praying mantids are stationary terrestrial predators, which use their extremely mobile necks to visually track prey until it is within reach. By using statistical models, we identified what factors elicited strikes and, importantly, their success rate. The timing of head movements greatly increased the chances of strike success, with earlier movements increasing the success rate.

The second experimental chapter addresses how darting robber flies, *Psilonyx annulatus*, aerially attack static prey. Prior to attacking, darting robber flies translate their body around a central point, assessing their prey. After assessment, they attack from a position correlated with the target's absolute size, not its angular size. Prey is beyond the robber fly's stereopsis range during the period of assessment. Assessments of differently sized targets have similarities with the behaviour exhibited by jumping insects, which use motion parallax, a form of active vision, to assess jump distance, suggesting darting robber flies also use motion parallax to predate.

The final experimental chapter considers killer flies, *Coenosia attenuata*, which chase moving targets aerially. Killer flies use a combination of gravity and wing

acceleration to increase their speed when chasing prey from above. This increased speed restricts the flies' ability to steer. However, killer flies create strong looming stimuli which may trigger their prey to produce evasive manoeuvres, thereby slowing down. Moreover, by travelling faster towards their prey, killer flies may avoid losing track of it, a real danger when chasing moving prey with low-resolution eyes potentially avoided thanks to active vision.

By employing active vision, each of the predators considered can achieve impressive performances, despite relying on very different strategies to capture prey. The use of active vision can increase the success of already excellent visual predators and improve the performance of predator with limited vision. However, active vision can also substantially alter predatory behaviour, leading to a trade-off between the advantages in visual perception active vision can bring and the disadvantage in behavioural efficiency of active vision strategies.

Acknowledgements

First and foremost, I would like to thank Prof. Jeremy Niven. His enthusiastic knowledge and expertise on every topic I have had the luck to talk to him about are only outshined by his warm reassurance and understanding. Much more than an accomplished scientist, he is an inspiration of kindness and support whom anyone can only learn from. I would also like to deeply thank Dr. Matthias Landgraf for his extensive help with my transitions between labs. Time is the most precious resource in academia, and I am grateful he decided to spend some to help me despite his huge workload. I am very thankful to Prof. Greg Sutton and Prof. Doekele Stavenga for assisting me with biomechanical and optical calculations respectively, and for their encouragement and appreciation of my findings. Thanks to Prof. Paloma Gonzalez-Bellido and Prof. Trevor Wardill for the collaboration.

Integral to this thesis and my academic life has been the help and shared experiences of the post-docs, PhD students and lab technicians I have met. Most thanks go to Dr. Sam Fabian for his enthusiastic availability, which I have definitely taken too much advantage of, and his guidance whenever maths and physics stop making sense. A deep thank you goes to Mary Sumner, for being the most helpful lab technician anyone could ever dream of. I must thank her for her help with data extraction from the worst quality videos ever taken and not blaming me, despite it being entirely my fault. Also thanks to Dr. Jack Supple for the dark jokes, self-commiseration, and shared sufferance; I am not sure any of that helped, but at least it came from the heart. To Dr. Rachael Feord, for supporting the résistance and partially succeeding in making me socialise. To Prof. Kate Feller, for the shared interest in raptorial appendages and for welcoming me to the New World with food, alcohol, and board game competition. And to Dr. Milly Sharkey, for believing in me when I could not and for keeping my head on my shoulders with sense, kindness, and humour. Many thanks also to the CCNR, especially Dr. Sofia David-Fernadez, Laura Corona, and Dr. Cornelia Bühlmann, for welcoming me back to Sussex.

My long-time friends were really invaluable in supporting me in my relocations and through the highs and lows of this journey. Thank you to Risky Business: Ollie, Lucia, Eachelle, Katie, Lucy, and Luciana, for the special moments of togetherness we have managed to find in busy calendars and adverse circumstances. I am so pleased to see how much we have grown as people since we first met, yet glad we still cannot play a game of Risk without drama. Thank you to the Tuculi: Lara, Nau, Elena, Hachi, and Dimi, for unreservedly taking my side no matter what, but also passionately arguing on every topic imaginable. And thank you to the Maricche: Lara, Giulia, and Ilaria, for always reminding me where my roots lie.

The friends I made along the way have made this experience unbelievably more exciting. Thanks to Amy, for being a normal human being, but also one of the weirdest people I could hope to meet. I will always regret not accepting her marriage proposal on the second night we met. To Dani, for his accent. But also for his thoughtfulness and sharp sarcasm, which he tries to mask as meanness. And to Navin, for the gossip, the drama, the struggles, and his hospitality during my visits to Cambridge. Thanks to the Magic 7: Aurora, Callum, Tom, Sophie, Matt, and Mara, for sharing the first moments of this experience in Cambridge, when I still thought I had everything under control. Thanks to Clare Boat Club for teaching me I can enjoy sports in the flatlands in a way I had not believed possible. A huge thank you goes to the Friends of Dorothy: Nels, Miguel, and Kirk, for welcoming me to the Minnesotan life, but also for often taking the mick and not letting me take myself too seriously. And to Will, for providing more emotional support than he had signed up for and for annoying me half as much as I annoy him.

Infine, il ringraziamento più profondo va alla mia famiglia. A mia sorella, per essere stata al mio fianco offrendo amore incondizionato da prima che ne abbia memoria, senza lasciare che la distanza o il tempo lo scalfissero. A mia madre, per avermi insegnato a prendere decisioni con coscienza e giudizio, e per aver rispettato ogni mia scelta nonostante l'apprensione. E a mio padre, per avermi trasmesso la sua dedizione al lavoro e la passione per il mondo naturale. La mia curiosità è iniziata alla fine del tuo dito, teso a puntare a un camoscio o una marmotta in lontananza. Ogni traguardo che raggiungo è tanto mio quanto loro.

Table of Contents

Declaration **V**

Summary **VII**

Acknowledgements **IX**

Table of Contents **XI**

1. General Introduction **1**

1.1. Visual Predation 1

1.1.1. The origin of predation 1

1.1.2. Sensory modalities in predation 3

1.1.3. Behavioural strategies of visual predators 5

1.2. Studying Predation in Animals 10

1.2.1. The study of predation 10

1.2.2. Choice of experimental animals. 13

1.3. The Visual System of Insects 16

1.3.1. Insect eyes 16

1.3.2. Visual processing in insects 20

1.3.3. Active vision strategies in insects 23

1.4. Thesis Structure 26

2. Active Vision Increases the Success of a 'Sit-and-Wait' Predator **29**

2.1. Introduction 29

2.2. Materials and Methods 30

2.2.1. Animals 30

2.2.2. Indoor testing 31
2.2.3. Videography and calibration 32
2.2.4. Data extraction 33
2.2.5. Statistics 34
2.3. Results 35
2.3.1. Variables affecting strike kinematics 35
2.3.2. Variables affecting head movements 40
2.4. Discussion 44
2.4.1. Experimental considerations 44
2.4.2. Prey speed 45
2.4.3. Environmental effects 46
2.4.4. Repeated presentations and learning 46
2.4.5. Mantids' weight and sex 47
2.4.6. Effects of head movements 48
2.5. Conclusions 49
2.6. Supplementary Information. 50

3. Aerial Predation by Motion Parallax in an Insect 53

3.1. Introduction 53
3.2. Materials and Methods 57
3.2.1. Animals 57
3.2.2. Indoor testing 57
3.2.3. Videography and digitisation 58
3.2.4. Kinematic analysis 58
3.2.5. Microscopy imaging 59
3.2.6. Visual parameter estimation 60

3.2.7. Data analysis and statistics. 62

3.3. Results 63

3.3.1. The attack strategies of damselflies and darting robber flies show marked differences when assessing prey 63

3.3.2. Darting robber flies are capable of flying with a smaller movement range than when assessing prey 66

3.3.3. Prey relief, background presence, colour or shape do not prevent darting robber flies from attacking 67

3.3.4. Effect of prey size on the prey assessment of darting robber flies 68

3.3.5. Prey is outside of the darting robber fly's stereopsis range when an attack is launched 72

3.4. Discussion 74

3.5. Supplementary Information 78

4. Gravity and Active Acceleration Limit the Steering Ability of an Active Predator When Attacking from Above 85

4.1. Introduction 85

4.2. Materials and Methods 87

4.2.1. Animals 87

4.2.2. Animal preparation. 87

4.2.3. Photography, videography and data extraction 88

4.2.4. Dynamic analysis 89

4.2.5. Steering model selection 90

4.2.6. Mapping the outcome of the engagement geometry 94

4.2.7. Data analysis and statistics. 94

4.3. Results 95

4.3.1. When attacking from the ceiling, killer flies accelerate with similar magnitudes in highly variable trajectories 95

4.3.2. Dive kinematics can be replicated using lateral acceleration-limited proportional navigation 98

4.3.3. Killer flies take off in region that should lead to shortest trajectory, but are impaired by limited lateral acceleration. . 101

4.3.4. Killer flies maintain wing force magnitude during dives, producing higher aerodynamic power than attacks from the walls or floor of the arena. 104

4.4. Discussion 108

4.4.1. Limited proportional navigation as steering controller. 108

4.4.2. Take-off timing 110

4.4.3. Potential advantages in early take-off 111

4.5. Conclusions 112

4.6. Supplementary Information. 113

5. Final Conclusions **121**

Bibliography **127**

1. General Introduction

1.1. Visual Predation

1.1.1. The origin of predation

Organisms need energy to complete biological functions and survive. Some organisms, autotrophs like plants and algae, are capable of producing that energy themselves (Mauseth, 2014). Others, heterotrophs like animals, acquire their energy by consuming autotrophs, or each other. Consumption of autotrophs, called herbivory, has the advantage that plants are abundant and cannot effectively escape due to reduced motility. However, plants are low in nutrients and high in fibre, requiring animal herbivores to have long and difficult digestions to extract energy and nutrients, both macronutrients and micronutrients (Horn, 1989; Hume, 2002). Moreover, most plants produce toxins as defence against excessive consumption by herbivores, which often need complex toxin removal systems (Dearing et al., 2000; Karban and Agrawal, 2002; Nishida, 2002). By contrast, animals that predate upon each other, called carnivores *sensu lato*, have much smaller digestive tracts because less processing is required to extract readily usable molecules (macronutrients and micronutrients). However, because prey and predators are more closely related, they compete in an evolutionary arms race based on quick movements and reactions.

Although predation has existed since the pre-Cambrian (Bengtson, 2002; Bengtson and Zhao, 1992), the evolutionary arms race between predators and prey has escalated in speed with the so-called 'Cambrian explosion' (Marshall, 2006; McMenamin and Schulte McMenamin, 1990). During the Cambrian Period, multicellular organisms started developing specialised structures to support mostly two specific functions.

One of these was vision. In the Cambrian, photosensitive cells grouped together to form primitive eyes (Nilsson, 2009; Parker, 1998). The presence of multiple photosensors meant that the noise of each one cell could be averaged with others,

thereby increasing signal reliability. Reliable vision allowed for reliable behaviour. For example, animals with reduced motility, like tubeworms and snails, possess the so-called 'shadow withdrawal reflex', where the shadow cast by a potential predator causes the animal to retract its soft body into a hard protective structure (Ferguson and Benjamin, 1991; Nicol, 1950). As eyes started becoming more complex with lenses focussing the light on the photosensitive cells, and neural circuits that could extract directional visual cues, animals became able to locate each other with reasonable accuracy (Nilsson, 2009; Sillar et al., 2016). This was useful to both prey and predators because directional attacks and escapes presumably improved the success rate of both.

The other important innovation animals evolved in the Cambrian Period is the development of hard structures covering the body, such as shells in some molluscs and exoskeletons in arthropods (Vermeij, 1989; Vermeij, 1993). Though the primary function of these was assumed to be protection from predators (Dzik, 2007; Vermeij, 1989), exoskeletons greatly enhance movement efficiency (Cisne, 1974; Cohen, 2005), making arthropods excellent at both predating and escaping. The efficiency provided by a hard exoskeleton also increased the evolutionary pressures on non-shelled animals. In response, some of these developed their own mechanical structures to support efficient movements. Some soft-bodied animals evolved a flexible rod within their bodies, called a notochord, to aid locomotion (Flood, 1970; Long et al., 2002; Webb, 2009), thereby establishing the phylum Chordata. The notochord, precursor of the inner skeleton, provided a semi-rigid structure for muscle attachment, which not only allowed fast escapes from arthropod predators, but also enabled early chordates to adapt to predatory life themselves (Jollie, 1973). This was accompanied by a series of morphological changes to cope with the increased metabolic rate associated with predation (Gans and Northcutt, 1983; Northcutt and Gans, 1983), including the appearance of elastic gills, a capillary circulatory system with central pumping, and muscular propulsion of food through the gut. Together with the appearance of sensory organs on a restructured head to detect prey (Bodznick and Northcutt, 1981; Bullock et al., 1983; Gans and Northcutt, 1983; Vinnikov, 1982), early vertebrates could turn into fully predatory animals and grow in size, eventually developing

inner skeletons as support structures (Northcutt and Gans, 1983), providing a similar functional advantage to arthropod exoskeletons.

Muscles can anchor to solid structures like exo- and endo-skeletons, which can transmit force, to create a lever (Westneat, 2004). Some levers have been adapted to maximise power, enough to break through an animal's hard shell (Elner and Campbell, 2009; Erickson et al., 1996; Westneat, 2004). Other levers have evolved to maximise speed, to produce a fast attack or escape response (Burrows and Morris, 2003; Lutz and Rome, 1994; McGowan and Collins, 2018; Westneat, 2004). The development of power-retaining structures in some joints has allowed power-amplified systems to develop, further exacerbating the speed and power limbs can generate (Bennet-Clark, 1975; Burrows, 2003; Deban et al., 1997; Gronenberg et al., 1993; Patek et al., 2004; Ritzmann, 1973; Wainwright and Bennett, 1992), which gives advantages to both prey and predators.

Although predation has been present since the pre-Cambrian (Bengtson, 2002; Bengtson and Zhao, 1992), the ability to quickly see other animals and quickly react to their presence, both evolved during the Cambrian, accelerated the arms race between predators and prey (Vermeij, 1993; Vermeij, 2004), which arguably increased evolution rates of both categories.

1.1.2. Sensory modalities in predation

Although vision has evolved in close connection with predation, predation is not strictly linked to any specific sensory cue. Different predators use different senses to capture their prey and often more than one sense is used. What are the advantages and disadvantages of vision compared to other sensory modalities used for predation?

Although vision is fast, somatosensory perception is arguably much faster than vision because mechano-transduction is three orders of magnitude faster than photo-transduction (Corey and Hudspeth, 1983; Laughlin and Weckström, 1993). For example, moles are insectivores living underground, in unfavourable light conditions. Instead of using vision, moles sense prey using their nose (Dalquest and Orcutt, 1942), which evolved prey-specific tactile organs (Catania, 2000). In the hyper-specialised star-nose mole, prey detection can lead to consumption in

120 ms (Catania and Remple, 2005). Although incredibly fast, this predatory modality is extremely close range, only detecting prey when contacting it. Some tactile predators are able to cope with this limitation. Water can transmit forces more effectively than air or soil, so underwater predators can use mechanoreception over modest distances (Catania et al., 2010). Soil can also be used to the predator's advantage however; for example, antlion larvae build pits to trap prey and capture it when sliding (Fertin and Casas, 2006; Lucas, 1982). Nevertheless, this predatory modality has a range much more limited than others, which some postulate might have led to the very origin of photoreceptors (Arendt, 2003; Arendt and Wittbrodt, 2001; Arendt et al., 2016; Schlosser, 2018).

The range of chemoreception-mediated predation is more extended. Many animals including lobsters (Derby et al., 2001), sharks (Gardiner and Atema, 2010) and catfish (Atema, 1971) are capable of orienting towards chemical cues released by their prey. Depending on the sensitivity of chemoreception and chemical concentration, this sensory modality can be used over impressive distances. Tube-nose seabirds, like albatrosses, are generalist marine predators with particularly sensitive chemoreception (Nevitt et al., 1995), that have evolved to detect prey over the thousands of kilometres separating their nesting and feeding sites (Van Buskirk and Nevitt, 2008). However, chemical plumes are imprecise indicators, often requiring lateral casting to ensure accuracy (Nevitt et al., 2008), which is a time and energy-consuming strategy consisting in periodically exiting and re-entering the plume. Following a false trail can waste considerable energy (Savoca et al., 2016).

A medium-range and direct way of localising prey can be through audition. Barn owls are nocturnal predators capable of hearing and capturing small rodents in thick vegetation (Knudsen and Konishi, 1979; Usherwood et al., 2014). Barn owls rely on their prey making noise, which rodents however tend to reduce in response to predator presence (Hendrie et al., 1998; Roche et al., 1999). Some predatory animals have evolved to avoid this problem. Instead of waiting for their prey to make noise, animals like bats and dolphins evolved echolocation, a form of active sensing. An animal performing active sensing emits a signal and is capable of detecting and processing how the environment affects this signal. Echolocating

animals emit soundwaves and listen to the echo of their call, which can signal the presence of objects around them (Thomas et al., 2004). This, however, has the disadvantage of prey being able to detect the presence of the predator. To avoid bats, prey can produce avoidance manoeuvres (Roeder, 1998; Yager et al., 1990) or response calls which interfere with the bat's attack strategy (Corcoran et al., 2009).

Other predators have evolved less common strategies to discover and follow prey. For example, many aquatic vertebrates are able to sense electric fields generated by other animals and use them for predatory purposes (Kalmijn, 1971; Mørup Jørgensen et al., 1972). Two groups of teleost fishes have evolved the ability to emit electric fields themselves and detect perturbances in these fields, caused by hiding prey (Lissman and Machin, 1958), another example of active sensing called electrolocation. Although fascinating, electroreception-mediated predation has evolved in a small group of aquatic vertebrates and its comparative power is limited.

Vision is a sense which is medium to long range, precise, conspicuous, and very widespread in predators. Although varied, behavioural paradigms of visual predators can be directly compared to acquire a sense of what general principles govern prey-capture behaviours.

1.1.3. Behavioural strategies of visual predators

In a context where efficient predation of fast-reacting prey is the key to survival, prey capture is crucially important. Predatory behaviour can be divided into prey search, prey pursuit, and prey handling (Sillar et al., 2016). Animals can invest their energy, time, and developmental resources in each of these phases depending on their ecological priorities (Griffiths, 1980). Although most predators centre their predatory strategy on one of these phases, they are often also effective in others; an animal's investment into each of the three phases of predation should not be used for strict categorisation, but as a useful conceptual tool to compare predators.

Animals who spend most of their time and energy searching for prey are usually filter feeders or young animals in development, who are focussed on maximising

energy intake and therefore hunt small, fairly defenceless prey (Griffiths, 1980). Filter feeders have evolved interesting microstructures to filter prey (Crisp and Southward, 1961; Hamner et al., 1983; Jenkin, 1957; Motta et al., 2010; Nelson, 1923; Sanderson and Wassersug, 1993). However, their behavioural complexity is low compared to other predators, at least with regards to feeding. As energy maximisers, filter feeders avoid engaging in energy-expensive behaviours (Griffiths, 1980). For this reason, it is often advantageous for them to avoid locomotion altogether and evolve a sessile lifestyle (Kirkegaard and Goldstein, 2016). This body design is advantageous enough to have evolved many times in animals, and disproportionately so in filter feeders (Harris, 1990). As a result, visual abilities of many filter feeders are severely reduced, as they do not need fast or precise signals for feeding.

Active predators invest most of their energy and feeding time in pursuing prey, hence the synonym "pursuit predators". A famous example of an active predator is the cheetah, which is also the fastest terrestrial animal (Sharp, 1997), and not by coincidence. Cheetahs predate on fast-running ungulates such as gazelles and impalas (Hayward et al., 2006). Although the speed difference between predator and prey is minimal, the cheetah is capable of much higher accelerations (Wilson et al., 2018) and rapid turns (Wilson et al., 2013). Although achieving less impressive absolute speeds, tiger beetles are pursuit predators reaching similar speeds relative to body size (Gilbert, 1997). Tiger beetles chase prey via pursuit, which uses their prey's actual position to determine the beetle's direction. This technique creates suboptimal trajectories (Haselsteiner et al., 2014), but tiger beetles are able to outrun their prey and hunt it down thanks to their incredible speed advantage. Both tiger beetles and cheetahs are highly adapted to fast, short-range chases, thanks to their light and compact bodies and their long legs (Evans and Forsythe, 2009; Hildebrand and Hurley, 1985). Other active predators avoid the energy expense linked to the active acceleration of cheetahs and tiger beetles by accelerating passively. When peregrine falcons detect prey, they dive towards it from high altitudes in what is called a stoop, letting gravity increase their speed with little energy expenditure (Alerstam, 1987; Ponitz et al., 2014; Rudebeck, 1950; Tucker, 1998; Tucker and Parrott, 1970). Hunting prey from above may save

energy but also makes it difficult to spot prey against the cluttered ground. For this reason, birds of prey have incredibly sharp vision (Fox et al., 1976; Shlaer, 1972).

Predators with less acute eyes, such as dragonflies, tend to chase prey upwards, making targets easily detectable against a clearer sky (Lin and Leonardo, 2017; Mischiati et al., 2015; Olberg et al., 2007; Supple et al., 2020). Although they do not use gravity to reduce their energy costs, dragonflies are capable of intercepting prey, using highly efficient flight paths. By keeping their target at a constant angle relative to their bearing, dragonflies can steer ahead of it, crucially reducing the duration of their chase (Olberg, 2012; Olberg et al., 2000). This requires them to use closed-loop feedback to continuously monitor their target's trajectory; using their targets' instantaneous position to steer during a chase is a common feature of active predators, even when using other chasing strategies (Gilbert, 1997). Coincidentally, the dragonfly's interception also masks the chaser's movement as a background object, as the chaser stays in a stable portion of the visual field of the chased animal (Srinivasan and Davey, 1995). Similar efficient paths have been recorded during the attacks of dipteran flies (Fabian et al., 2018; Wardill et al., 2017), but also hawks (Kane et al., 2015) and falcons (Brighton et al., 2017). Some predators, however, exploit rather than avoid their prey's escape manoeuvres. Flush pursuers, like the painted redstart, use conspicuous body parts to elicit escape manoeuvres in their prey, thereby directing it towards their preferred attack zone (Jabłoński, 1999; Jabłoński, 2001).

Contrary to active predators, sit-and-wait or ambush predators invest much less in chasing prey. Instead, most of the feeding resources are invested in subduing and handling prey. For example, tigers spend most of their foraging time quietly stalking possible targets (Seidensticker and McDougal, 1993). Once their prey is within reach, tigers use their heavy bodies to immobilise it and their large teeth and powerful jaws to kill it. The effect of two different predatory techniques on the body morphology of cheetahs and tigers, both felines, is remarkable. As ambush predators, tigers preferentially hunt in high grass or thick vegetation, which conceals them from their prey's sight (Karanth and Sunquist, 2000). Many ambush predators hide, thereby reducing the distance at which their prey might notice them. Crocodiles, for example, hide in muddy water pools in otherwise dry

areas (Brito et al., 2011; Johnson, 1973). This firstly has the advantage of concealing them whilst still being able to see prey through the water. More importantly however, these pools are necessary resources other animals obtain water from, meaning crocodiles have evolved to hide in a place their prey is naturally drawn to. Some ambush animals have taken this a step further, having evolved to resemble objects that attract their prey. Female anglerfish have evolved an appendage where they harbour bacteria which emit bioluminescence (Baker et al., 2019; Freed et al., 2019), which acts as a lure to small fish eaten by the anglerfish (Grobecker and Pietsch, 1979; Munk, 1999; Pietsch and Grobecker, 1978). Crab spiders have adapted their whole body to the purpose. They have evolved to not only predate on flowers which match their body colour, but also to reflect ultraviolet light, which attracts pollinators (Heiling et al., 2004; Heiling et al., 2005). One family of praying mantids, the orchid mantids, has also evolved to attract potential prey by resembling flowers (Mizuno et al., 2014; O'Hanlon et al., 2014). However, most mantids use camouflage to go unnoticed by potential predators and prey (Svenson et al., 2015), an important but largely unexplored component of sit-and-wait predators to allow targets to get within their reach (Pembury Smith and Ruxton, 2020).

Most notably, praying mantids have evolved specialised forelimbs, featuring spines that mechanically and behaviourally aid prey capture (Copeland and Carlson, 1977; Loxton and Nicholls, 1979; Prete, 1990). The structure of these raptorial forelegs is so well adapted for capturing prey that similar morphologies evolved independently in at least two other predatory arthropods: mantispids (Kral et al., 2000; Pérez-de la Fuente and Peñalver, 2019) and mantis shrimps (Burrows, 1969; Patek et al., 2013). Mantis shrimps are ambush predators which have been particularly studied for the evolution of a latch-mediated spring in their predatory appendages (Burrows and Hoyle, 1972), which produce extremely fast and powerful movements to subdue prey, which is why these are also called "power-amplified" movements. This type of movement is not unusual among ambush predators, and is also used by snapping shrimps (Ritzmann, 1973), chameleons (Wainwright and Bennett, 1992), salamanders (Deban et al., 1997) and toads (Lappin et al., 2006). Power-amplified movements are ballistic and can

only be modulated prior to movement initiation (Kagaya and Patek, 2016). In opposition to the closed-loop controllers used by active predators to chase prey, ambush predators which use power-amplified movements can be described as open-loop actuators (Longo et al., 2019).

Another commonality among many ambush predators is their ability to gather depth-related information about their prey, such as absolute size and distance. Whilst chameleons can do so monocularly by adjusting their lens's focus (Harkness, 1977), praying mantids use binocular stereopsis for range estimation (Rossel, 1983), which has been suspected to be used by mantis shrimps (Schiff et al., 1985) and mantispids (Kral, 2013) too. In mantids, visual perception has been linked to species-specific forelimb morphology (Oufiero, 2020), which highlights the close connection between ambush predation and vision. Somewhat similarly, net-casting spiders have evolved the largest lenses of any terrestrial arthropod, which makes their eyes uniquely sensitive (Blest and Land, 1977; Stafstrom and Hebets, 2016) to support prey capture via silk nets held by the front pair of legs (Coddington and Sobrevilla, 1987; Robinson and Robinson, 1971). The relationship between vision and predation, both pursuit and ambush, will be examined in section 1.3.

Predation can also be a social strategy to feed. Many animals have been recorded hunting socially, including insects (Schneirla, 1934), fish (Merron, 1993), birds (Bednarz, 1988) and mammals (Creel and Creel, 1995; Gazda et al., 2005; Packer et al., 1990). Although how animals achieve the coordination necessary for social predation is a fascinating question, especially in more basal clades, the challenges that each animal faces during a predatory episode are similar to ones faced by solitary predators. The predatory group can employ the same behavioural strategy (Bednarz, 1988; Creel and Creel, 1995; Merron, 1993) or have individual roles (Bednarz, 1988; Gazda et al., 2005; Stander, 1992; Strübin et al., 2011), which has crucial effects on the type of prey captured. Nevertheless, the strategies exhibited by each member of the group have parallels with solitary predators. The challenges posed by predatory lifestyle and solutions to overcome them can therefore be isolated more easily in solitary predators, without the added complexity of the social interaction between predators.

In summary, predation has evolved in conjunction with faster visual perception and faster appendage movements. Visual predation among extant animals is a unique field to look at principles of animal evolution in sensory ecology, structural morphology and behaviour. Visual predation can be broadly divided into active predation and sit-and-wait predation. Active predators chase their prey monitoring its position via closed-loop feedback. They can steer their path via either pursuit, by moving to their target's location, or interception, by anticipating future prey positions. To increase the success of their chases, active predators have compact bodies with light and long limbs, which allows them to achieve impressive speeds and accelerations, which they use to gain an advantage over their target. By contrast, sit-and-wait predators remain hidden, usually thanks to their camouflage, waiting for prey to get near them, although they do sometimes stalk it. In a few instances, predators have even evolved features attractive to prey. When close, they use powerful specialised appendages or tools to capture it. Some of these appendages use latch-mediated springs to amplify the power used to capture prey, which require the predator to rely on open-loop feedback.

The advantages of studying predation, both pursuit and ambush, in insects will be highlighted in the following section, before considering their visual systems and adaptations to predation.

1.2. Studying Predation in Animals

1.2.1. The study of predation

As explained in the previous section, animals have evolved many adaptations to pursue predatory life. Consequently, predation has been studied through many different approaches. One such approach is sensory ecology, the study of how information in the environment is detected and processed by animals (Dusenbery, 1992; Stevens, 2013), which is highly relevant for the study of predation. Prey tend to mask the signals that inform potential predators about their presence through camouflage, which in turn creates innovative and fascinating adaptations to break it (Galloway et al., 2020). For example, many teleosts have evolved reflective scales to match the luminosity of the sea background and therefore camouflage (Denton

and Nicol, 1966). However, the light reflected by the scales does not match the polarisation of the background. Some predators such as cuttlefish and octopus can detect polarised light, which allows them to break the camouflage and makes them able to predate on teleosts (Shashar and Cronin, 1996; Shashar et al., 1998; Shashar et al., 2000). To spot prey, many predators use matched filters, whereby a signal given by prey is matched by the sensitivity of a receptive channel of the predator (Wehner, 1987). Sensory ecology approaches to predation, therefore, consider signals given by prey and how they are elaborated by predators.

Predators evolved their hunting paradigm by adapting the neuronal circuitry specific to their phylogeny to exploit an ecological niche. Neuroethology integrates neuroscientific approaches with ecological and evolutionary theories to untangle the causal and functional reasons behind animal behaviour, i.e. the how and why predators behave in the way they do (Sillar et al., 2016). Predation has played a central role in the development of neuroethology as a field, with many of its founding fathers having worked on predatory animals such as vipers (Bullock and Diecke, 1956), weakly electric fish (Heiligenberg, 1989; Lissman, 1958), toads (Ewert and Hock, 1972) and praying mantids (Roeder, 1937; Roeder et al., 1960). The toad provides perhaps the first example of a comprehensive explanation of the circuitry used by a predator to identify its prey (Ewert, 1987). A neuroethological approach to predation aims to describe how salient stimuli are extracted by peripheral sensory systems, overlapping with sensory ecology, but also how they are processed centrally and generate motor outputs. By comparing how different predators carry out the same task, it is possible to understand the general underlying principles of predation as well as the specific differences in how similar behaviours are implemented by different animals.

Animals generate behaviour by active muscular activity, which interacts with forces in the environment. The study of how active and passive forces are used to generate behaviour in animals is called biomechanics. The adaptation to predatory life produces selective pressures that tend to increase the speed and efficiency of animal movements; any delay or energy dissipation during predator-prey interactions may result in the early termination of an animal's life. For this reason, both predators and prey have evolved mechanisms to produce efficient, fast,

and/or high-power movements. For example, some animals have found a way out of the binary choice between muscular speed or power (Alcazar et al., 2019), by loading power-retaining structures via slow but powerful muscle contractions. These structures, or springs, can be locked in place by a latch, controlled by a weak but fast muscle. Once the latch is disengaged, these appendages release vast amounts of power in a short amount of time. These catapult mechanisms have been found in predators and prey (Bennet-Clark, 1975; Burrows, 2003; Burrows and Hoyle, 1972; Deban et al., 1997; Gronenberg et al., 1993; Lappin et al., 2006; Ritzmann, 1973; Wainwright and Bennett, 1992), some of which have been described in the previous section. Although it may initially seem that biomechanics is a relatively isolated field in the study of predation, an animal's predatory style heavily influences its limb morphology. Active predators possess stable and relatively inflexible limb joints adapted to running, while ambush predators have very flexible limb joints to handle prey effectively (Andersson, 2004). In turn, the biomechanical tools an animal uses heavily influence its sensory perception and predatory behaviour. As already stated in the previous section, catapult movements are ballistic, which means that they cannot be modulated after they begin. Consequently, they rely on open-loop feedback, which requires the animal to pre-set its muscular activity pattern before initiating the actual movement (Kagaya and Patek, 2016). By contrast, animals with similar appendages and predatory strategies who do not rely on catapult mechanisms can alter their attack more easily and even halt it (Gray and Mill, 1983; Rossoni and Niven, 2020).

Studying a predator from a truly integrative perspective means being able to understand what information it extracts from its prey, how its attack is generated by both intrinsic and extrinsic factors, and the function behind its predatory behaviour. By using principles of sensory ecology, neuroethology and biomechanics together, scientists have been able to draw otherwise invisible links between various aspects of predation (Combes et al., 2012; Higham et al., 2016; Moore and Biewener, 2015), providing a more comprehensive framework to understand predation as a phenomenon.

1.2.2. Choice of experimental animals

Although the theoretical approach to predation can be open and draw from various sources, the practicalities of experimentation often start with one question. What animal to consider when studying predation? A common strategy in biology is to use so-called "model organisms" (Leonelli and Ankeny, 2013), animals that have been studied in depth for many years, resulting in their genomes being sequenced in large part or even in full, as in fruit flies (Adams et al., 2000) or mice (Waterston et al., 2002). Whole-genome sequencing of an animal hugely contributes to understanding of its physiology and, importantly, unlocking a number of genetic tools available to study the organism even further (Hales et al., 2015). Model animals have mostly been selected for their quick generational turnover and ease to breed and maintain in the lab. Most of them have a herbivorous or filter-feeding lifestyle to avoid the complications of having to keep two animal species in laboratories. As a consequence, most model animals are not suitable as a model of predatory behaviour. One notable exception to this is the zebrafish, which was originally studied as model organisms for vertebrate development, but, after their genome was sequenced (Howe et al., 2013), they became central models for many fields, including the study of predation. In fact, although considered an omnivore (Spence et al., 2007b), zebrafish can predate upon suitably sized arthropods (Spence et al., 2007a), which has led into insightful studies of its predatory behaviour (Bianco et al., 2011; Gahtan et al., 2005; McElligott and O'Malley, 2005; Soto and McHenry, 2020).

The model-organism approach has been criticised by some researchers (Bolker, 2012), who suggest that focussing research efforts on a small number of model animals has huge risks for the scientific world. Mainly, the use of model organisms is supported by the assumption that some aspects of their physiology are shared with many, or most, other animals and that findings in one species could direct and inform research in others. Although broadly true, the similarities and differences between model organisms and other animals will not be known until investigated. As stated above, understanding the function of behaviour means drawing similarities between phylogenetically distinct species, a fundamental concept in neuroethology. It should not therefore come as a surprise that a rival strategy to

the model-organism approach comes from one of the founding fathers of neuroethology. Heiligenberg suggests that some animals have specialised for a particular task by optimising specific neuronal circuits (Heiligenberg, 1991), the study of which can conveniently highlight their functions, hidden in other animals by less efficient performances. Insights of how these "champion animals" process specific stimuli and produce specialised behaviour can in turn inform researchers on how analogue circuitry in other animals can support similar functions. For example, dragonflies are "champion" predators, who predate upon smaller flying insects with a success rate up to over 95% (Combes et al., 2012; Olberg et al., 2000). They have adapted to this predatory lifestyle by developing eyes with the highest resolution among compound eyes (Horridge, 1978; Sherk, 1978), but their acute eyes would be useless without being able to extract salient visual features. Neuronal recordings in the dragonfly's optic lobe revealed the presence of neurons highly responsive to prey-like objects (O'Carroll, 1993). Although first identified in the dragonfly, analogues of these neurons have been found in other non-predatory flies (Keleş and Frye, 2017; Nordström and O'Carroll, 2006), supposedly underlying sexual selection. This approach is so popular in neuroethology that champion animals may be referred to as model animals by some, though with a different meaning from what geneticists and physiologists define as a model organism. Eventually, the choice of what organism to select when investigating behaviour should come down to practicalities of experimentation, as well as ease of husbrandry and how generalisable the findings can be. Effectively put into words by August Krough, "For a large number of problems there will be some animal of choice or a few such animals on which it can be most conveniently studied" (Krogh, 1929), a maxim which has become famous as Krogh's principle and has, consciously or not, guided several advances in animal physiology (Krebs, 1975).

Comparisons between champion predators, encouraged by a neuroethological approach to the study of predation, should however be mindful of phylogenetic differences between clades. When two predators show differences in their predatory pattern, that could be due either to their evolutionary history or to differences in the ecological niche to which they are adapted. Unless ecological

conditions are similar, the further apart the two compared animals are on the phylogenetic tree, the more information about their evolution is needed to understand why their behaviour is different. For this reason, it is useful to compare predators with similar sensorimotor abilities. One large evolutionary divide exists between vertebrate and invertebrate animals. The chordates (phylum Chordata) are thought to have evolved in the early Cambrian (Shu et al., 1999), around the same time arthropods (phylum Arthropoda) evolved (Edgecombe, 2020). As discussed above (see section 1.1.1), at that time animals were evolving visual abilities and solid structures to support movement. For this reason, fundamental differences exist between chordates and arthropods in terms of eye morphology (Nilsson, 1996), body architecture (Arendt and Nübler-Jung, 1994), and motor control (Belanger, 2005). Parallels between animals can be made more easily within each group, although general principles of arthropod behaviour can inform the study of chordate behaviour and vice versa.

When faced with the choice of studying predation in either chordates or arthropods, there are many advantages of using arthropods, and specifically the insects (subphylum Hexapoda), its largest subphylum. Firstly, insects are generally smaller than vertebrates. This means that they can be reared in smaller spaces and with less food than vertebrates, which drastically reduces the cost of their maintenance. Insects are not only smaller, but their nervous system also possesses fewer neurons, many orders of magnitude fewer than in vertebrate nervous systems (Azevedo et al., 2009; Menzel and Giurfa, 2001; Zheng et al., 2018). Given the moderate effect of increasing numbers of neurons on the production of qualitatively different behaviours (Chittka and Niven, 2009), this makes insects excellent models to study complex behaviour. Many neurons in insects, though not all, are identifiable between individuals of the same species (Comer and Robertson, 2001; Meinertzhagen, 2016; Rowell, 1989), due to developmental processes that produce neurons recognisable by morphology and physiology (Meinertzhagen et al., 2009). Some insect neurons can even be compared between different species as described above (Keleş and Frye, 2017; Nordström and O'Carroll, 2006; O'Carroll, 1993), although this makes it harder to distinguish between neuronal analogues and homologues.

All of the advantages just outlined would be completely useless if insects only evolved few examples of predatory behaviours. Luckily, that could not be further from the truth. Insects are the most diverse class of all animals (Stork, 2018), having evolved to exploit the majority of terrestrial ecosystems. The phylogenetic tree of insects is vast (Misof et al., 2014) and includes many predatory species (Grimaldi and Engel, 2005). As already outlined, insects include active predators such as dragonflies, tiger beetles, and robber flies, while among ambush predators are praying mantids, ambush bugs, water stick insects, and mantispids. Many others, including damselflies and water bugs, can switch between predatory strategies depending upon the context. All these predators possess bodies of approximately similar size, with similar eye structures and motor systems and are therefore highly comparable.

Although a model-system approach to studying predation would advocate choosing genetically tractable predators, like the zebrafish, a champion-animal approach is more compatible with principles of neuroethology. Insects are a diverse and abundant class of predators with tractable nervous systems, whose predatory behaviour is highly comparable; this makes them invaluable assets to the study of predation.

1.3. The Visual System of Insects

1.3.1. Insect eyes

Photons, the elementary particles of light, are transformed into electrical signals by photoreceptive cells via a process named phototransduction (Rayer et al., 1990). During phototransduction, photons bind to proteins called opsins on the photoreceptor's cell membrane. Photons can change the structural conformation of opsins, thereby initiating a signalling cascade within the photoreceptor (Yau and Hardie, 2009), which in insects causes the membrane potential to depolarise. Increasing the number of opsins on a photoreceptor makes it more sensitive, as it increases the likelihood of photon capture. Because opsins are trans-membrane proteins, photoreceptors have a considerable amount of cell membrane to increase their sensitivity (Nilsson, 2009). In insects, this is achieved by

evaginations of the photoreceptor's membrane called microvilli, which are densely packed with opsins. In most insects, the microvilli from neighbouring photoreceptors are grouped to form a rhabdom. An additional boost in sensitivity is given by a lens, which focuses light onto the rhabdom by refraction (Nilsson, 2009). Insects have compound eyes, where each rhabdom in the eye has a corresponding lens, contrary to vertebrates which possess one lens per eye, a design called camera or simple eye. A compound eye is made up by repeats of basic units, called ommatidia, composed by: a) a rhabdom, b) its lens, c) a refractive structure between a lens and the rhabdom called a crystalline cone, d) pigment cells that optically isolate the unit, and e) other support cells.

Any eye evolves as the product of a trade-off between resolution and sensitivity (Snyder, 1977), the balance of which needs to match the visual ecology of the animal. The higher the ommatidium density in the eye, the more resolved the imaged formed by it. However, more densely packed ommatidia necessarily decrease in size, reducing their sensitivity. This trade-off can be measured in compound eyes. An eye evolved for resolution will have more ommatidia with smaller angular separations. Therefore, a good indicator of resolution is the angle between ommatidia ($\Delta\Phi$), which can be calculated from the distance between the photoreceptors (x_{photo}) and the focal length of their lenses (f):

$$\Delta\phi = x_{photo}/f \qquad \text{Equation 1.1}$$

The resolution of the eye increases as the interommatidial angle decreases. A better approximation of eye resolution is the receptive field of its photoreceptors which, rather than being determined by the distance between them, is determined by their diameter (d_{photo}). Better known as the acceptance angle ($\Delta\rho$), it can be calculated as:

$$\Delta\rho = d_{photo}/f \qquad \text{Equation 1.2}$$

Sensitivity can be measured as the focal ratio (also known as the F-number), obtained by dividing the focal length of a lens (f) and its diameter (d_{lens}):

$$F = f/d_{lens} \qquad \text{Equation 1.3}$$

The sensitivity of the eye increases as the focal ratio decreases. A crucial bottleneck in the balance between sensitivity and resolution is eye size. Increasing the number of ommatidia in an eye would improve its resolution, and increasing the

diameter of each ommatidia would benefit the eye's sensitivity. However, eyes are not only under physical constraints, especially in flying insects (Swallow et al., 2000), but also energetically very expensive to maintain (Niven et al., 2007). Rather than evolving impractically huge eyes, many insects, and particularly predators, evolved eyes where ommatidia are more numerous, or larger, or at lower interommatidial angles, only in certain areas of the eye (Barros-Pita and Maldonado, 1970; Gonzalez-Bellido et al., 2011; Horridge, 1978; Laughlin and McGinness, 1978; Rossel, 1979; Sherk, 1978; Wardill et al., 2017). These areas, called acute zones or foveae, are usually positioned on the eye in a location of ecological relevance, where it is more convenient to see with higher resolution or more sensitivity.

Generally speaking, compound eyes can be divided in three groups: apposition eyes, optical superposition eyes and neural superposition eyes (Land and Nilsson, 2002). Apposition compound eyes have optically and anatomically isolated ommatidia (Horridge, 1978; Horridge, 1980). Because light rays outside of an ommatidium's optical axis are absorbed by surrounding pigment cells, much of the light captured by the lens is not transduced. The design of apposition compound eyes, therefore, favours resolution over sensitivity. This explains why most insects who possess an apposition compound eye are diurnal, such as dragonflies and praying mantids. In superposition compound eyes (Exner, 1891), lenses are separated from the photoreceptive layer by a clear zone that lacks isolating pigments. By refracting light from many lenses onto individual photoreceptors, superposition compound eyes more than double the photon catch of individual photoreceptors (Miller et al., 1968). Such a large superposition aperture can, however, encounter many aberrations resulting in a somewhat blurred image (Caveney and McIntyre, 1981; Warrant and McIntyre, 1990). For this reason, superposition eyes are common among night active insects or otherwise living in low-light conditions, such as forest-dwelling tiger beetles (Brännström, 1999). A third type of eye evolved in dipteran flies, called a neural superposition eye (Kirschfeld, 1966). Much like apposition eyes, the ommatidia of neural superposition eyes are isolated. In each ommatidium however, the photoreceptors separated into 8 different rhabdomeres (R1-8). Aside from colour-sensitive

rhabdomeres (R7-8), which are stacked on top of each other, each rhabdomere has its own optical axis. The optical axis between two rhabdomeres within an ommatidium is matched by the optical axes between two ommatidia (Stavenga, 1975). The signals from rhabdomeres that sample the same point in space in neighbouring ommatidia are then pooled post-synaptically, thereby increasing sensitivity without sacrificing resolution (Agi et al., 2014).

As explained, the effect of an animal's light environment on the design of its compound eyes has been investigated in detail. However, an animal's foraging strategy impacts its eye morphology as much as the light intensity of its environment or its locomotory strategy (Feller et al., 2021; Land, 2003). Although a predatory lifestyle was likely a big determinant in the evolution of compound eye acuity (Paterson et al., 2011), the effects of predation on eye evolution have been largely understudied.

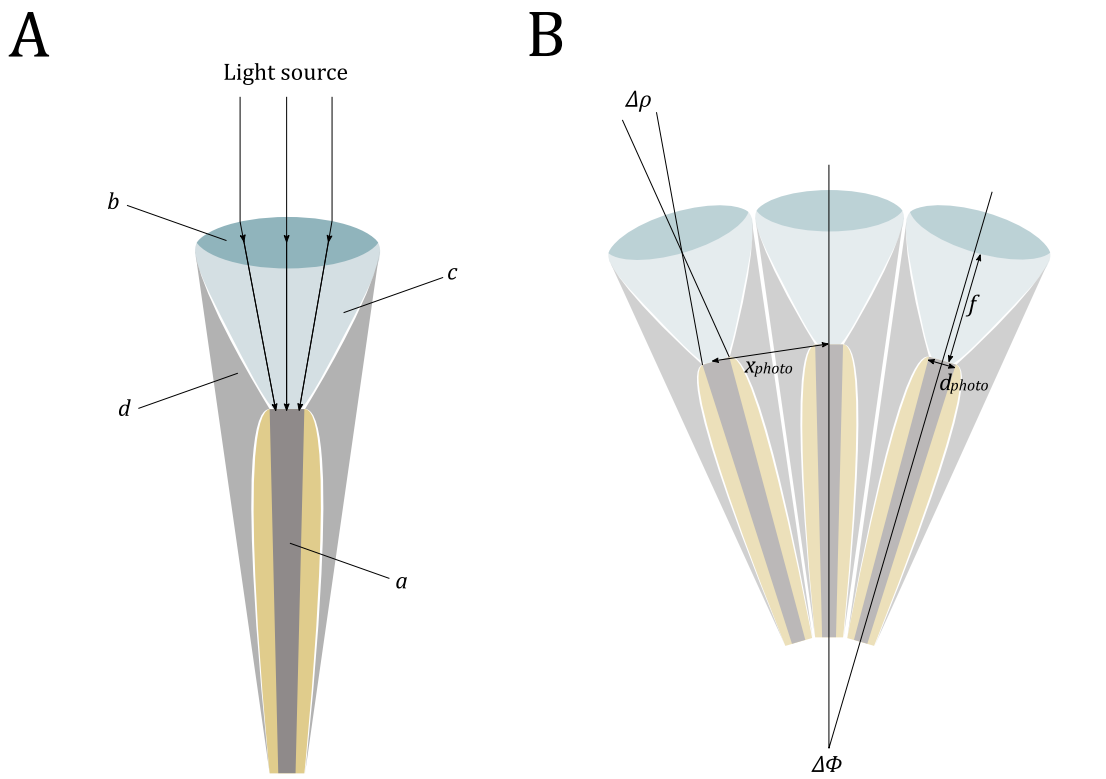

Figure 1.1. The structure of the insect compound eye. A) Schematic cross section of an ommatidium, showing: *a*, the rhabdom; *b*, the lens; *c*, the crystalline cone; *d*, screening pigments. B) An illustration of some measurements used to estimate eye resolution and sensitivity in a compound eye: $\Delta\Phi$, the interommatidial angle; x_{photo}, the distance between photoreceptor tips; *f*, the focal length of the lens (approximate); d_{photo}, the photoreceptor diameter; $\Delta\rho$, the acceptance angle.

1.3.2. Visual processing in insects

Light transmitted through the lens array is processed by successive layers of the optic lobe. The insect optic lobe is comprised of five neuropils, called the retina, lamina, medulla, and lobula. The retina, composed primarily from photoreceptors, is responsible for phototransduction, while the other neuropils use information from the retina to extract salient visual information. All the neuropils of the optic lobe are retinotopically arranged, meaning that neighbouring cartridges, or columns, of neurons in the different neuropils process visual input from neighbouring ommatidia.

Achromatic photoreceptors project medially to the first neuropil of the optic lobe, called the lamina. Each column in the lamina has the same subsets of neurons to refine the output from photoreceptors. The large monopolar cells (LMCs) in the lamina amplify the signal from photoreceptors and directly filter the incoming

information to enhance contrast detection (Laughlin and Hardie, 1978), responding to light increments and decrements rather than absolute values. The rest of the neurons are responsible for modulating this feedforward signal with feedback information coming from the medulla (Tuthill et al., 2013), possibly being responsible for the light-adaptation of LMCs. Most of the information is processed in parallel via microcircuits (Meinertzhagen and Sorra, 2001), to be sent to the medulla.

There is an extensive divergence of circuitry from the lamina to the medulla. In fact, the medulla receives signals from the laminar columns retinotopically, but also is stratified in layers along the proximo-distal axis (Fischbach and Dittrich, 1989). This arrangement suggests that the medulla is capable of processing wide-field stimuli. Indeed, medullar neurons have been shown to respond to wide-field motion, with instances of preferred direction responses (DeVoe, 1980; Gilbert et al., 1991). The medulla also processes small-field motion. Early, more distal layers are responsible for elementary processes like edge detection (Wiederman et al., 2008), while later, more proximal layers extract motion information, with both directional and non-directional preferences (Douglass and Strausfeld, 1995; Douglass and Strausfeld, 1996). Some of both wide-field and small-field neurons in the medulla feedback to the lamina (Fischbach and Dittrich, 1989), while others project directly to the central brain (Otsuna and Ito, 2006). Most neurons, however, project to the lobula, carrying information about both wide-field and small-field motion.

The lobula has a very diverse structure depending on the phylogeny of the animal considered and its visual ecology. Most dipterans possess a lobula complex, which can be divided in the lobula and lobula plate (Fischbach and Dittrich, 1989). In most lower insects, a single lobula is comprised of a number of lobes (El Jundi et al., 2009; Fabian et al., 2020; Immonen et al., 2017; Rosner et al., 2017), which varies depending on the complexity of visual information needed by the animal, including navigation and foraging strategy. The physiology of lobula neurons also depends on the general ecology of the animal. Most generally, the lobula is responsible for discriminating objects in the visual field from the background (Egelhaaf, 1985). The presence of such a defined structure responsible for the

visual processing of object motion has meant that the study of motion detection has greatly benefitted from research done in the insect lobula, the findings from which can indicate computational principles common amongst many, if not all, animals (Borst and Egelhaaf, 1989). In the lobula of flying animals, wide-field neurons are tuned to patterns of visual field motion matched by specific aerial manoeuvres generated by self-motion (Krapp et al., 1998). Some neurons can encode for differential angular movements of objects in the visual field in response to self-movement (Longden et al., 2017), possibly extracting three-dimensional information about an animal's surroundings. Parallel to and separate from wide-field motion, the lobula also processes object detection. Among object-detecting neurons are looming detectors, present in a variety of insects (de Vries and Clandinin, 2012; O'Shea and Williams, 1974; Rind and Simmons, 1992; Yamawaki, 2018). Other neurons are tuned to the detection of small targets travelling across the visual field, and are for this reason called small target motion detectors (STMDs) (Keleş and Frye, 2017; Nordström and O'Carroll, 2006; O'Carroll, 1993; Wu et al., 2016). Of these cells, some respond to seemingly quite complex stimuli. For example, neurons can attend a single stimulus out of two identical targets (Wiederman and O'Carroll, 2013), or respond to stimuli with certain matching coordinates between the two eyes (Rosner et al., 2019).

Neurons from the lobula project onto many brain areas, where information about salient visual features is integrated with other sensory information, including motivational state and behavioural goals. Eventually, however, visual information is transmitted by descending neurons from the brain to the ventral nerve cord of the animal. Circuits in the ganglia are then responsible for correctly activating motor neurons controlling leg or wing muscles. Descending neurons are orders of magnitude fewer than both neurons in the optic lobe or in the ventral ganglia (Namiki et al., 2018), so they must encode visual information efficiently. Similarly to neurons in the lobula, descending neurons are divided in two classes, one that responds to wide-field motion and the other that detects object motion (Nicholas et al., 2018; Olberg, 1981a). Predatory insects need fast and precise information about object motion; for this reason they evolved target-selective descending neurons (TSDNs) with large axons, producing faster conductance

(Supple, 2019). In active predators, TSDNs code for precise target location and direction vector (Frye and Olberg, 1995; Gonzalez-Bellido et al., 2013; Nicholas et al., 2018; Supple et al., 2020), thereby providing motor centres with the essential information necessary to steer towards prey. The descending neurons of sit-and-wait predators have been somewhat less studied. Some neurons have been described that respond to small targets, with preference towards targets moving in a certain direction (Yamawaki and Toh, 2009b); however, these neurons also respond to widefield movement in the same direction, suggesting that they do not strictly mediate predation alone. Other descending neurons identified in ambush predators respond to looming stimuli (Yamawaki and Toh, 2009a). Although it is easy to imagine they might trigger an attack towards looming prey, these neurons have been shown to mediate defensive behaviour (Sato and Yamawaki, 2014), again suggesting they are not involved in predatory behaviour alone. One class of target-sensitive descending neurons has been described in the praying mantid (Gonka et al., 1999). These neurons seem to be fewer than the TSDNs of active predators and they do not seem to encode precise information about prey location and direction. Rather, they have been suggested to signal the presence of a target in the capture zone. The proposed function of these neurons has therefore been to release a predatory strike. This circuitry seems however extremely simplistic compared to the complex behaviours recorded in praying mantids (Cleal and Prete, 1996; Cleal and Prete, 1996; Rossoni and Niven, 2020), suggesting that there might be a larger, not yet identified circuitry implementing the full behavioural complexity of ambush predators.

1.3.3. Active vision strategies in insects

Contrary to most vertebrate eyes, the eyes of insects are fixed on their heads. This does not mean, however, that insects' eyes are static, as their gaze shift paradigms can be as complex as the ones of vertebrates (Land, 1999). During saccadic movements, insects alternate periods of stable eye positions, called fixations, to periods of fast eye movement, called saccades. By separating bouts of eye movements and eye immobility, both vertebrates and invertebrates minimise the impact of motion blur on their visual input, while also allowing for visual scanning

(Land, 2019). For example, tiger beetles interpose brief pauses, fixations, in their predatory chase, during which they move so fast that their visual scene is heavily blurred (Gilbert, 1997).

The opposite gaze shift strategy is called smooth visual tracking. During a smooth tracking sequence, an animal moves its eyes to follow a moving target so that it occupies the same position on the retina. During an attack, dragonflies rotate their heads to compensate for body movement and also target movement, so to minimise the retinal slip of the target (Mischiati et al., 2015; Olberg et al., 2007). Similarly, praying mantids have been shown to smoothly track a target moving against a uniform background, thereby centring the target on the fovea throughout the tracking sequence (Levín and Maldonado, 1970; Rossel, 1980). On a non-uniform background, mantids switch to saccadic tracking of a moving target (Rossel, 1980).

The manipulation of gaze with the intent of extracting more accurate information from the visual environment is called active vision. A concept originally introduced for artificial systems (Aloimonos et al., 1988), active vision has been used to describe eye movement strategies of both vertebrates (Choi and Henderson, 2015; Dawkins and Woodington, 2000; Mazer and Gallant, 2003; Mitchell et al., 2014) and invertebrates (Buatois et al., 2018; Cellini and Mongeau, 2020; Egelhaaf et al., 2009; Lehrer and Srinivasan, 1994). In contrast to active sensing with sound (e.g. bats) or electricity (e.g. electric fish), active vision does not require signal emission by the sensing animal. Active vision can substantially boost an animal's visual abilities; animals with extremely narrow retinae can achieve a considerable visual field by means of active vision, allowing visually challenging behaviours like predation (Buschbeck et al., 2007; Dzimirski, 2010; Land, 1969; Land, 1982). Similarly, apparently complex cognitive abilities such as numeracy (Vasas and Chittka, 2019) and pattern discrimination (MaBouDi et al., 2021) could be explained by relatively simple active vision strategies. The entire visual ecology of an animal can benefit from active vision in ways that cannot be simply evaluated by eye morphology alone (Land et al., 1990).

As already mentioned, a major visual challenge of predatory animals is to extract three-dimensional information about the visual environment from two-

dimensional retinae. Simply put, in a two-dimensional image a small target at close distance might look the same as a large target farther away. Praying mantids (Rossel, 1983) have evolved the ability to do so by triangulating the target's position from its retinal coordinates on the two eyes, an ability known as stereopsis. Without using stereopsis, active predators can select for targets of matched angular size and speed, which usually leads them to chase targets of suitable absolute size (Lin and Leonardo, 2017; Wardill et al., 2015). Although both of these tactic can benefit from active vision (Levín and Maldonado, 1970; Mischiati et al., 2015; Olberg et al., 2007; Rossel, 1980), neither of them is a product of active vision.

There are, however, animals who can use active vision to gather three-dimensional information. An animal's movement causes a shift of its visual scene, which is known as optic flow (Gibson, 1950). While during rotational movements the entire visual scene rotates uniformly, a translational movement causes differential optic flow, with nearby objects slipping more, and faster, than objects farther away. The animal's absolute movement, or velocity, can be then used to extract objects' absolute parameters (Kral, 2003). Animals can translate with the only aim of extracting three-dimensional information. This behaviour, known as motion parallax, is another example of active vision, and its use is widespread in animals (Collett, 1978; Davies and Green, 1988; Ellard et al., 1984; Goulet et al., 1981; Lehrer and Collett, 1994; Lehrer et al., 1988; Poteser and Kral, 1995; Ravi et al., 2019; Rogers and Graham, 1979; Ruiz and Theobald, 2020; Sobel, 1990; Srinivasan et al., 1989; van der Willigen et al., 2002; Wallace, 1959; Zeil, 1993). Motion parallax can be as sensitive (Rogers and Graham, 1982) and more effective than stereopsis (Poteser and Kral, 1995), but it has not been recorded in predation, likely because it is slow and might give away the presence of a predator.

Overall, active vision is an effective way to compensate for suboptimal eye morphology. In predation, active vision has been identified mainly in the form of scanning, smooth visual tracking, and saccadic tracking. Even these forms of active vision have only been studied in isolation; whether and how they support successful predation are questions that remain largely unanswered.

1.4. Thesis Structure

The range of possible ways in which active vision affects the behaviour of predatory animals has been understudied. Insects offer a suitable model for this investigation by combining convenient experimental conditions with an extensive literature on their vision and predatory strategies. The aim of this thesis is to investigate the role of active vision in predation using predatory insects, with an approach based on sensory ecology, neuroethology and biomechanics. Visual strategies of both active and sit-and-wait predators will be considered with a comparative approach.

Chapter 2 will consider the praying mantid, a relatively well-studied ambush predator with foveated, high-resolution compound eyes. The visual tracking strategy of the praying mantid will be investigated in response to prey moving linearly in front of it, at different speeds and with different initial head orientation. This will establish how mantids combine the need to turn their gaze towards their target with the need to track it as it moves. Crucially, the role of head movements in the initiation of attacks and their success will be investigated with an ecological approach, bridging an important behavioural gap which has been overlooked in the literature.

In chapter 3, the hunting behaviour of darting robber flies will be described. Darting robber flies are ambush predators much smaller than praying mantids, which poses many challenges to their visual ability. Our behavioural analysis shows that darting robber flies use absolute prey size when attacking, yet the reduced size of their eyes severely affects their ability to use stereopsis. We suggest that darting robber flies overcome some of the limitations imposed by their small size by means of active vision, without which it would be otherwise much more challenging for miniature predators to exist. The effectiveness of depth estimation can therefore be compared between animals that achieve it by means of active vision, such as darting robber flies, and animals that have adapted their eye morphology for the task, such as praying mantids, hence highlighting the advantages and disadvantages of active vision strategies.

Chapter 4 will be focussed on killer flies, active predators with limited visual abilities. Killer flies have been shown to predate without relying on depth-related information about their prey, seemingly using a simple interception strategy during their attacks. During downward dives, the effectiveness of this interception strategy is impaired by the force of gravity, which adds to active acceleration during downwards attacks. Rather than correcting their interception path to improve efficiency, killer flies conduct high-acceleration attacks. We suggest this might trigger avoidance manoeuvres in the prey, therefore forced to slow down. Moreover, killer flies might prioritise visual tracking of their targets over flightpath efficiency. This chapter will highlight the large impact that active vision can have on behaviour of animals.

2. Active Vision Increases the Success of a 'Sit-and-Wait' Predator

2.1. Introduction

Tracking a moving target is an important ability for many animals, as it underpins their capacity to capture prey or find a mate. Prey is not only erratic, but also actively evasive (Domenici et al., 2011). Improving visual resolution increases accuracy allowing predators to successfully intercept prey, thereby directly increasing an animal's chance of survival. Due to the high cost of eye maintenance (Niven et al., 2007), however, visual predators have usually evolved only a portion of their eye with maximal visual resolution, called an acute zone or fovea. Active eye movements allow these animals to scan the visual scene with their foveas (Land, 1999; Land, 2019), but the role of eye movements in ecological contexts has been overlooked (Billington et al., 2020).

In insects, local regions of increased resolution can be evaluated relatively easily from external eye morphology (Perl and Niven, 2016; Perl et al., 2017; Stevenson et al., 1995). The presence of an acute zone in the eyes of insect predators (Barros-Pita and Maldonado, 1970; Gonzalez-Bellido et al., 2011; Horridge, 1978; Laughlin and McGinness, 1978; Rossel, 1979; Sherk, 1978; Wardill et al., 2017) has been documented extensively. Evidence of how their foveas are directed during targeted behaviour has proven more difficult to gather. Some active predators have been found to stabilise their target's position on their eyes by head rotation, which is known as smooth tracking (Mischiati et al., 2015; Olberg et al., 2007), even performing predictive movements. Other active predators do not foveate their prey until they start chasing it, however (Wardill et al., 2015). The efficacies of different strategies of active vision have been difficult to quantify precisely during predatory behaviour because of a lack of variation in the active

movements used by individual predators, hence only allowing comparisons to be made between species.

Although praying mantids can stalk prey when hungry (Bertsch et al., 2019; Holling, 1966; Milledge, 1990), they primarily capture prey by ambushing it with specialised raptorial limbs (Copeland and Carlson, 1977; Loxton and Nicholls, 1979; Prete, 1990). Mantids have adapted to visual predation by developing eyes with frontal foveas (Barros-Pita and Maldonado, 1970; Rossel, 1979) that they use for range estimation (Nityananda et al., 2018; Rossel, 1983). Despite their sit-and-wait strategy, praying mantids have extremely mobile necks, seemingly adapted to support active vision. In fact, mantids can visually track prey moving slowly against a uniform background by smooth tracking (Rossel, 1980). When the speed increases, their head movements lag behind prey, which they correct with fast, ballistic head rotations called saccades (Lea and Mueller, 1977; Rossel, 1980). During a saccade, mantids can rotate their heads up to 400 °/s (Lea and Mueller, 1977). However, mantids have been shown to strike at prey moving at very high speed (Rossoni and Niven, 2020), reaching over 1300 °/s.

Here, we use a combination of high-speed three-dimensional videography and generalised linear models to investigate the role of active vision in the initiation, success, and abandonment of the raptorial strike of the praying mantid. We manipulated the animals' head orientation before the strike and monitored the movements of the head before and during the strike. We show that the mantid's sex, its head orientation, the speed of prey, and the number of prey presentations affect strike initiation, whereas the head orientation, the timing of head movements, the speed of prey, and the number of prey presentations affect the success of the strike. Prey speed is the only factor influencing strike abandonment. As a crucial factor affecting strike success, head movements in turn are affected by the mantid's head orientation, its sex, temperature and the speed of prey.

2.2. Materials and Methods

2.2.1. Animals

African mantids (*Sphodromantis lineola* (Burmeister, 1838)) were purchased from a local supplier (BugzUK, Norwich, UK) as L4 nymphs. They were maintained in individual cages in the School of Life Sciences, University of Sussex, UK, with a 12/12 hour light/dark cycle at room temperature (21-23°C). Mantids were fed live larval and adult green bottle blowflies (*Lucilia sericata*) and offered water weekly. Animals were raised this way to at least L6 nymph stage for experiments. During the experimentation period, the 12 mantids (males = 5, females = 7) were individually tracked. To account for a range of motivational states in relation to feeding status, once a week and at least two days before experiments, mantids were fed either to satiation or one blowfly larva and offered water until rejected.

2.2.2. Indoor testing

Prior to each trial, mantids were weighed. To record their strikes, they were placed on a 26 x 26 cm raiseable metal plate, in the middle of a 75 x 60 x 60 cm white arena, illuminated from overhead. Mantids were presented with a manually operated 4 mm wide, black faceted bead (target) to assess their willingness to hunt. Visual tracking of prey, stalking, and attempting to attack prey were all taken as signs that the animal intended to hunt. This also served to lead them to the stimulus presentation area, where the distance between the mantid and the target was less than the mantid's forelimb length, meaning the stimulus was within reach. Once in position, the mantids' heads were oriented towards their left, their right, or the centre of the arena, hereafter referred to 0°, 180° or 90° head orientation, by quickly presenting a manual target in the desired direction. An identical target attached to a transparent fluorocarbon wire with diameter of 0.3 mm (Asso fishing line, Genova, Italy) was then moved from left to right, at constant speeds ranging from 20 mm/s to 500 mm/s using a motor (RE-385, MFA Como Drills, Worth, Kent, UK). These speeds reflect a variety of locomotion speeds from a walking fruit fly (DeAngelis et al., 2019) to flying blowflies (Yurkiewicz and Smyth, 1966). Praying

mantids have been shown to be responsive to target speeds above 500 mm/s (Rossoni and Niven, 2020).

Praying mantids were presented the same stimulus over several trials, interspersed by brief pauses up to 2 minutes, until they completed a strike. Between stimulations, the manually moved target was presented to check their willingness to continue hunting; mantids tracking the target with their head and/or attempting to walk towards it were considered as still willing to hunt. For each stimulus presentation, the temperature and humidity in the behavioural arena were recorded (Electronic Temperature Instruments, Worthing, UK), as well as the time of the day.

2.2.3. Videography and calibration

Mantids were filmed from behind, so as to avoid disrupting their visual tracking. The animals were filmed with a resolution of 1280 x 720 pixels, using the high-speed feature at 240 frames per second on a smartphone camera (iPhone SE first generation, Apple Inc., Cupertino, CA, U.S.A.), held in place by custom cut 6-mm thick panels of acrylic. To obtain stereo images of the animal, we took inspiration from a double-periscope mirror arrangement used in a prototype for rotational stereo videography (de Margerie et al., 2015), and adapted it to a static design. The smartphone camera was pointed at two inner mirrors, positioned perpendicularly to each other, which reflected the view of two outer mirrors, looking out towards the behaving animal (**Fig. 2.1A-B**). We used 3-mm thick mirrors of size 75 x 100 mm (outer mirrors, H x W) and 75 x 50 (inner mirrors). We compared back-surfaced mirrors on acrylic to front-surfaced mirrors on glass (Edmund Optics, Barrington, NJ, USA). The mirrors were supported by custom cut 6 mm thick panels of acrylic, fixed on a wooden board. Although the relative positions of the mirrors were fixed, a calibration video was taken after each trial, to account for potential small changes in filming angles. Calibrations were obtained by filming a laser-printed chequerboard in orientations visible by both cameras (**Fig. 2.1C**).

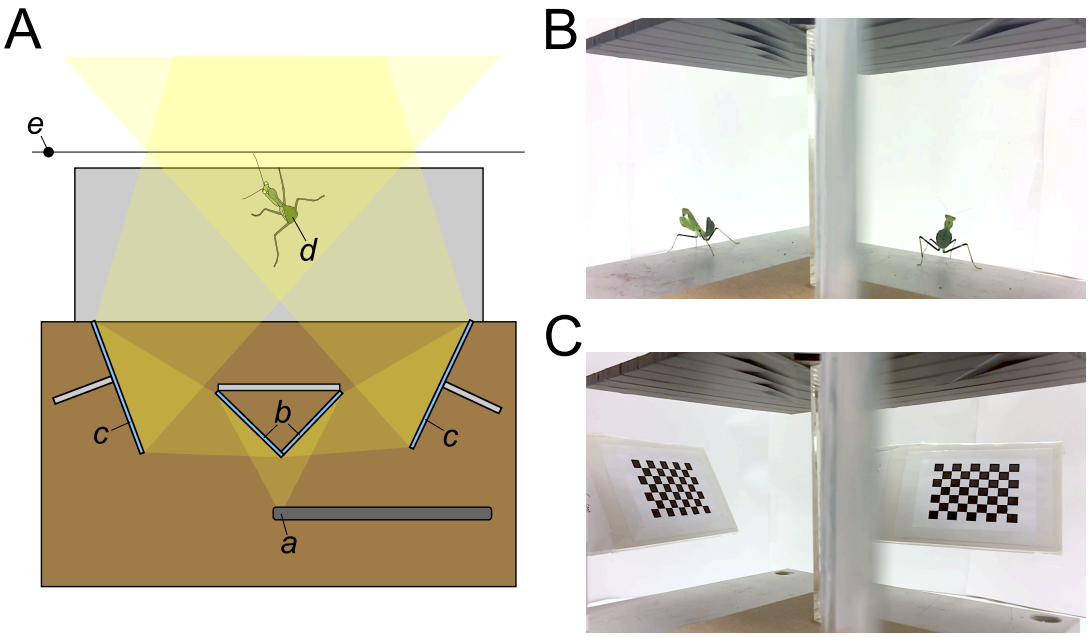

Figure 2.1. The experimental configuration for recording the strikes of praying mantids in stereo. A) Top view of the experimental setup showing: *a*, the recording smartphone; *b*, inner mirrors; *c*, outer mirrors; *d*, a praying mantid; *e*, a target. The raiseable metal plate is shown in grey, the wooden board onto which the mirror setup is glued is brown, and the field of view of the smartphone camera is shown in yellow. B) A still frame showing a praying mantid recorded from two views simultaneously. C) A still frame from a calibration video, showing two simultaneous views of the calibration grid.

2.2.4. Data extraction

All videos were analysed offline. Firstly, the behavioural responses of the mantids were scored. Mantids were given a binary score for head movement (present/absent) and strike initiation (attempted/not attempted). Tarsal flexion, tibial extension, and femoral depression were all considered attempted strike initiations. For each head movement recorded, whether the movement happened before or after strike initiation was also scored (before/after). For each strike initiated, strike completion, which was marked by full tibial flexion, was recorded (completion/abandonment). Finally, whether completed strikes were successful in capturing prey was also recorded (success/failure).

As the target entered and exited the arena during a presentation, it made a distinctive clicking sound, which we used to trim the recorded sequence. To digitise animal positions, each video was split down the midline so to isolate the two stereo views. Five frames were taken from a sample of 100 videos (50 for each stereo view), and the positions of the target and both eyes of the mantids were

marked using DeepLabCut, version 2.1 (Mathis et al., 2018) running in Python (version 3.8.5). We used the marked frames to train a DeepLabCut deep learning algorithm for 650,000 iterations. After visual evaluation of the trained network, it was used by a pose estimator algorithm (Karashchuk et al., 2020) that also obtained triangulation matrices from calibrations, and then used for three-dimensional reconstruction. The distances between the eyes were fixed during the reconstruction to represent a fixed distance on the animal.

The reconstructed 3D coordinates of the marked body parts were analysed using MATLAB R2020a (version 9.8). We considered the three-dimensional coordinates of the target when visible from both cameras. A straight line was fitted to the target trajectory using the method of least squares. Because targets were travelling at constant speed, we used the average triangulated speed to reconstruct the entire target motion from its entry into the arena. We then used this trajectory to calculate the minimal distance between the target's trajectory and the midpoint between the digitised eye coordinates in the first videoframe. This was considered as the distance between mantid and target trajectory.

We used target velocity as a measure of the accuracy of our stereo calculations because it could easily be measured manually and incorporated both spatial accuracy and temporal precision. Target velocities calculated via stereo videography were highly correlated to the velocities measured manually (Pearson's correlation, $r = 1.00$, $p < 0.001$, **Fig. 2.S1**), indicating that that our stereo setup was both accurate and precise. A linear model revealed that the correlations between target velocities calculated manually and in stereo were not significantly different depending on mirror type, front-surfaced *versus* back-surfaced mirrors ($p = 0.263$). Both mirror setups were therefore reliable in extracting three-dimensional measurements.

2.2.5. Statistics

Statistical tests were run on R studio software, version 1.3.959, and R software, version 4.0.2 (R Core Team, 2017). In this chapter, mean ± standard error ($m \pm SE$) are used as descriptive statistics, calculated using the *pastecs* package.

Generalised linear mixed-effects models were fitted using the *glmer* command in the *lme4* package (Bates et al., 2015). As all outcome variables in the models were binary, logistic regressions were obtained by using a binomial family within the mixed-effects models, which in R studio defaults to a logit link function. Continuous predictors were scaled to standard deviation (*SD*) = 1 and centred on mean (*m*) = 0. Raw data was used during statistical testing, but some figures present data smoothed with a Savitzky-Golay filter (Savitzky and Golay, 1964). Model selection was performed by stepwise removal of non-significant ($p < 0.05$) fixed effects, from least significant to least non-significant. Random predictors were then added in a stepwise fashion and discarded if non-significant. The individual mantid was retained as a random effect in all models due to the experimental design. For some cases, addition of random predictors caused non-convergence in the model, meaning that those variables could not be assessed.

2.3. Results

2.3.1. Variables affecting strike kinematics

Individual African mantids (*S. lineola* (Burmeister, 1838)) (n = 12 animals) were tested over multiple trials (n = 62 trials) involving repeated presentations of an artificial prey item (hereafter referred to as the target; n = 230 presentations). During the presentations, the distance between the mantid and the target trajectory, i.e. the minimum distance between the mantid's initial head orientation and the target trajectory as outlined in the methods, was 14.9 ± 0.33 mm. Animals were tested at a temperature of 26.0 ± 0.144 °C and a humidity of 26.9 ± 0.291 %.

Mantids initiated a strike on 77.4 ± 4.32 % of the presentations. To understand the factors influencing strike initiation, we implemented a generalised linear mixed-effects model (see Materials and Methods) and simplified it stepwise by removing effects from least significant to least non-significant (**Table 2.1**). Sex had a significant effect on strike initiation, with males initiating fewer strikes than females (**Fig. 2.2A**). Strike initiation also decreased with increasing target speed (**Fig. 2.2B**), although the second-slowest speed led to strike initiations at every presentation. Higher head orientation angles also decreased the likelihood of a

strike initiation, although orientations of 90° and 0° elicited a similar proportion of strikes (**Fig. 2.2C**). Finally, mantids were more likely to initiate a strike in response to successive presentations. However, this effect might be non-linear; very early presentations were more likely to lead to strike initiation, but so were very late presentations (**Fig. 2.2D**). Neither temperature nor humidity affected the probability of strike initiation, and the same was true for the time of the day of each presentation. There was no significant change in the likelihood of strike initiation between trials. The distance between mantid and target trajectory also did not affect the likelihood of strike initiation, and neither did the presence or absence of a head movement. Individual mantids' head widths did not affect their ratio of strike initiation, and neither did their individual weights.

Of all strikes initiated, only 47.2 ± 7.30 % were completed, which was indicated by full tibial flexion. A simplified generalised linear mixed-effects models (**Table 2.2**) revealed that speed was the only significant predictor of strike completion, with higher speeds decreasing strike completion likelihood. All presentations of the second-slowest target speed led to strike completion (**Fig. 2.3**).

Of all strikes completed, 58.2 ± 6.54 % were successful. A simplified generalised linear mixed-effects model (**Table 2.3**) revealed that mantids were less likely to successfully strike targets with repeated presentations (**Fig. 2.4A**). To check whether this effect was caused by the excessive number of presentations required by high-speed targets to elicit a strike (**Fig. 2.S2**), we substituted the presentation number in our model with an interaction term between presentation number and target speed. This interaction was not significant (p = 0.847), suggesting indeed that mantids are more likely to be successful during earlier presentations at all target speeds. Mantids were also more likely to be successful if they moved their head before initiating a strike (**Fig. 2.4B**). A strike was less likely to be successful the higher the initial head orientation angle (**Fig. 2.4C**). Finally, mantids' strikes were less likely to be successful when the target was moving at higher speeds (**Fig. 2.4D**). Neither room temperature, nor humidity, nor the time of the day affected the probability of strike success. There was no significant change in the likelihood of strike success between trials. The distance between mantid and target trajectory did not affect strike success, and neither did the mantids' sex.

Table 2.1. Simplification of generalised linear models shows that sex, target speed, initial head orientation, and presentation number influence strike initiation. Rows in bold represent the most parsimonious model with only significant effects. Mantid identity was included as a random effect, with rows in italics indicating inclusion as random coefficients. Significance values: * = $p < 0.05$, ** = $p < 0.01$ *** = $p < 0.001$.

Outcome variable	Predictors	*p* value	Estimate	S.E.
Strike initiation	Presence of head movement prior to strike	0.599		
	Target trajectory distance	0.806		
	Time of the day	0.737		
	Temperature	0.882		
	Trial number	0.187		
	Humidity	0.262		
	Weight	*0.973*		
	Head width	*0.459*		
	Intercept	**0.006****	**1.186**	**0.430**
	Sex (male)	**<0.001*****	**-2.348**	**0.706**
	Target speed	**<0.001*****	**-1.712**	**0.357**
	Initial head orientation	**<0.001*****	**-1.183**	**0.294**
	Presentation number	**<0.001*****	**0.145**	**0.030**

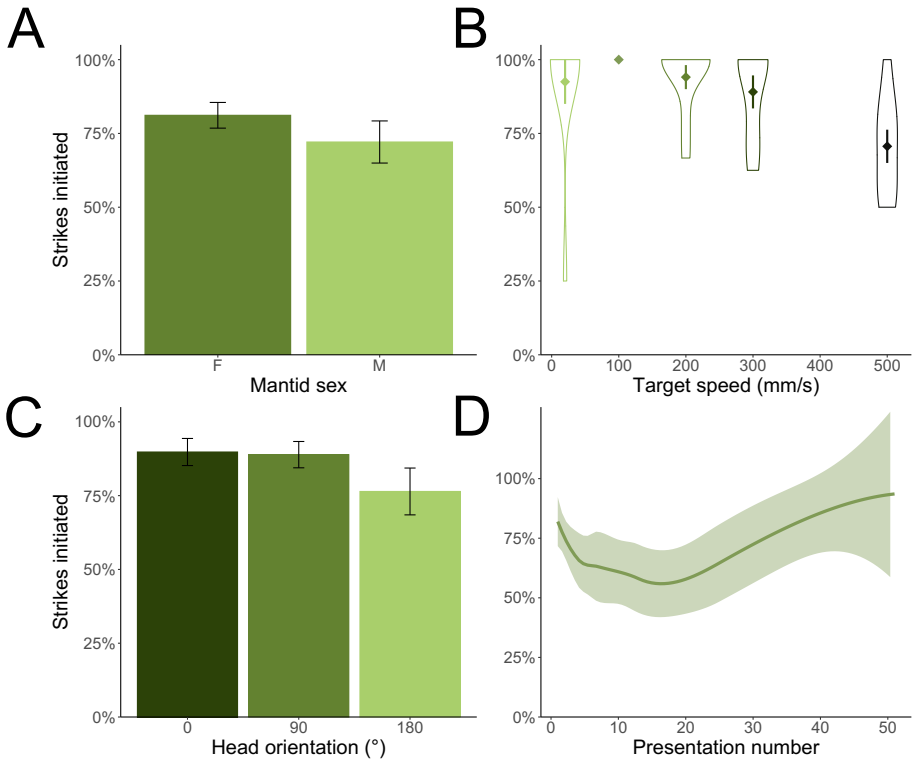

Figure 2.2. Strike initiation is influenced by mantid sex, target speed, initial head orientation, and presentation number. A) Differences in the proportion of initiated strikes in male and female mantids. B) Strike initiation frequency varies with target speed. C) Difference in strike initiation depends on head orientation. D) Percentage of strikes initiated depends on presentation number (data smoothed using a Savitzky-Golay filter). In all panels, bars represent ± standard error of individual mantids and shaded areas represent 95% confidence intervals.

Table 2.2. Simplification of generalised linear models shows that target speed influences strike completion. Rows in bold represent the most parsimonious model with only significant effects. Mantid identity was included as a random effect, with rows in italics indicating inclusion as random coefficients. Significance values: * = $p < 0.05$, ** = $p < 0.01$ *** = $p < 0.001$.

Outcome variable	Predictors	*p* value	Estimate	S.E.
Strike completion	Presentation number	0.760		
	Trial number	0.760		
	Time of the day	0.530		
	Initial head orientation	0.463		
	Temperature	0.406		
	Humidity	0.256		
	Target trajectory distance	0.185		
	Presence of head movement prior to strike	0.078		
	Sex	0.273		
	Weight	*0.169*		
	Head width	*0.159*		
	Intercept	**<0.001*** **	**-0.909**	**0.217**
	Target speed	**<0.001*** **	**-1.55**	**0.227**

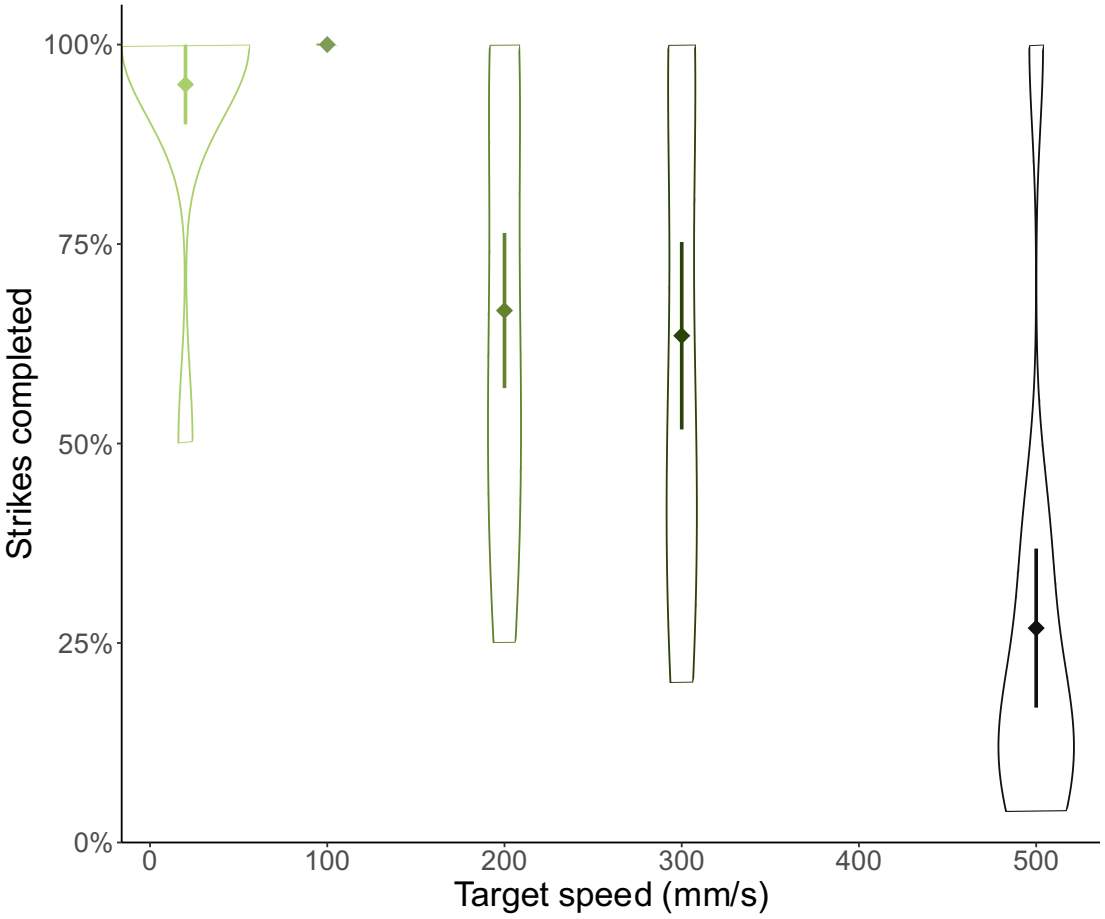

Figure 2.3. The proportion of strikes that are completed depends on the target speed. Bars represent ± standard error.

Table 2.3. Simplification of generalised linear models shows that presentation number, head movement timing, initial head orientation, and target speed influence strike success. Rows in bold represent the most parsimonious model with only significant effects. Mantid identity was included as a random effect, with rows in italics indicating inclusion as random coefficients. Significance values: * = $p < 0.05$, ** = $p < 0.01$ *** = $p < 0.001$.

Outcome variables	Predictors	*p* value	Estimate	S.E.
Strike success	Humidity	0.891		
	Temperature	0.843		
	Target trajectory distance	0.698		
	Trial number	0.429		
	Time of the day	0.241		
	Sex	0.187		
	Intercept	**0.084**	**-21.6**	**12.5**
	Presentation number	**0.015***	**-3.76**	**1.55**
	Presence of head movement prior to strike	**<0.001*****	**51.0**	**11.3**
	Initial head orientation	**<0.001*****	**-30.3**	**7.69**
	Target speed	**<0.001*****	**-84.5**	**18.4**

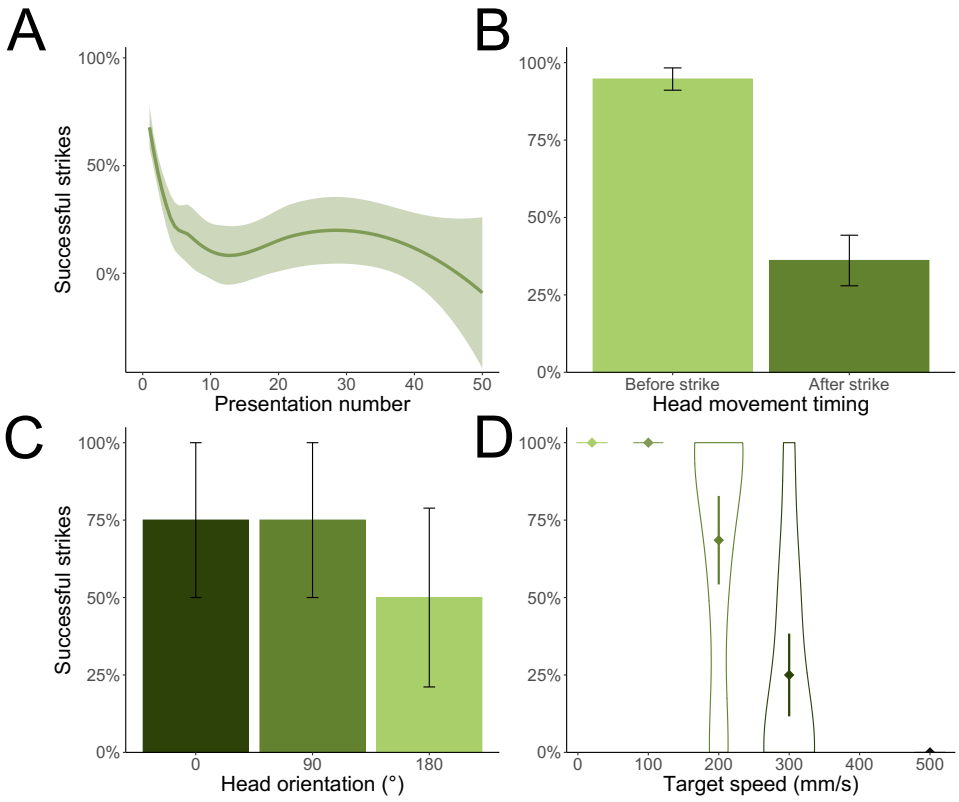

Figure 2.4. Strike success is influenced by presentation number, timing of head movements, initial head orientation, and target speed. A) Percentage of successful strikes depends on presentation number. B) Movement of the head before strike initiation improves success. C) Initial head orientation influences the success of the strike (shown only for prey speed equal to 200 mm/s). D) Strike success depends on target speed. In all panels, bars represent ± standard error of individual mantids and shaded areas represent 95% confidence intervals.

2.3.2. Variables affecting head movements

The timing of head movements, i.e. whether mantids turned their head before or after the strike was initiated, was the only variable that significantly affected the likelihood of strike success but not its initiation. To investigate this further, we first tested what factors affected the likelihood of head movements happening, using generalised linear mixed-effects models (**Table 2.4**). Mantids were less likely to move their head the higher their head orientation angle (**Fig. 2.5A**). Head movements were more likely to happen at higher room temperatures (**Fig. 2.5B**) and less likely to happen at higher prey speeds (**Fig. 2.5C**). Humidity and time of the day did not affect the probability of head movements, and neither did the mantids' sex. The probability of head movement did not vary with either the trial number or the presentation number. Head movements were also unaffected by the distance between the target trajectory and the mantid. Individual mantids' head widths did not affect the likelihood of a head movement, and neither did their individual weights.

Strikes were more likely to be successful if mantids moved their heads prior to strike initiation. We investigated what influenced the timing of head movements, i.e. if they happened before or after strike initiation, using generalised linear mixed-effects models (**Table 2.5**). Female mantids moved their heads before the strike more frequently than male mantids (**Fig. 2.6A**). Mantids were also more likely to move their heads before striking as temperatures increased, although this effect might not be linear, with a possible peak in the likelihood that mantids moved their heads prior to a strike around 30°C (**Fig. 2.6B**). Mantids were more likely to move their heads before the strike the higher the head orientation angle (**Fig. 2.6C**). And finally, mantids were increasingly less likely to move their heads before the strike for higher target speeds (**Fig. 2.6D**). Humidity and time of the day did not affect the likelihood of head movements occurring before the strike. This likelihood did not vary with either trial number or presentation number. The chance of head movements prior to the strike was also unaffected by the distance between the target trajectory and the mantid. The head widths of individual mantids did not affect the likelihood of head movements prior to a strike, and neither did their individual weights.

Overall, head movements were significantly influenced by room temperature, initial head orientation and target speed. These factors affected both the likelihood of head movements occurring and whether mantids moved their head before or after strike initiation. The mantid's sex was the only variable with a significant effect on whether head movements happened before or after strike initiation, but not on the likelihood of head movements happening at all during a target presentation.

Table 2.4. Simplification of generalised linear models shows that initial head orientation, temperature, and target speed influence the presence of head movements. Rows in bold represent the most parsimonious model with only significant effects. Mantid identity was included as a random effect, with rows in italics indicating inclusion as random coefficients. Significance values: * = $p < 0.05$, ** = $p < 0.01$ *** = $p < 0.001$.

Outcome variable	Predictors	*p* value	Estimate	S.E.
Presence of head movements	Trial number	0.839		
	Time of the day	0.520		
	Humidity	0.262		
	Presentation number	0.518		
	Target trajectory distance	0.310		
	Sex	0.099		
	Head width	*0.839*		
	Weight	*0.821*		
	Intercept	**<0.001*** **	**-0.721**	**0.196**
	Initial head orientation	**0.048***	**-0.400**	**0.202**
	Temperature	**<0.001*** **	**0.725**	**0.217**
	Target speed	**<0.001*** **	**-1.28**	**0.194**

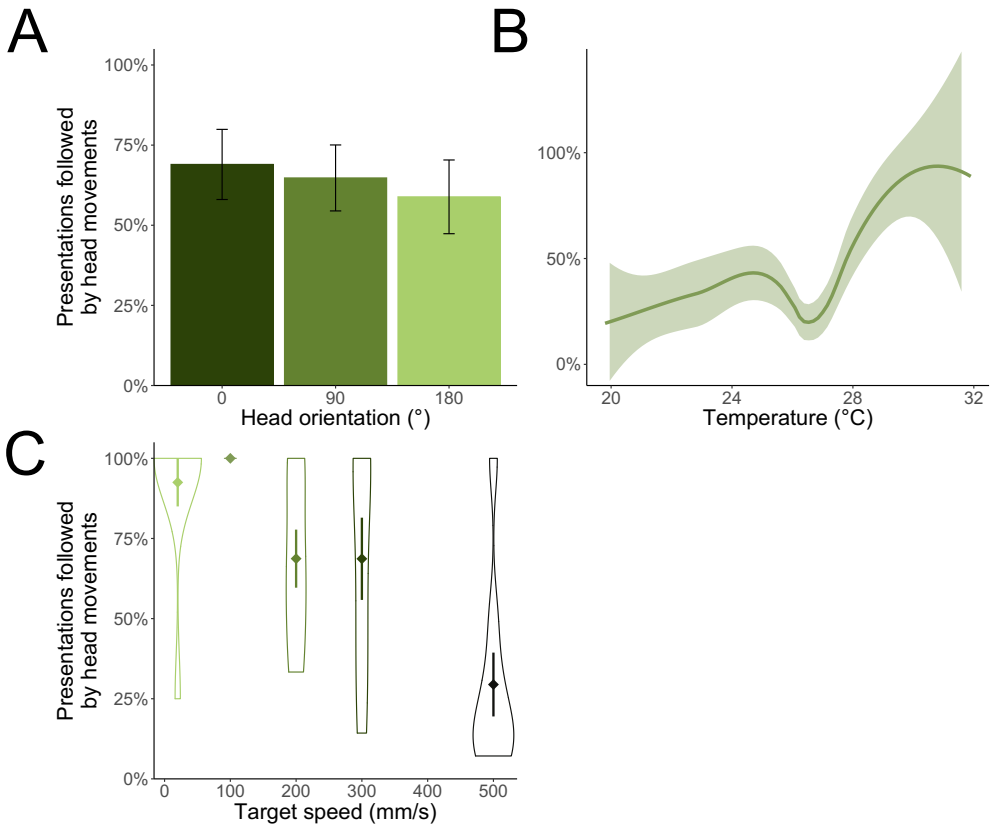

Figure 2.5. The presence of a head movement is influenced by initial head orientation, temperature, and target speed. A) Presence of head movements depends on initial head orientation. B) Temperature influences the presence of head movements. C) The presence of a head movements depends on target speed. In all panels, bars represent ± standard error of individual mantids and shaded areas represent 95% confidence intervals.

Table 2.5. Simplification of generalised linear models shows that sex, temperature, initial head orientation, and target speed influence the timing of head movements. Rows in bold represent the most parsimonious model with only significant effects. Mantid identity was included as a random effect, with rows in italics indicating inclusion as random coefficients. Significance values: * = $p < 0.05$, ** = $p < 0.01$ *** = $p < 0.001$.

Outcome variable	Predictors	*p* value	Estimate	S.E.
Head movement occurrence prior to strike	Time of the day	0.860		
	Trial number	0.817		
	Humidity	0.539		
	Presentation number	0.330		
	Target trajectory distance	0.131		
	Head width	*0.413*		
	Weight	*0.190*		
	Intercept	**0.142**	**-0.621**	**0.423**
	Sex (male)	**0.005****	**-2.26**	**0.810**
	Temperature	**0.003****	**1.18**	**0.392**
	Initial head orientation	**<0.001*****	**1.36**	**0.410**
	Target speed	**<0.001*****	**-2.00**	**0.469**

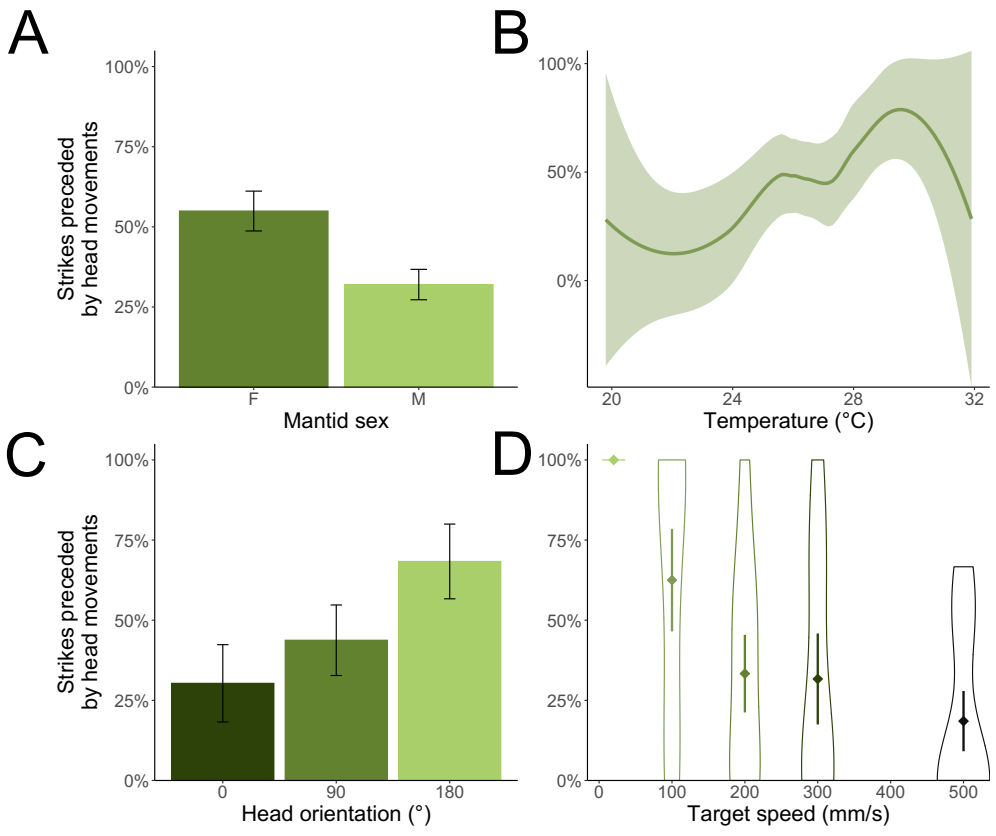

Figure 2.6. The likelihood that head movements happened before a strike is influenced by mantid sex, temperature, initial head orientation, and target speed. A) Differences in head movement timing in male and female mantids. B) Temperature influences head movement timing. C) Head movement timing depends on initial head orientation. D) Head movement timing varies with target speed. In all panels, bars represent ± standard error of individual mantids and shaded areas represent 95% confidence intervals.

2.4. Discussion

African mantids (*S. lineola*) reliably attacked targets presented to them in our experimental setup. We aimed to determine the impact of head orientation on the initiation, abandonment, and success of strikes. Using a strategy of orientating the head by presenting a target manually prior to the start of the experiments, we were able to test the impact of head orientation at the time of stimulus presentation. Head orientation affected head movements as well as strike initiation and success, but not strike abandonment. We also varied the speed of the prey presented to the mantids, to see how it affected the mantids' performance. Prey speed affected the initiation, completion, and success of the strike, as well as head movements towards prey. The mantids' sex affected strike initiation and whether head movements happened before or after strike initiation. Temperature influenced the presence of head movements and whether they happened before or after initiating a strike, the latter variable in turn determining strike success. The distance between mantid and target trajectory, the mantid's weight, its head width, and the trial number had no effect on the variables considered of strikes and head movements.

2.4.1. Experimental considerations

Mantids could be filmed via mirrors from behind, so not to disrupt their strike kinematics. The double-periscope mirror arrangement presented here produced two separate views which we could use to extract behavioural data, as done in other prototypes (de Margerie et al., 2015). We show that this setup can also be used for tracking body parts in the two views and then triangulating their three-dimensional positions, using easy to obtain calibration videos. This double-periscope arrangement can produce three-dimensional data using only one camera, hence avoiding synchronisation issues, thereby greatly reducing setup costs. Reliable measures could be extracted from both front-surfaced and back-surfaced mirrors, also reducing the cost of the mirrors themselves. Our setup is also light and easily portable which, in conjunction with using portable cameras, makes it suitable for field experiments, as well as laboratory experiments.

We aimed to present mantids with the most naturalistic conditions possible. Therefore, we tested mantids with constant linear prey speed, contrary to constant angular prey speeds used in previous literature (Rossel, 1980). We also presented mantids with three-dimensional targets, as opposed to projected two-dimensional stimuli (Yamawaki, 2000a). By testing mantids with naturalistic conditions, we could evaluate environmental and internal factors affecting strike and head movements. However, a full picture of the role of head tracking in praying mantids can only be painted by integrating evidence gathered in different experimental conditions.

2.4.2. Prey speed

Target speed affected every aspect we considered of strike kinematics and head movements. Although prey speed has already been shown to affect the structure of the strike of praying mantids (Rossoni and Niven, 2020), here we show that slower prey speeds are more likely to trigger head movements, and these head movements are more likely to happen prior to a strike in response to slower compared to faster prey. Slower prey speeds also increase the likelihood of strike initiation and, crucially, the success of a strike. Prey speed is also the only variable we found that affects the decision to abandon or complete a strike. That strikes can be abandoned has been documented (Nityananda et al., 2016a; Rossoni and Niven, 2020), but our evidence strictly links strike abandonment to prey speed. The slowest prey speed we used (20 mm/s) led to slightly fewer strikes initiated, more strike abandonments, and fewer head movements than the second-slowest prey speed (100 mm/s).

Although our results indicate that mantids preferentially strike slower prey, but this preference peaks around 100 mm/s, others indicate that mantids strike more frequently in response to faster prey over 300 mm/s (Prete et al., 1993). A few methodological differences exist with the experiments reporting preferential hunting of faster prey, including using a primarily looming stimulus and a flat target. In response to this kind of prey, mantids were indeed more likely to strike at prey of higher speed, but also more likely to stalk prey when moving slowly. It is not however clear how the two behavioural responses could interact and

whether increased stalking could be linked to an increased chance of striking. Further research is needed to bridge the gap between our and existing findings, and to clarify the impact of target trajectory and three-dimensionality on speed preference.

2.4.3. Environmental effects

While humidity had no effect on any dependent variables considered, temperature affected both the likelihood and the timing of head movements, although it had no effect on strike initiation, completion, or success. Although temperature influences how insect muscles respond to contraction frequencies (Machin et al., 1962) and neuronal and synaptic conductances (Abrams and Pearson, 1982; Alonso and Marder, 2020; Burrows, 1989; Heitler et al., 1977; Tang et al., 2010), further experimentation is needed to pinpoint whether the effect of temperature on head movements is mechanical, physiological, or behavioural. Temperature does not affect jumping performance of jumping insects (Heinrich, 1993; Snelling et al., 2013), but it has been shown to affect their inclination to engage in a jump (Maeno et al., 2019). The temperature independence of the strike reported here suggests that mantids may maintain foraging over a range of temperatures. However, it is worth highlighting the relatively small range of temperatures considered here (20-32°C). Extending this range might highlight temperature dependencies of the strike missed in our analysis.

A final environmental factor considered was the time of the day, which had no effect on either head or strike kinematics. African mantids might engage in locomotory activity differently during the day but their movements when in close range of prey do not seem to follow circadian patterns.

2.4.4. Repeated presentations and learning

The likelihood of African praying mantids to initiate a strike fell in response to repeated presentations up to 20 successive presentations, as previously described (Prete et al., 1993). However, our results show that beyond 20 presentations, the likelihood that mantids initiated a strike rose again. This might be an adaptive trait in two possible explanatory frames. On the one hand, it could be likely for prey to

be restricted within certain areas, as they might be territorial or drawn to an attractive stimulus in that area. On the other hand, the presence of a potential target might indicate that other, similar targets could be in the area, attracted by the same feature. The increased likelihood of praying mantids to strike at prey after repeated presentations might be advantageous in both hypothetical scenarios. The likelihood of striking prey was not affected by learning to strike or avoid our target between strikes. Mantids reduce strike likelihood after repeated strike attempts (Maldonado, 1972; Rilling et al., 1959), but a single strike instance, as executed in our experiments, was not enough to induce learning.

2.4.5. Mantids' weight and sex

We found that body weight had no effect on the likelihood to strike at prey or to engage in head movements. Previous literature found that satiation levels affect the hunting behaviour of praying mantids in mixed ways. Increased satiation seems to clearly decrease the locomotory response of praying mantids to prey, resulting in decreased rate of stalking and decreased distance at which stalking is initiated (Bertsch et al., 2019; Prete et al., 1993). However, the distance at which strikes are initiated is not affected by satiation levels (Prete et al., 1993). It is not therefore clear whether the decreased strike likelihood also observed (Bertsch et al., 2019; Prete et al., 2002) is an effect of reduced stalking. Our experiments seem to answer this question; by ensuring that targets were within the mantids' reach before all presentations, we controlled for the effect of stalking on the likelihood of strike initiation, which was not affected by the mantids' body weight.

The sex of mantids affected the likelihood to initiate a strike. Just like most insects, male mantids are smaller than females and famously subject to sexual cannibalism (Birkhead et al., 1988; Kynaston et al., 1994; Lawrence, 1992). By striking less, male mantids might reduce the chance of catching the attention of predators, including female conspecifics. Females mantids are known to predate more aggressively than males, especially in cannibalistic species (Fisher et al., 2020). Females produce more costly gametes than males, which easily explains their increased likelihood to strike. Increased energetic demands of females has resulted in some insects in males providing nourishment to females prior to

mating (Gwynne, 2008). Males were also less likely to move their heads prior to a strike than females. This could again be due to the male tendency to reduce movements, or to inferior visual abilities determined by their smaller size. Head width was however not a significant factor in any of the models considered, although this might be an important effect when considering mantids in a range of developmental phases.

2.4.6. Effects of head movements

An important question considered by this chapter is what role head movements play in the strike. Mantids can correct visual tracking of prey on a uniform background by performing fast saccades in between smooth tracking (Rossel, 1980), however, they produce head rotations up to 400 °/s (Lea and Mueller, 1977). In this chapter, we tested their response to prey speed of angular velocity up to approximately 1900 °/s, which they still tried to strike. Head rotations cannot match target rotation at these speeds. In fact, head rotations were less likely to happen, and tended to happen after rather than before a strike, in response to faster prey speed. By doing so, praying mantids might reduce the motion blur caused by a head movement, which would not be able to match prey speed anyway. Mantids have been shown to respond to specific ratios of angular size and speed of their prey (Nityananda et al., 2016b). Whether they might use this ratio to estimate prey absolute size at high prey speeds, as found in other insect predators (Lin and Leonardo, 2017; Wardill et al., 2015), remains an open question. Even if this was the case, successful strikes heavily relied on head movements prior to strike initiation. Mantids use their large frontal foveas (Barros-Pita and Maldonado, 1970; Horridge and Duelli, 1979; Rossel, 1979) to triangulate prey position (Rossel, 1983). It is therefore not surprising that tracking targets with their eyes prior to strike initiation increases strike success. However, a more precise reconstruction of the dynamics of mantids' head movements, including the overall trajectory, timing, and following behavioural output would be beneficial to understand the role that mantids' foveas have during predatory behaviour.

2.5. Conclusions

Overall, we present a cheap, versatile, and robust way to extract three-dimensional behavioural data using a single camera. We show that the praying mantid's strike and head movements can be affected by a range of environmental and internal factors. The mantid's sex, head orientation, and the timing of its head movements can affect the likelihood to strike and the strike success. External factors like prey speed and the number of stimulus presentation can also affect strike performance. Although temperature can influence the mantid's head movements, strikes seem temperature independent.

2.6. Supplementary Information

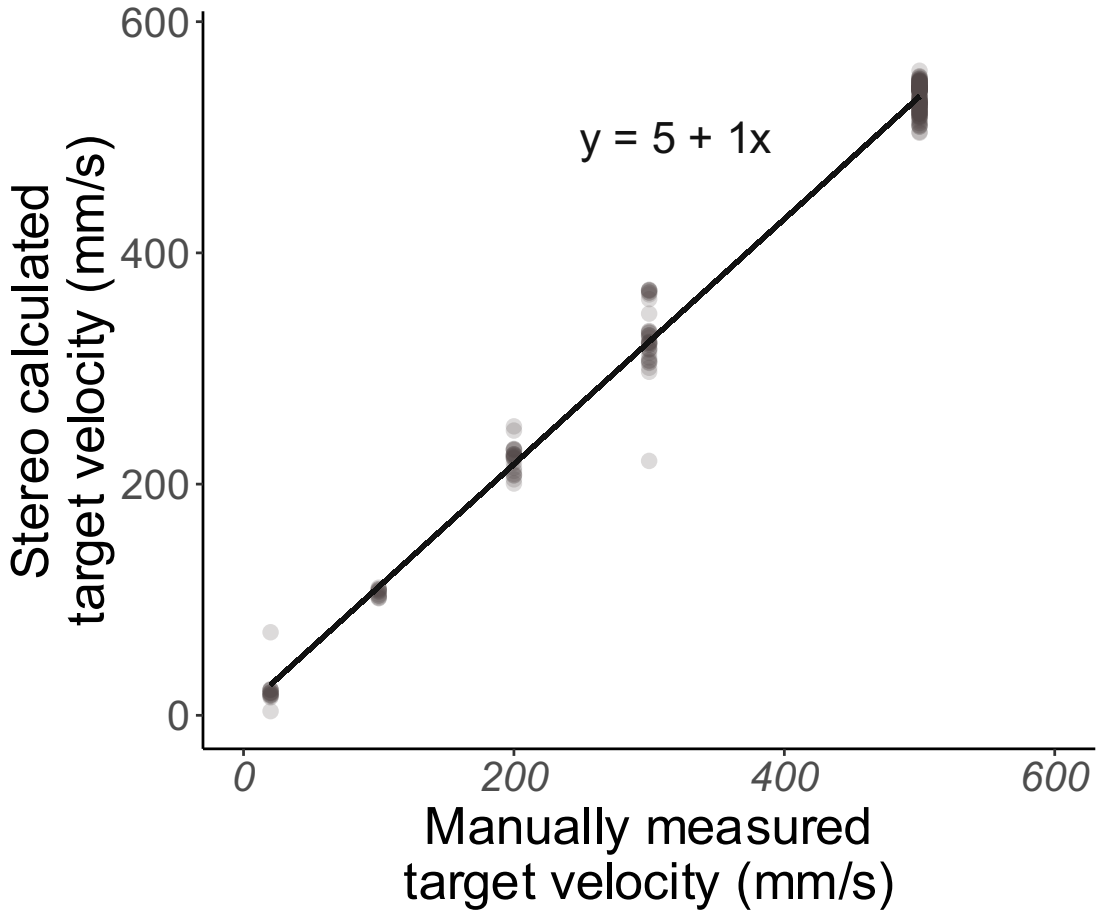

Figure 2.S1. Target velocity calculated via stereo-view triangulation, plotted against manually measured target velocity.

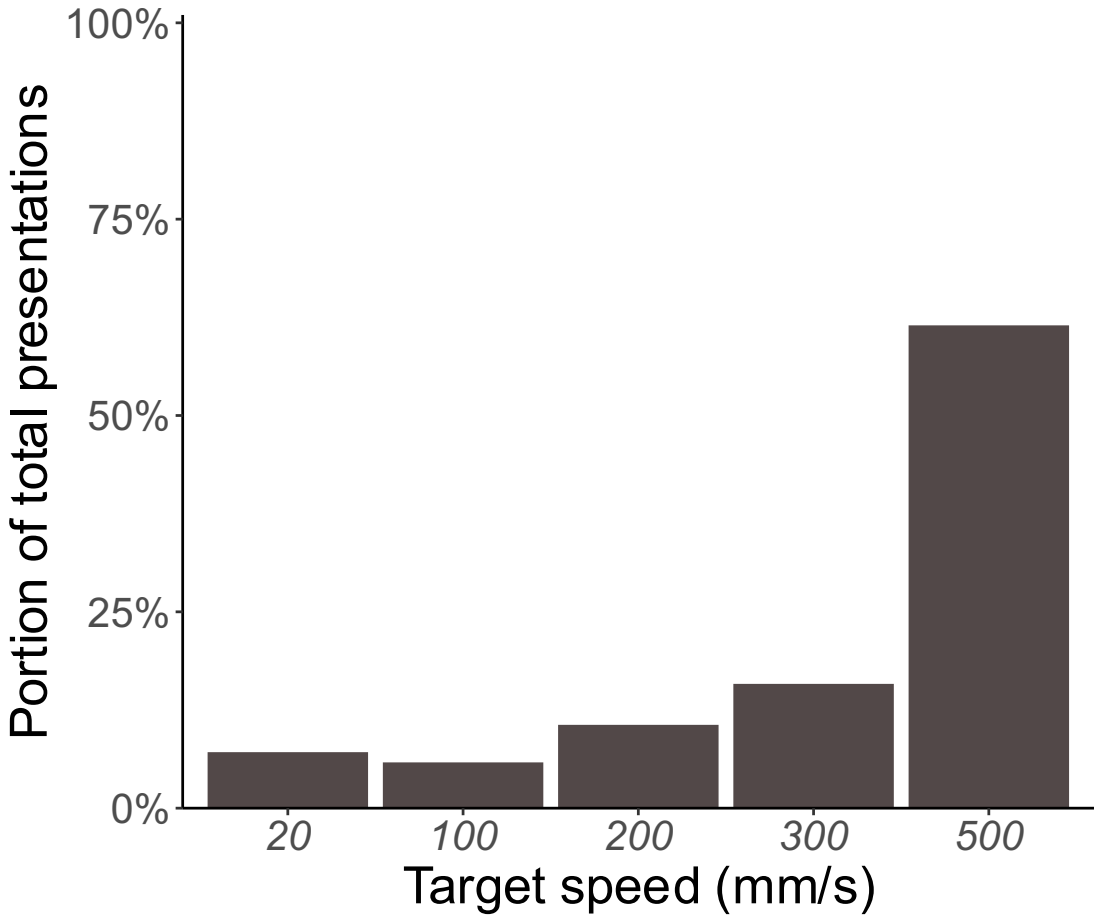

Figure 2.S2. Percentage of stimulus presentations for each target speed.

3. Aerial Predation by Motion Parallax in an Insect

3.1. Introduction

A predator's success is often dependent on its ability to estimate the size of potential prey and its distance from it. This is particularly important for ambush predators, who rely on a surprise element and usually predate upon still prey in close proximity. To obtain such information, many ambush predators use the binocularity afforded by the overlapping fields of view of their frontal eyes (Cartmill, 1974; Nityananda and Read, 2017), an ability called stereopsis. Because stereopsis relies on the visual disparity between the two eyes, the higher the distance between the eyes and the higher their spatial resolution, the more accurate the distance calculation is and the longer its effective range (Burkhardt et al., 1973). Thus, due to their small heads and their low-resolution compound eyes, insects have a very limited stereopsis range. Nevertheless, praying mantids use stereopsis (Nityananda et al., 2016a; Rossel, 1983) and damselflies rely on binocular vision (Horridge, 1978; Supple et al., 2020) when assessing prey. By contrast, predators that chase moving prey can use their prey's movement to infer its size. Closer prey will look bigger, subtending a larger size on the predator’s retina, and appear to move faster, moving at a higher angular velocity across the predator’s retina, than prey far away. Indeed, the correlation between the prey's angular size to its angular velocity predicts the likelihood of an attack in dragonflies (Lin and Leonardo, 2017) and killer flies (Wardill et al., 2015).

Another way to obtain 3D information is for an animal to correlate its own movement to the perceived displacement of objects in its visual field, a phenomenon known as optic flow (Gibson, 1950). For optic flow to be reliable, the target must be static, or moving in a predictable trajectory. For a given predator’s linear displacement, nearby objects will appear to move further and faster than distant objects. Animals can exploit this principle by performing translational

movements with the only intent of generating optic flow for 3D calculations. By correlating the apparent movement, or velocity, of a nearby object to the movement, or velocity, of their own head, animals can compute 3D information (Kral, 2003), which is known as motion parallax. The use of motion parallax to calculate distance is very widespread in the animal kingdom, from humans to insects (Collett, 1978; Davies and Green, 1988; Ellard et al., 1984; Goulet et al., 1981; Poteser and Kral, 1995; Rogers and Graham, 1979; Srinivasan et al., 1989; van der Willigen et al., 2002). Insect motion parallax has been studied mostly in relation to their jumping behaviour. Before jumping, some insects such as locusts (Collett, 1978; Wallace, 1959), mantids (Poteser and Kral, 1995) and crickets (Goulet et al., 1981) perform side-to-side movements called peering. The angular velocity of their target on their visual field is correlated to their jump velocity (Collett and Paterson, 1991; Sobel, 1990), which in turn determines the distance travelled to the target. Although flying insects have been less studied in relation to motion parallax, evidence suggests that bees and wasps can use motion parallax to assess the width of a gap before going through it (Ravi et al., 2019), to select flowers, and use landmarks to navigate (Lehrer and Collett, 1994; Lehrer et al., 1988; Srinivasan et al., 1989; Zeil, 1993), while flies can use motion parallax to adjust their flight (Ruiz and Theobald, 2020). Motion parallax can be effective over longer distances than stereopsis (Poteser and Kral, 1995), it has a similar sensitivity threshold (Rogers and Graham, 1982), and could be as effective against prey camouflage (Galloway et al., 2020). However, to our knowledge, no case has been documented of predators using motion parallax to assess prey. A notable exception are anecdotal reports of praying mantids performing small-amplitude peering movements in response to some prey stimuli (Yamawaki, 2000b; Yamawaki, 2003), though this behaviour does not seem to be used for range estimation and therefore lacks a clear function. This is likely because the movements required for motion parallax might give away the presence of a predator, allowing the prey to escape.

Gleaning is a predatory strategy which involves plucking prey from a substrate. Although the term is mainly used for birds, some insects, like the damselfly (Corbet, 1999; von Reyn et al., 2014) are also capable of this. Grass flies of the

family Asilidae, hereafter called darting robber flies to avoid confusion with the grass flies of the Chloropidae family (Sabrosky, 1989), are also gleaning predators. They are thought to be the most basal lineage of the robber fly family (Bybee et al., 2004) and have many striking differences with other robber flies (Martin, 1968): they populate the shaded undergrowth, cluttered with grass and bushes, where they attack a variety of static prey (Martin, 1968; Newkirk, 1963). Despite the striking similarity in body morphology between darting robber flies and other gleaners (**Fig. 3.1A-B**), their eyes are very unique. Darting robber flies have eyes very close to the midline of their small head, which also contrasts with other robber fly species (Wardill et al., 2017). Instead, the damselfly's eyes are on the side of its wide head (**Fig. 3.1C-D**), as expected for a predator using binocular cues to capture prey (Cartmill, 1974; Nityananda and Read, 2017; Supple et al., 2020).

The striking difference in eye morphology between darting robber flies and damselflies indicate that their gleaning strategies could also differ substantially. To investigate this, we selected a darting robber fly, *Psilonyx annulatus*, and show that it attacks similar prey than another gleaner, the damselfly *Ischnura posita*. The attacks of darting robber flies were compared to the attacks of damselflies, showing more lateral movement whilst the prey was assessed. We show that darting robber flies use prey size, not their angular size, to determine the distance at which to attack prey, attacking from further away and moving more when attacking larger prey. We show that prey is outside the stereopsis range of the darting robber fly, suggesting these animals use motion parallax to assess prey before attacking.

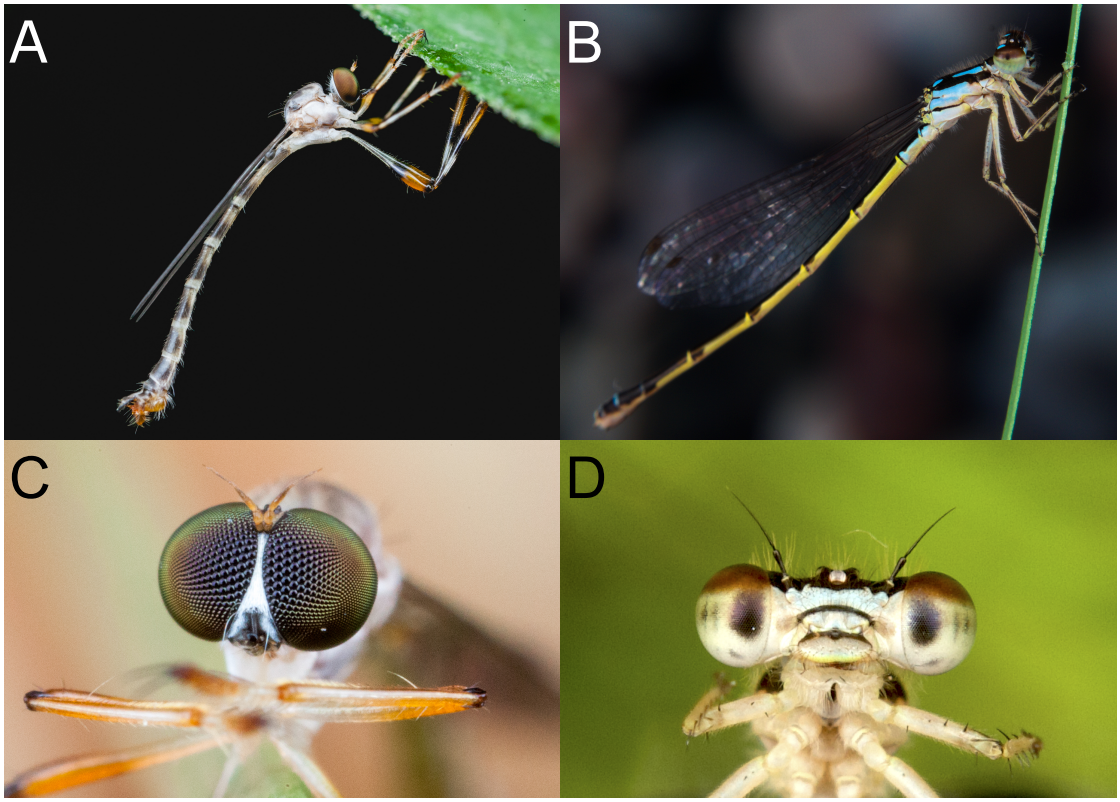

Figure 3.1 Darting robber flies evolved characteristic eye morphology compared to other gleaning predators, despite strikingly similar bodies. A) A side picture of a live darting robber fly (*Psilonyx annulatus*). B) A side picture of a live fragile forktail damselfly (*Ischnura posita*). C) A frontal picture of the eyes of a live darting robber fly. D) A frontal picture of the eyes of a live fragile forktail damselfly.

3.2. Materials and Methods

3.2.1. Animals

Darting robber flies (*Psilonyx annulatus*) (Say, 1859) were collected from the wild in regional parks of York, PA (U.S.A.), with research permits obtained from local authorities. Collected animals, both males and females, were kept in an indoor tent at 40-50% humidity and 20-25°C temperature, and fed live fruit flies (*Drosophila melanogaster*).

Fragile forktail damselflies (*Ischnura posita*) (Hagen, 1861) were acquired from an animal supplier (Carolina Biological Supply Company, Burlington, NC, U.S.A.) in nymph from. Nymphs were kept in pond water and fed live blackworms (*Lumbriculus variegatus*) until their final moult. Adult damselflies, both males and females, were kept in an indoor tent at 65-70% humidity and 20-30°C temperature, and fed live fruit flies.

3.2.2. Indoor testing

The darting robber flies were collectively transferred to a transparent 300 x 195 x 205 mm tank, placed vertically on a table. The arena was illuminated with standard ceiling room lights (60Hz current) directly above and was placed in front of a white board, illuminated with infrared light, to increase the contrast of the flies in the camera without affecting ambient light. In these conditions, darting robber flies were recorded responding to two types of stimuli. To test responses to natural prey, live fruit flies of different species and sizes (*Drosophila melanogaster, Drosophila affinis,* or *Drosophila virilis*) were released in the arena. To test responses to artificial prey, we placed a display outside the transparent wall of the arena. The display (Apple Inc., Cupertino, CA, U.S.A.) had dimensions 180 x 288 mm (1600 x 2560 px) and a refresh rate of 60 Hz. The stimuli were manually created using the GNU Image Manipulator Program (version 2.8.22, The GIMP Development Team).

The fragile forktail damselflies were collectively transferred to either a 300 x 195 x 205 mm tank or a 1 x 1 x 1 m arena. The arena was illuminated with ceiling

room lights directly above. The damselflies hunted live fruit flies (*Drosophila melanogaster*) present in the arena.

3.2.3. Videography and digitisation

We recorded videos with a resolution of 2048 x 2048 pixels at a rate of 1000 frames per second using two time-synced SA2 or WX100 Photron cameras (Photron Ltd., Tokyo, Japan). The system was calibrated using an altered version of the J.Y. Boguet's Laboratory's MATLAB toolbox (Caltech, http://www.vision.caltech.edu/bouguetj/calib_doc/), running on MATLAB R2014a (version 8.3, MathWorks Inc., Natick, MA, U.S.A.).

The movements of the thorax and abdomen of the darting robber flies and fragile forktail damselflies were digitised offline using supervised automatic tracking software (Wardill et al., 2017), as well as the body position of their target. The digitised coordinates for each camera were then analysed by a stereo software to reconstruct the three-dimensional trajectory of the object of interest. Both the tracking and the reconstruction were run with MATLAB 2012a (version 7.14).

The 3-D coordinates were then smoothed using a Savitzky-Golay filter (Savitzky and Golay, 1964) (polynomial order = 3, window size = between 101 and 251, manually selected according to trajectory length and noise); the third dimension, or depth, was smoothed twice with the same filter, because of the additional noise due the stereo calculations. The filter was applied using MATLAB R2018b (version 9.5) and was preferred to other smoothing algorithms (Dey and Krishnaprasad, 2012) because of its considerable speed.

3.2.4. Kinematic analysis

All kinematic analysis was run offline on smoothed trajectories, using MATLAB 2019b (version 9.7). The flights were trimmed so that they started when the body angle with the prey was less than 20° (**Fig. 3.S1**) and ended with the shortest distance between the target and the predator (**Fig. 3.2A**). The position of the target was taken as the median value for each axis to minimise the impact of errors in the digitisation.

We calculated the fly's velocity as the derivative over time of its position, and then smoothed this vector with a Savitzky-Golay filter (polynomial order = 3, window size = 101). The fly's acceleration was taken as the derivative over time of the velocity, smoothed again with the same Savitzky-Golay filter parameters. We found the minima in the velocity and considered the last minimum of the flight as t = 0, the time point determining the end of the assessment phase and the beginning of the attack phase (**Fig. 3.2B**).

The straightness index of a phase was calculated as the ratio between a) the distance between the beginning and the end of the phase, and b) the path length travelled between the two timepoints (Benhamou, 2004). To calculate the movement range of the assessments, we first calculated the central position of the flight portion as the mean value during the assessment of each axis. Then, we calculated the distance of each flight timepoint from such centre point and used the standard deviation of this distance as an estimate of flight movement range.

3.2.5. Microscopy imaging

Protocols for darting robber fly head fixation and imaging were adapted from previous imaging work on other robber flies (Wardill et al., 2017). Summarising, we dissected and fixed whole heads 48 hours in a 4% paraformaldehyde (PFA) and phosphate-buffered saline (PBS) solution, at room temperature. After three PBS rinses, the heads were bleached for 7 days in 35% hydrogen peroxide to clear the cuticle and eyes from screening pigments (Smolla et al., 2014), and rinsed again in PBS. We then placed heads on ascending and subsequently descending solutions of PBS-diluted ethanol (30%, 50%, 70%, 80%, 90%, 95%, and ethanol absolute). Finally, we placed heads in an ascending dilution series of 2,2'-thiodiethanol (TDE) and PBS (from 10% to 90% TDE in steps of 10, and a final concentration of 97% TDE solution) (Gonzalez-Bellido and Wardill, 2012). We then imaged the whole heads with an oil-immersion objective (Olympus XLSLPLN25XGMP, Tokyo, Japan), using 97% TDE solution as mounting medium. A Bruker two-photon microscope (Billerica, MA, U.S.A.) was used to image tissue autofluorescence to 810 nm light, produced by a Spectra-Physics Insight® DS+ TM laser (Santa Clara, CA, U.S.A.). Images voxel resolution was 0.4 μm^3.

Eye cross-sections for TEM imaging were obtained by preparing specimens as done in previous literature (Gonzalez-Bellido et al., 2011; Meinertzhagen, 1996; Meinertzhagen and O'Neil, 1991). Briefly, heads were fixed in a modified Karnovsky fixative, containing 2.5% glutaraldehyde and 2.5% PFA aqueous solutions diluted in cacodylate buffer (Shaw et al., 1989). Heads were then rinsed in PBS three times. Samples were left in 2% osmium and 0.2M cacodylate buffer solutions for two hours and dehydrated in a 30-minute step alcohol series (50%, 70%, 80%, 90%, 95%, and two ethanol absolute immersions), followed by a 30-minute immersion in acetonitrile absolute. We then placed the heads in a 50% mix of acetonitrile and Epon resin (Poly/Bed 812, PolySciences, Warrington, PA, U.S.A.) and left, agitated, to evaporate overnight. Following this, we placed the heads in Epon resin and left agitated, overnight. Finally, we embedded the heads in fresh resin left at 60°C overnight. We sectioned the embedded heads using cross-sections centred on the fovea of one of the two eyes. The sections were then transferred over copper disks, coated with 2% Formvar (Sigma-Aldrich, St Louis, MO, U.S.A.), and stained with 3% uranyl acetate and Renolds lead citrate. The grids were imaged using a JEOL JEM-1400Plus 120kV transmission electron microscope (TEM).

3.2.6. Visual parameter estimation

Visual acuity parameter estimation of the darting robber flies was based on previous literature on fruit flies and robber flies (Stavenga, 2003; Wardill et al., 2017). Using ImageJ (Meijering, 2008), we rotated the two-photon scans on all axes using the head's midline and so that the robber fly's largest two lenses had heir base parallel to the head's cross section. We considered the 13 largest lenses for each eye as that eye's fovea. For each lens, we calculated the fly's lens diameter (d_{lens}) by averaging the three diagonals of the hexagonal crystalline cone under each lens (Wardill et al., 2017). We then resliced the scan to have a coronal view of the retina. For each lens, we considered a coronal section cutting that lens in half, to calculate the optical features of the lens (Stavenga, 2003). As the lens had a flat proximal surface, we fitted a circle on the outer surface of each lens and extracted the radius (r).

Using the radius of each lens's outer surface (r), we calculated the lens power (P) as:

$$P = \frac{(n_{lens} - n_{air})}{r} \qquad \text{Equation 3.1}$$

where n_{air} is the refractive index of air, 1.00, and n_{lens} is the refractive index of the lens, assumed to be 1.43 (Stavenga et al., 1990). Using the lens power (Eq. 3.1), we calculated the image-space focal length (f') as:

$$f' = n_{image}/P \qquad \text{Equation 3.2}$$

with an image space refractive index (n_{image}) equal to 1.34 (Seitz, 1968). The object-space focal length (f) was similarly calculated as:

$$f = n_{air}/P \qquad \text{Equation 3.3}$$

Using the object-space focal length (Eq. 3.3), we calculated the lens's F-number:

$$F = f/d_{lens} \qquad \text{Equation 3.4}$$

where d_{lens} is the lens diameter extracted from the two-photon stack.

For each ommatidium, we approximated the optimal distance of the rhabdomere from the back of the lens, to compare it with the actual distance of the rhabdomere tip from the lens. First, we measured the thickness of the lens (t_{lens}) and used it to calculate the distance of the image space principal point from the front surface of the lens (H'):

$$H' = t_{lens} \cdot (1 - \frac{n_{image} \cdot P}{n_{lens} \cdot P}) \qquad \text{Equation 3.5}$$

We then used this distance (Eq. 3.5) to calculate the position of the focal plane from the proximal surface of the lens, which is where rhabdomere tips ought to be located (x_{rh}):

$$x_{rh} = f' - (t_{lens} - H') \qquad \text{Equation 3.6}$$

We compared this measure to the actual position of the rhabdomere tip, measured using the two-photon scans, to validate our approximations.

Using the acquired transmission electron micrographs of the photoreceptor tip (Wijngaard and Stavenga, 1975), we fitted ellipses around each rhabdomere of the ommatidia in the fovea. We averaged the major and minor axes of the ellipse and used this as a measure of photoreceptor diameter (d_{photo}). We then approximated the acceptance angle (Stavenga, 1979) as:

$$\Delta\rho = d_{photo}/f \qquad \text{Equation 3.7}$$

Then, we used the coordinates of the centroids of the fitted ellipse to calculate the average distance between photoreceptors R7 and all surrounding photoreceptors (x_{photo}), excluding photoreceptor R3 as the corresponding rhabdomere is not neighbouring (Stavenga, 1975). We used these measures to estimate the interommatidial angle ($\Delta\Phi$) (Stavenga, 2003), which is approximately 20% smaller than the interphotoreceptor angle (Pick, 1977):

$$\Delta\Phi = \frac{x_{photo}}{f} - 20\% \qquad \text{Equation 3.8}$$

Finally, we measured the distance between the biggest lenses on the right and left eye (x_{fovea}) to calculate the flies' stereopsis range (E_∞) (Burkhardt et al., 1973):

$$E_\infty = \frac{x_{fovea}}{2\tan(\Delta\Phi/2)} \qquad \text{Equation 3.9}$$

3.2.7. Data analysis and statistics

Statistical tests were run on R studio software, version 1.2.5001, and R software, version 3.6.1 (R Core Team, 2017). In this chapter, mean ± standard error ($m \pm SE$) are used as descriptive statistics, unless data is not normal, in which case the median and interquartile range (med, IQR) are used instead. The interquartile range was calculated using the basic package. Means, medians and standard deviations were calculated using the *pastecs* package, as was data normality testing using the Shapiro-Wilk test. Variance homogeneity was tested using the Levene's test, within the *car* package. Significance value (p) was 0.05 for all tests, except where p values were adjusted.

To test if a value was part of a non-normal data distribution, we used a one-sample Wilcoxon signed rank test in the *stats* package. For comparisons between two groups with normally distributed data and homogeneous variance between the groups, we used a two-sample Student's *t*-test, also in the *stats* package. If the data was non-normally distributed or if the variance was heterogeneous, we used a Wilcoxon rank sum test in the *stats* package. For comparisons between multiple groups with normally distributed data and homogeneous variance amongst the groups, we used the Analysis of Variance (ANOVA) in the *stats* package. To test for linear trends in ordinal data, we used trend analysis contrasts based on a 1-degree

polynomial, in the *stats* package. If data was not normally distributed or the variance was heterogeneous, we used a Kruskal-Wallis test in the *stats* package. To test for linear trends in ordinal data, we used a Jonckheere-Terpstra test in the *DescTools* package. Correlations between normally distributed variables were tested using a Pearson's *r* test in the *Hmisc* package. Correlations between not normally distributed data were tested using a Spearman's *r* test, also in the *Hmisc* package.

3.3. Results

3.3.1. The attack strategies of damselflies and darting robber flies show marked differences when assessing prey

Both darting robber flies (*P. annulatus*, *n* = 16 flights) and fragile forktail damselflies (*I. posita, n* = 14 flights) hunted static fruit flies in our arena by orienting their bodies towards the prey once it was detected (robber fly: **Movie 3.M1,** damselfly: **Movie 3.M2**). The start of the behavioural sequence was marked when the angle between the predator's body and the prey, i.e. the angle described by the prey, the predator's abdomen, and its head, first fell below 20° (**Fig. 3.S1**). The distance from the prey at this point was not significantly different between the two predators (darting robber flies: *med* = 53.9 mm, *IQR* = 22.3; fragile forktail damselflies: *med* = 55.9 mm, *IQR* = 36.7; Wilcoxon rank sum test, *W* = 130, *p* = 0.467, **Fig. 3.2A**). Both darting robber flies and damselflies showed a consistent velocity pattern across their trajectories, which was used to divide the attack of both predators in two phases (**Fig. 3.2B-F**). In the first phase, which we called the *assessment*, both species maintained a lower velocity, with their body oriented towards their prey. In the second phase, which we called the *attack*, the flies rapidly accelerated towards the target, capturing it with their legs and pulling it away for consumption (**Movies 3.M1, 3.M2**).

Although the overall structure of the predatory behavioural sequence was similar between the two groups, during the assessment phase we found group-specific hallmarks (**Figs. 3.2G-H, 3.S2**). When compared to damselflies, the robber fly's assessment phase had *i)* longer duration (robber flies: *med* = 1105 ms, *IQR* =

647; damselflies: *med* = 292 ms, *IQR* = 360; Wilcoxon rank sum test, $W = 15$, $p < 0.001$) and *ii)* lower velocity (robber flies: 0.056 ± 0.004 m s^{-1}; damselflies: 0.139 ± 0.015 m s^{-1}, *m* ± *SE*; Wilcoxon rank sum test, $W = 215$, $p < 0.001$). In addition, the flight path during the assessment phase appeared more convoluted in darting robber flies than in damselflies. To quantify this, we calculated the straightness index for both predators; straightness values closer to 0 indicated more tortuous trajectories. The assessment flight paths of robber flies were significantly more tortuous than that of damselflies (robber flies: *med* = 0.39, *IQR* = 0.24; damselflies: *med* = 0.75, *IQR* = 0.26; Wilcoxon rank sum test, $W = 185$, $p = 0.003$). The presence of such tortuous assessments was not always followed by an attack. Darting robber flies were seen assessing targets such as conspecifics and flat pieces of paper without launching an attack towards them (**Fig. 3.S3, Movie 3.M3**). This suggests that the darting robber flies' convoluted assessments may play an active role in evaluating possible targets. In contrast to the assessment, the attack phase was very similar between robber flies and damselflies. There were no significant differences for *i*) the distance from the prey at which the predator initiated the attack (robber flies: *med* = 39.2 mm, *IQR* = 30 and damselflies: *med* = 35.6 mm, *IQR* = 20; Wilcoxon rank sum test, $W = 97$, $p = 0.547$), *ii*) the duration of the attack (robber flies: 207 ± 11 ms, damselflies: 176 ± 19 ms, *m* ± *SE*; Wilcoxon rank sum test, $W = 79$, $p = 0.177$), *iii*) the peak velocity (robber flies: *med* = 0.42 m s^{-1}, *IQR* = 0.33; damselflies: *med* = 0.30 m s^{-1} and *IQR* = 0.16; Wilcoxon rank sum test, $W = 86$, $p = 0.289$) and *iv*) peak accelerations (robber flies: *med* = 3.97 m s^{-2}, *IQR* = 1.49; damselflies: *med* = 3.53 m s^{-2}, *IQR* = 3.04; Wilcoxon rank sum test, $W = 103$, $p = 0.724$). Tortuosity of the attack trajectory was the only significantly different measure between the two predators, with robber flies having straighter attacks than damselflies (robber flies: *med* = 0.99, *IQR* = 0.017; damselflies: *med* = 0.96, *IQR* = 0.045; Wilcoxon rank sum test, $W = 59$, $p = 0.029$).

Our results indicate that darting robber flies and fragile forktail damselflies have key differences in prey assessment strategies. Robber flies assessed prey by performing higher-tortuosity, lower-velocity manoeuvres than damselflies. In contrast, the attacks of the two species had similar duration, velocity and acceleration, though robber flies had straighter attacks than damselflies.

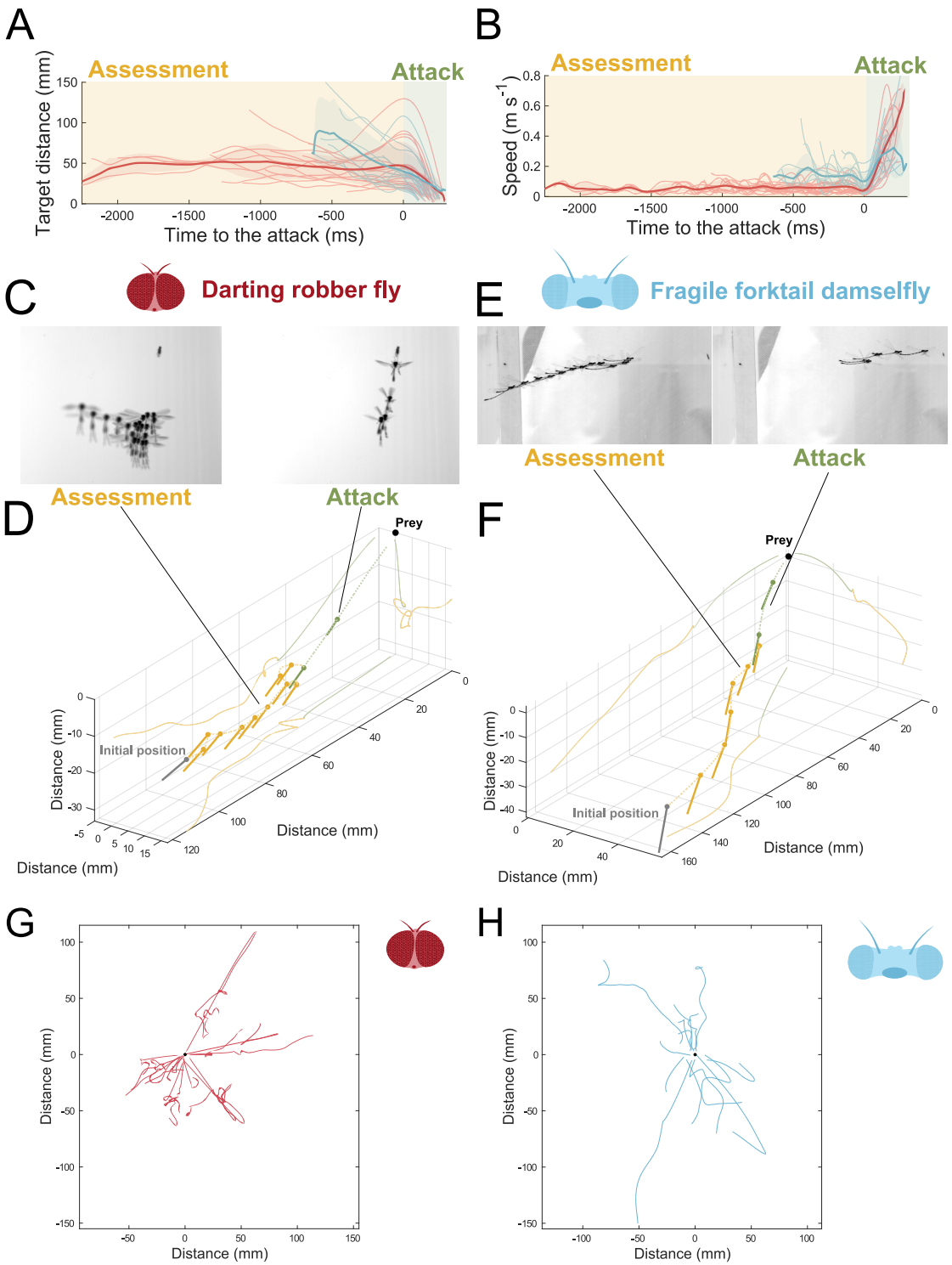

Figure 3.2 Variability and phase division in the hunting behaviour of darting robber flies and fragile forktail damselflies attacking static fruit flies. A) The distance from prey over time for darting robber fly attacks (red thin lines) and fragile forktail damselfly attacks (blue thin lines). B) The velocity plots over time for darting robber fly attacks (red thin lines) and fragile forktail damselfly attacks (blue thin lines). Thick lines in panels A-B show the mean profiles for each predator, smoothed. Shaded red and blue lines represent ± standard deviation. The *attack* (green) was identified as the final acceleration towards the static target. The *assessment* (yellow) preceded the attack. B) Two 50 ms overlays of a

darting robber fly attack towards a static fruit fly, one for frames within the assessment and one for frames within the attack. C) A digitised trajectory (dotted line) of a darting robber fly hunting a static fruit fly. The position of the fly every 100 ms is shown as a point (thorax) and line (abdomen), colour-coded according to its behavioural phase classification, assessment in yellow and attack in green. The trajectory is projected on each of the three two-dimensional planes. The prey position is represented as a black point. D) Two 50 ms overlays of a fragile forktail damselfly attack towards a static fruit fly, one for frames within the assessment and one for frames within the attack. E) A digitised trajectory of a fragile forktail damselfly hunting a static fruit fly. Plot details are as in panel C. F) Top views of darting robber flies (n = 16, trajectories in red) attacking a static fruit fly (black dot). G) Top views of fragile forktail damselflies (n = 14, trajectories in blue) attacking a static fruit fly (black dot).

3.3.2. Darting robber flies are capable of flying with a smaller movement range than when assessing prey

The tortuosity displayed by darting robber flies during their assessment is three dimensional (**Fig. 3.2C-E**), so that the body of the animal appears to translate around an imaginary centre point, without changing its body orientation (**Fig. 3.S1**). Darting robber flies might bob during prey assessment because they are incapable of a more stable flight. However, when freely flying in the arena, robber flies showed good flight control skills, sometimes hovering in place (**Fig. 3.S4**) (Newkirk, 1963). We recorded these instances of hover flights (n = 10 flights) and compared them to prey assessments (n = 16 flights). The minimal velocities of hovering events were significantly lower than during assessments (hovers: 0.0039 ± 0.0008 m s^{-1}; assessments: 0.0119 ± 0.0018 m s^{-1}, $m \pm SE$; Wilcoxon rank sum test, W = 18, p = 0.001). Since the hovering sequences were of shorter duration than assessments (hovers: *med* = 373 ms, *IQR* = 165; assessments: *med* = 1292 ms, *IQR* = 717; Wilcoxon rank sum test, W = 18, p = 0.001), for further comparison the assessment flights were trimmed to the mean duration of hovering flights (392 ms). The 392 ms window for each assessment trajectory was taken so that the time point of minimal velocity was as close to the midpoint as possible, while still having 392 ms of duration. We then calculated the movement range as the standard deviation of the fly's distance from the centre of the flight volume during this trimmed portion. During the trimmed portions of the assessments, robber flies had a movement range (*med* = 0.896 mm, *IQR* = 0.77) which was significantly higher than the movement range during hovering flights (*med* = 0.523 mm, *IQR* = 0.42; Wilcoxon rank sum test, W = 35, p = 0.019). These results show that the tortuous

assessments are therefore unlikely to arise from a lack of flight control, as when not assessing prey, darting robber flies can fly with much less lateral displacement. Instead, we suggest that the tortuous trajectories performed during the assessment phase are actively implemented and serve a role in prey assessment.

3.3.3. Prey relief, background presence, colour or shape do not prevent darting robber flies from attacking

The tortuous flightpaths during prey assessment of the darting robber flies could arise if motion parallax was being used to make camouflaged prey 'pop out' from the background through figure relief transformation (Galloway et al., 2020; Gårding et al., 1995; Nityananda and Read, 2017). To test this possibility, we presented darting robber flies with a computer screen that displayed images of flies (2.8 mm body length), scaled to those of real fruit flies (2.45 ± 0.06 mm; m ± SE, n = 10 animals). The attacks to fruit fly images (n = 8 flights) and to real fruit flies (n = 16 flights) did not differ significantly in any of the parameters measured (distance from the prey at the beginning of the assessment, duration and straightness index of the assessment phase, distance from prey at the beginning of the attack, peak velocity and acceleration during the attack; see **Table 3.S1** for a summary of the statistics). Because darting robber flies reliably hunted fly images in a way that is indistinguishable from real fruit flies, relief information on its own cannot be the determinant cue for the outcome of the assessment.

It may however be possible that, whilst incapable of perceiving relief details of their prey, darting robber flies compare target movement to background movement during the assessment. Target images shown on a uniform background do not test this, as uniform backgrounds do not provide movement information. Therefore, we instead displayed images of fruit flies overlayed on two-dimensional textured backgrounds on a computer screen. Motion parallax movements performed for targets on two-dimensional textured backgrounds result in a coherent movement between target and background, as they are on the same plane; target and background have therefore no differential motion. We tested two backgrounds, one picturing foliage and one with netting. Darting robber flies attacked images of fruit flies on both textured backgrounds (n = 3 and n = 9 flights,

respectively, **Movie 3.M4**), suggesting that attacks do not rely on differential movement information between a target and its substrate.

We also tested the robber flies for prey shape or colouration (**Movie 3.M4**). Darting robber flies attacked coloured pictures of fruit flies (n = 8 flights), black and white pictures of the same size (n = 3 flights), or grey circles of the same length and width (n = 5 flights). This suggests that prey colour or shape are not cues that strictly dictate whether to attack potential prey.

3.3.4. Effect of prey size on the prey assessment of darting robber flies

It is possible that the motion parallax information obtained during tortuous assessment flights allows darting robber flies to estimate prey distance and size. We then tested if prey size was a key cue for the attack. In the wild, darting robber flies attack a variety of prey, ranging from dipterans to spiders (Newkirk, 1963). In our experimental arena, robber flies readily attacked real fruit flies of different sizes: *Drosophila melanogaster* with a body length of 2.45 ± 0.05 mm (m ± SE, n = 10 animals), *Drosophila affinis* with a body length of 2.68 ± 0.09 mm (n = 10 animals) and *Drosophila virilis* with a body length of 3.57 ± 0.06 mm (n = 10 animals). Notably, the attacks to capture *D. melanogaster* (n = 16 flights), *D. affinis* (n = 9 flights) and *D. virilis* (n = 7 flights) were launched at an increasingly greater distance from the target. Prey size was positively correlated with the distance between predator and prey at the start of the attack. (Jonckheere-Terpstra test; J = 259, $p < 0.001$, **Fig. 3.3A**). A longer attack translates into additional time for acceleration. Accordingly, peak velocities were significantly higher for larger prey (trend analysis contrasts; $F(1,29) = 0.186$, $p = 0.003$) and peak velocity was positively correlated with distance from the target (Pearson's correlation, $r = 0.9$, $p < 0.001$). To achieve this, darting robber flies could start attacking at a distance where targets subtend a set angular size; the larger the target, the larger the distance and the higher the peak acceleration. However, when the attack was launched, the subtended angular sizes of the three drosophila species were significantly different (*D. melanogaster*: 3.83 ± 0.48 °; *D. affinis*: 1.78 ± 0.20 °; *D. virilis*: 2.31 ± 0.39 °, m ± SE; Kruskal-Wallis test; $\chi^2(2) = 8.33$, $p = 0.016$). Indeed, for

D. affinis and *D. virilis* to subtend the same size as *D. melanogaster* (3.83°), attacks towards them would have needed to be launched at distances of 40.0 and 53.3 mm, respectively. However, the recorded distance from prey at the start of the attack were significantly different (*D. affinis*: *med* = 87.7 mm, *IQR* = 31.1 ; *D. virilis*: *med* = 93.4 mm, *IQR* = 70.9; Student's t-tests, $t(8) = 5.62$, $p < 0.001$, and $t(6) = 2.86$, $p = 0.029$, respectively).

To further investigate the role of prey size while controlling for other variables, we recorded attacks to the same image of a *D. melanogaster*, scaled such that their body length was 1.58 mm ($n = 9$ flights), 2.81 mm ($n = 8$ flights), 3.09 mm ($n = 8$ flights), 4.33 mm ($n = 7$ flights) and 6.53 mm ($n = 7$ flights)). For each attack, we found the central point in space of the assessment and calculated the target's angular size at this point. At this central point, the angular size of the target did not increase with the target's absolute size (target's angular size at central assessment point: *med* = 6.60°, *IQR* = 10.0, $n = 39$; Jonckheere-Terpstra test; $J = 346$, $p = 0.150$). This suggests that the target's angular size, not its absolute size, was used to determine where robber flies performed their assessments. The robber fly's mean speed during the assessment did not differ between attacks to prey of different size (Kruskal-Wallis test; $\chi^2(4) = 2.17$, $p = 0.705$). However, larger targets elicited longer and more tortuous assessments (Jonckheere-Terpstra test; $J = 450$, $p < 0.001$, **Fig. 3.3B**, and $J = 223$, $p = 0.024$, **Fig. 3.3C**, respectively). The movement range, i.e. standard deviation from the central point of the assessment, also increased with prey size (Jonckheere-Terpstra test; $J = 395$, $p = 0.012$, **Fig. 3.3D**) and was correlated with the distance from the target at the central point of the assessment (Spearman's correlation, $r_s = 0.54$, $p < 0.001$). After the assessment, darting robber flies positioned themselves at a distance from the target that increased with target size (Jonckheere-Terpstra test; $J = 423$, $p = 0.001$, **Fig. 3.3E**). Crucially, targets did not subtend the same angular size at this position, where the attack was launched (Kruskal-Wallis test; $\chi^2(4) = 16.13$, $p = 0.002$, **Fig. 3.3F**. This suggests that, by the time the assessment was completed, the target's absolute size, not its angular size, was used to determine at what distance to launch the attack, though this does not necessarily mean that the target's absolute size is explicitly calculated by the predator.

To summarise, larger prey, which was assessed at greater distance to subtend the same angular size, elicited longer and more tortuous assessment flights, which were performed with a larger movement range. After assessing prey, darting robber flies launched the attack from further away, the larger the target was. However, the position where the attack was launched did not vary with the target's angular size, but its absolute size.

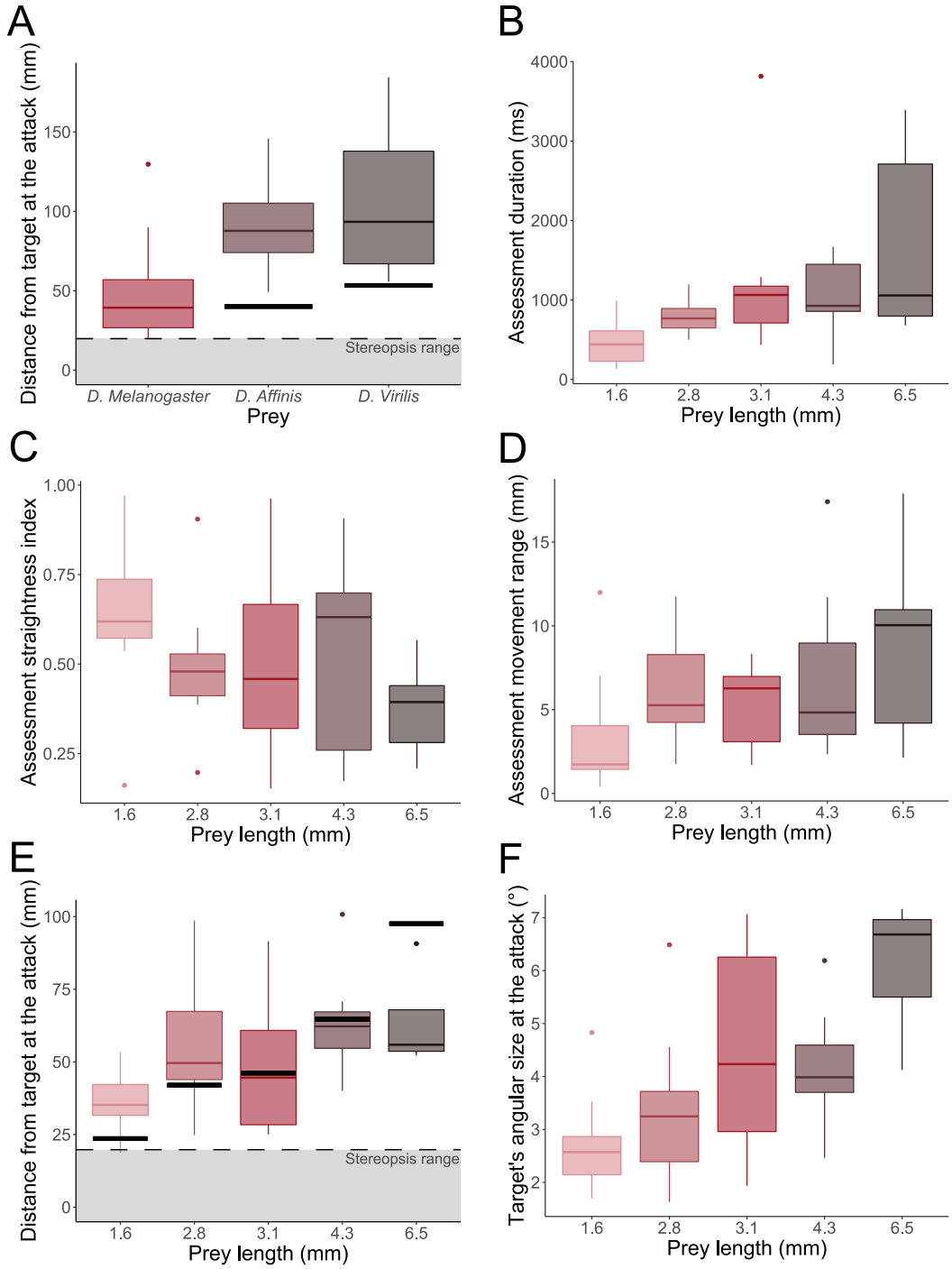

Fig. 3.3. Prey of different size is at different distances from the darting robber fly when the attack is launched, subtending different angular sizes. A) The darting robber fly's distance when the attack is launched from prey of three different sizes, *D. melanogaster* with size 2.45 ± 0.19 mm, *D. affinis* with size 2.68 ± 0.29 mm and *D. virilis* with size 3.57 ± 0.19 mm. B) Duration of the assessment for prey of different sizes. C) Straightness index of the assessment for prey of different sizes. D) The standard deviation of distance from the central point of the assessment, called movement range, for prey of different sizes. E) The darting robber fly's distance when the attack is launched from prey of different length shown on a computer display. F) Angular size of prey of different sizes when darting robber flies launch the attack. In A: n = 16 attacks for *D. melanogaster*, n = 9

attacks for *D. affinis*, $n = 7$ attacks for *D. virilis*. In B-F: $n = 9$ attacks for prey size 1.6 mm, $n = 8$ attacks for prey size 2.8 mm, $n = 8$ attacks for prey size 3.1 mm, $n = 7$ attacks for prey size 4.3 mm, $n = 7$ attacks for prey size 6.5 mm. In A and B, black lines represent the distance required for prey to subtend the same angular size *D. melanogaster* subtends in A; the grey area represents the stereopsis range of the darting robber fly (see Materials and Methods).

3.3.5. Prey is outside of the darting robber fly's stereopsis range when an attack is launched

To test if darting robber flies could calculate absolute prey size using stereopsis, we looked at these predators' visual system (**Fig. 3.4A, Movie 3.M5**). Using two-photon microscopy, we imaged the 13 biggest lenses of each eye ($n = 3$ animals, $n = 78$ lenses). From the resulting 3D stack, a coronal view was taken through each lens (**Fig. 3.4B**). Lenses were curved on the outer surface and flat on the inner surface. We fit a circle to the outer surface of each lens and measured its radius. Using this radius (*med* = 41.2 µm, *IQR* = 3.79), the refractive index of air (1.00) and the refractive index of the lens (1.43 (Stavenga et al., 1990)), we calculated the power of the lens, $P = 10.4\ mm^{-1}$. We then used these values to calculate the object space focal length, $f = 95.8$ µm, and the image space focal length, $f' = 128$ µm, using 1.34 as the refractive index of the image space (Seitz, 1968). The object space focal length was divided by the median diameter of the lenses (*med* = 69.9 µm, *IQR* = 6.97) to calculate the lens' F-number, $F = 1.37$.

To validate these calculations, we calculated for each lens the position of the focal plane where the rhabdomere tips ought to be located (*med* = 97.8 µm, *IQR* = 8.28). The distance between the distal surface of the lens and the tip of the rhabdomeres, measured using two-photon scans, (*med* = 95.8 µm, *IQR* = 17.3) was not significantly different to the calculated position of the focal plane (Wilcoxon rank sum test, $W = 2573$, $p = 0.097$). Thus, both calculations are supportive of a focal plane positioned approximately 96.5-97 µm from the proximal surface of the lens.

Transmission electron micrographs of the robber fly's rhabdoms were taken at the distal portion of the fovea's rhabdoms (**Figs. 3.4C, 3.S5**). We calculated the average between the two axes of an ellipse fitted to each rhabdomere (0.779 ± 0.023 µm, $n = 5$ animals measured for one ommatidium each, $n = 35$ rhabdomeres) and divided this by the object space focal length to calculate the acceptance angle,

$\Delta\rho$ = 0.47°. The electron micrographs were also used to extract the distance between the photoreceptors (1.74 ± 0.159 µm, n = 5 animals measured for one ommatidium each, n = 25 rhabdomere distances). We divided this value by the object space focal length, and applied Pick's correction (Pick, 1977), which gives the interommatidial angle of the darting robber fly's fovea, $\Delta\Phi$ = 0.831°. We measured the distance between the biggest lenses from the two-photon scan (285 ± 3.06 µm, *med ± IQR*). We divided this number by twice the tangent of half the interommatidial angle, to approximate the stereopsis range of darting robber flies, E_∞ = 19.8 mm (**Fig. 3.4D**).

The stereopsis range is significantly less than the distance from which the darting robber fly launched the attack to *D. melanogaster* (n = 16 flights, *med* = 49.3 mm, *IQR* = 30, Wilcoxon signed rank test, W = 135, p < 0.001), the distance between the central point of the assessment and *D. melanogaster* (n = 16 flights, 42.5 ± 3.72 mm, Wilcoxon signed rank test, W = 135, p < 0.001), and the minimal distance between predator and *D. melanogaster* during the assessment (n = 16 flights, 31.7 ± 3.07 mm, Wilcoxon signed rank test, W = 128, p < 0.001). This suggests that darting robber flies are unlikely to use stereopsis to gather 3-D information such as the size of their prey and their distance from it.

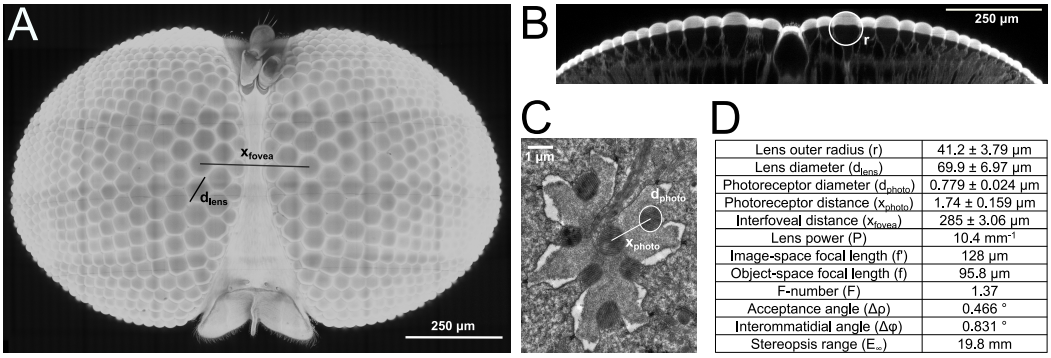

D

Lens outer radius (r)	41.2 ± 3.79 µm
Lens diameter (d_{lens})	69.9 ± 6.97 µm
Photoreceptor diameter (d_{photo})	0.779 ± 0.024 µm
Photoreceptor distance (x_{photo})	1.74 ± 0.159 µm
Interfoveal distance (x_{fovea})	285 ± 3.06 µm
Lens power (P)	10.4 mm^{-1}
Image-space focal length (f')	128 µm
Object-space focal length (f)	95.8 µm
F-number (F)	1.37
Acceptance angle (Δρ)	0.466 °
Interommatidial angle (Δφ)	0.831 °
Stereopsis range (E_{∞})	19.8 mm

Fig. 3.4. Optical measurements from the darting robber fly eyes. A) Two-photon scan of the darting robber fly's head showing the enlarged frontal facets close to the midline. The black lines show the measurement of lens diameter and interfoveal distance between the two eyes. B) Coronal section of the two-photon stack showing a circle fitted to the outer curvature of a lens, the radius of which was used as a measurement. C) Transmission electron micrograph showing the cross-section of an ommatidium in the acute zone. The ellipse fitted to one of the photoreceptors is shown as well as the distance between the centroids of rhabdomeres R7 and R1. D) A summary of the morphological measurements taken from darting robber flies heads (upper part), and the subsequently calculated features of the fly's visual system (lower part).

3.4. Discussion

In this chapter, we show that the predatory attacks of darting robber flies and fragile forktail damselflies can be divided in two behavioural phases. In the first phase, which we call the assessment, both robber flies and damselflies orient their body and assess their prey. In the second phase, both predators accelerate towards the prey for capture, performing the attack. Despite attacks being very similar between the two species, darting robber flies assess their prey for longer, at lower speed, and with more convoluted trajectories than damselflies. Darting robber flies are capable of flying at lower speed and with a smaller movement range when not hunting, compared to when they assess prey; the more convoluted assessments seem therefore to be actively performed. Moreover, the fact that robber flies and damselflies performed so similarly during attacks suggests that the difference in flight during prey assessment is not due to the physical constraints the smaller robber flies face during flight.

Darting robber flies treated prey images shown on a computer monitor as real prey. Being generalist hunters (Newkirk, 1963), darting robber flies seem unlikely to assess prey by shape or colour. This is confirmed in our experiments, where

darting robber flies hunted prey images of different shapes and colours. Instead, their convoluted assessments seem to be used to evaluate prey size. Darting robber flies hunted both real prey and pictures of prey of a range of sizes in our arena. Attacks towards prey of larger size were launched from a higher distance, which allowed the darting robber flies to achieve higher peak velocities. High peak velocities at the end of the attack are possibly achieved to produce a large impact force onto the prey, as seen in other predators (deVries et al., 2012). Darting robber flies may therefore launch the attack towards bigger targets from further away to produce enough force to snatch the prey. Theoretically, if prey of different absolute size subtended the same angular size on the darting robber fly's retina when the attack is launched, then the robber fly's distance from the target would be larger for bigger prey. However, our data suggests that this is not how darting robber flies determine where to initiate the attack, as targets of different lengths subtended different angular sizes at the beginning of the attack. By contrast, prey of different lengths have the same angular size at the central point of the assessment. This suggests that darting robber flies use the target's angular size to determine where to assess prey, but use its absolute size to determine where to launch the attack. Although it is tempting to suggest that darting robber flies calculate their target's absolute size during assessment, there is no evidence for this explicit calculation and implicit, simpler rules-of-thumb could be used by the predators.

To answer the question of whether darting robber flies could rely on stereopsis, we used morphological data from the robber fly's eyes. The curvature of the lens of each rhabdomere can be used to calculate its power and focal lengths (Stavenga, 2003). We calculated the focal lengths of the largest rhabdomeres on each eye, with which we could also found the optimal distance between the lens and the rhabdomere. The optimal distance was not significantly different than the measured distance between the lens and the rhabdomere, confirming our approximations were reliable. We used the focal lengths and rhabdomere distances to calculate the interommatidial angles (Wardill et al., 2017). Ideally, we would have liked to confirm these results with more established pseudopupil measurements (Horridge and Duelli, 1979), but the dark pigments in the darting

robber fly's eyes made it impossible. Nevertheless, the interommatidial angles found in the acute zone of this miniature ambush predator are comparable to other formidable sit-and-wait predators like praying mantids (Horridge and Duelli, 1979). This underlines that small predators can meet the visual challenges of larger competitors, as found in other robber flies (Wardill et al., 2017). We used the interommatidial angle to calculate the approximate stereopsis range for the darting robber fly. The stereopsis range was much smaller than the distance at which the darting robber fly assesses prey, suggesting that these animals do not use stereopsis to calculate prey size. Considered the actively convoluted prey assessment they use, we suggest that darting robber flies use motion parallax to determine at what distance from their target they ought to launch an attack.

The assessments of robber flies do indeed have some features in common with other animals that use motion parallax. When trying to jump towards a distant object, both locusts (Collett, 1978) and mantids (Poteser and Kral, 1995) perform larger peering movements than when targeting an object nearby, to increase their accuracy. However, the velocity of the peering stays constant, which suggests that they use the target's angular velocity, rather than its angular displacement, to calculate its size (Kral, 1998; Kral, 2003). We see the same pattern with darting robber flies. When assessing larger prey, which is farther away, the movement range increases and the straightness index decreases, but their velocity stays constant. Darting robber flies also assess bigger prey for longer, which could be a way to compensate for the reduced accuracy of farther away prey (Collett, 1978). Other insects which use motion parallax (Collett and Paterson, 1991; Ravi et al., 2019; Srinivasan et al., 1989; Walcher and Kral, 1994; Zeil, 1993) are able to use absolute motion parallax, calculating the absolute distance of one object, and relative motion parallax, to understand how objects are positioned in relation to each other. It is not clear if the darting robber fly can use relative parallax cues. Indeed, when presented with a two-dimensional prey image attached to a two-dimensional background, darting robber flies readily attacked it, showing that they do not compare target motion to background motion. Whether darting robber flies would be able to use relative parallax in other contexts however, for example if an obstacle is present in front of their target, needs further investigation.

Darting robber flies have evolved motion parallax to capture prey, but why they have done so? Their large lenses allow them to spot prey at similar distances to damselflies, but their much smaller heads only allow them to use stereopsis with a very limited range. If darting robber flies used binocular cues to calculate absolute prey parameters, they would be too close to their prey, with the risk of being spotted and their prey escaping. Motion parallax has a much longer range for them, as the distance they have from prey at the moment of attack is the same as damselflies. Their small bodies and head could even turn to their advantage, as this might be the reason why they are not spotted by their prey when assessing it. 3D calculations in predatory behaviour have long been thought to rely on the binocularity of animals with large eyes and/or high visual acuity (Nityananda and Read, 2017; Rossel, 1983; Wardill et al., 2017). However, this and other examples (Wardill et al., 2015) show that animals with less sophisticated visual systems can still successfully predate by using simple rules applicable to perceived imaged at lower resolution.

3.5. Supplementary Information

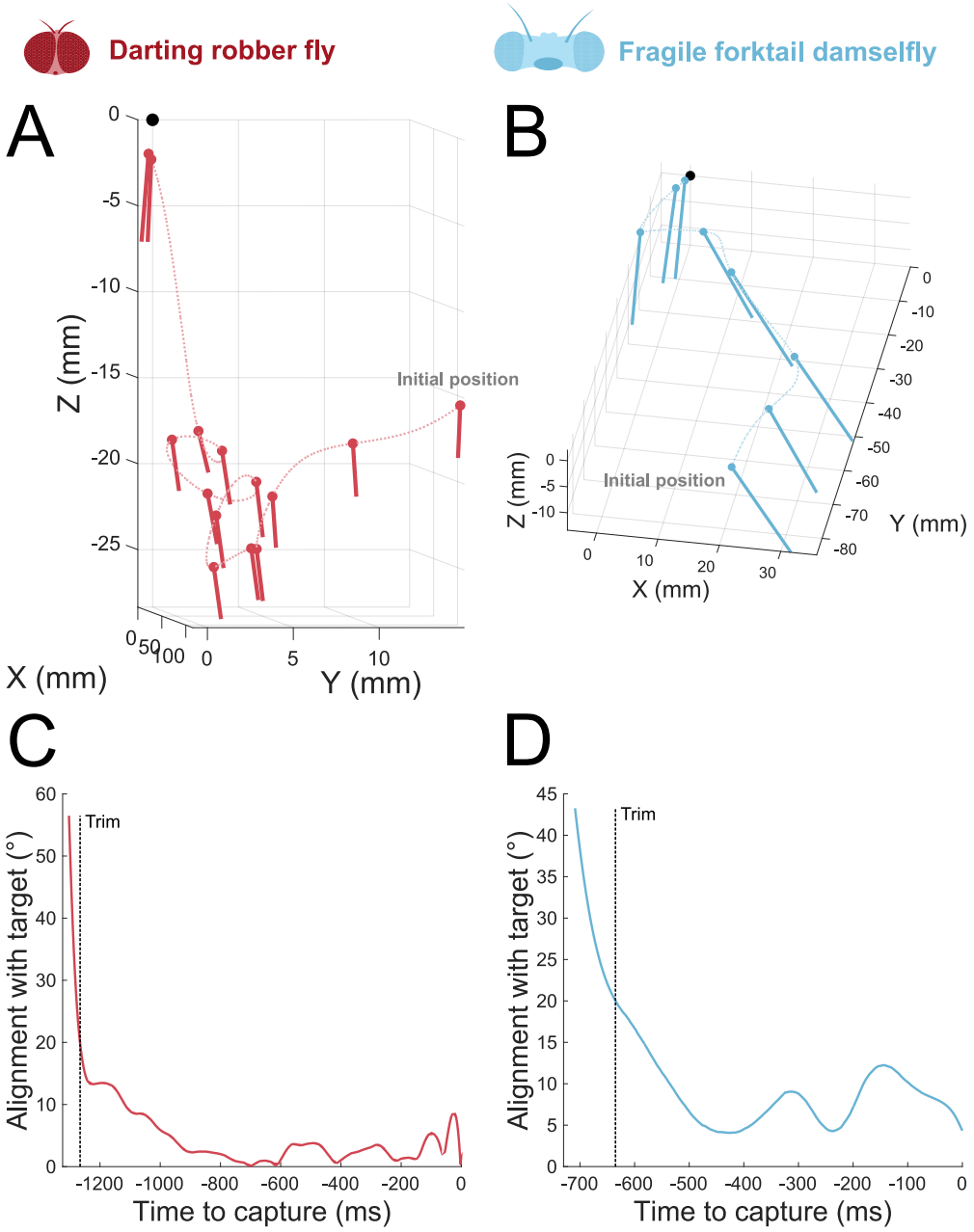

Fig. 3.S1. Predator body angle when assessing and attacking prey. A) The trajectory of a darting robber fly (dotted line) assessing and attacking a fruit fly. The position of the fly every 100 ms is shown as a point (thorax) and line (abdomen). The target position is represented as a black point. B) The trajectory of a fragile forktail damselfly assessing and attacking a fruit fly. Details are as in panel A. C) The body alignment with the target over time of the robber fly's assessment and attack shown in A. The vertical line represents the timepoint when the fly's body aligns under 20° with the target, which was used to trim attacks. D) The body alignment with the target over time of the damselfly's assessment and attack shown in B. Details are as in panel C.

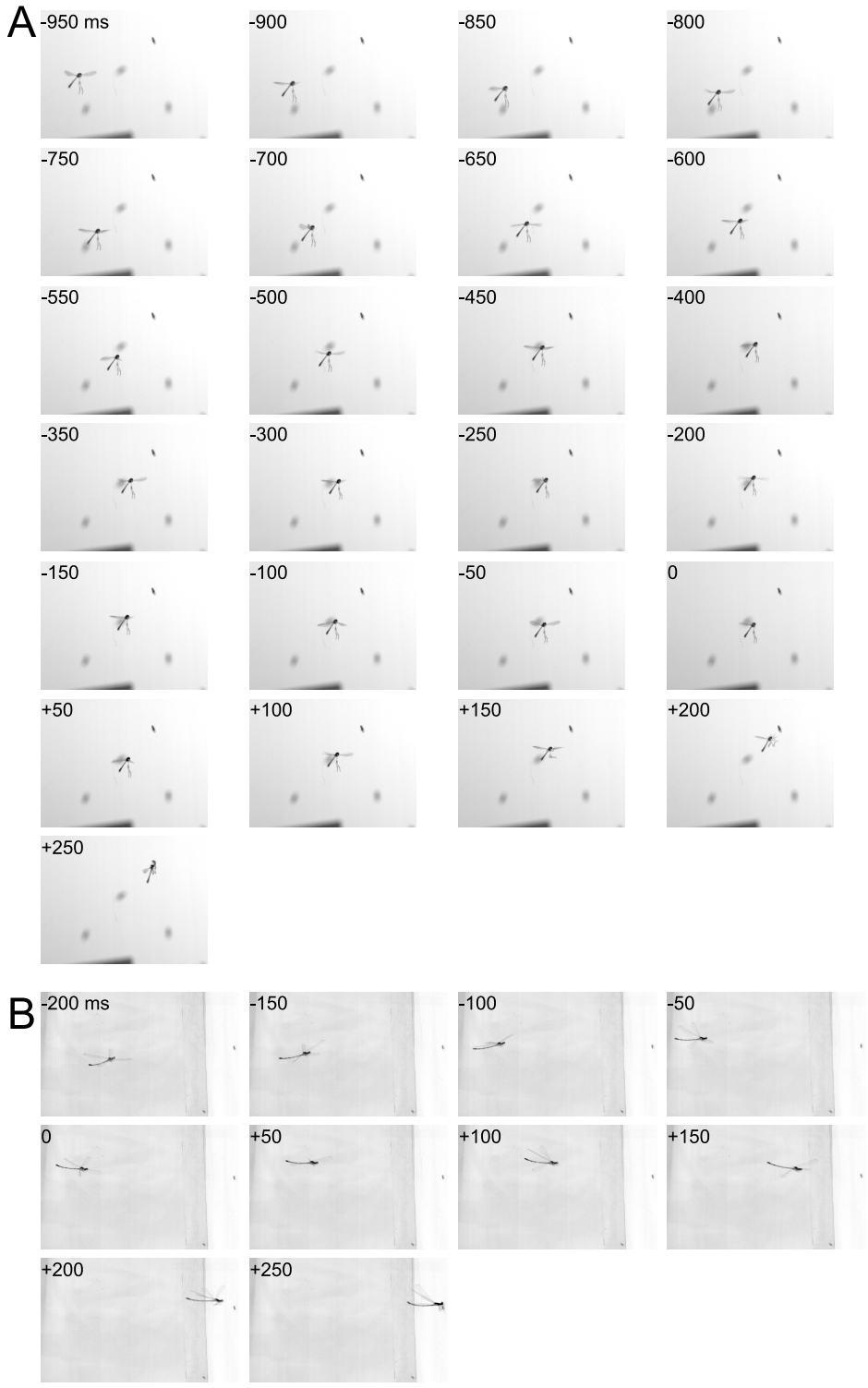

Fig. 3.S2. Sequential images of darting robber flies and fragile forktail damselflies gleaning static prey. A) Sequential still frames at 50 ms intervals showing a darting robber fly attacking a fruit fly. B) Sequential still frames at 50 ms intervals showing a fragile forktail damselfly attacking a fruit fly.

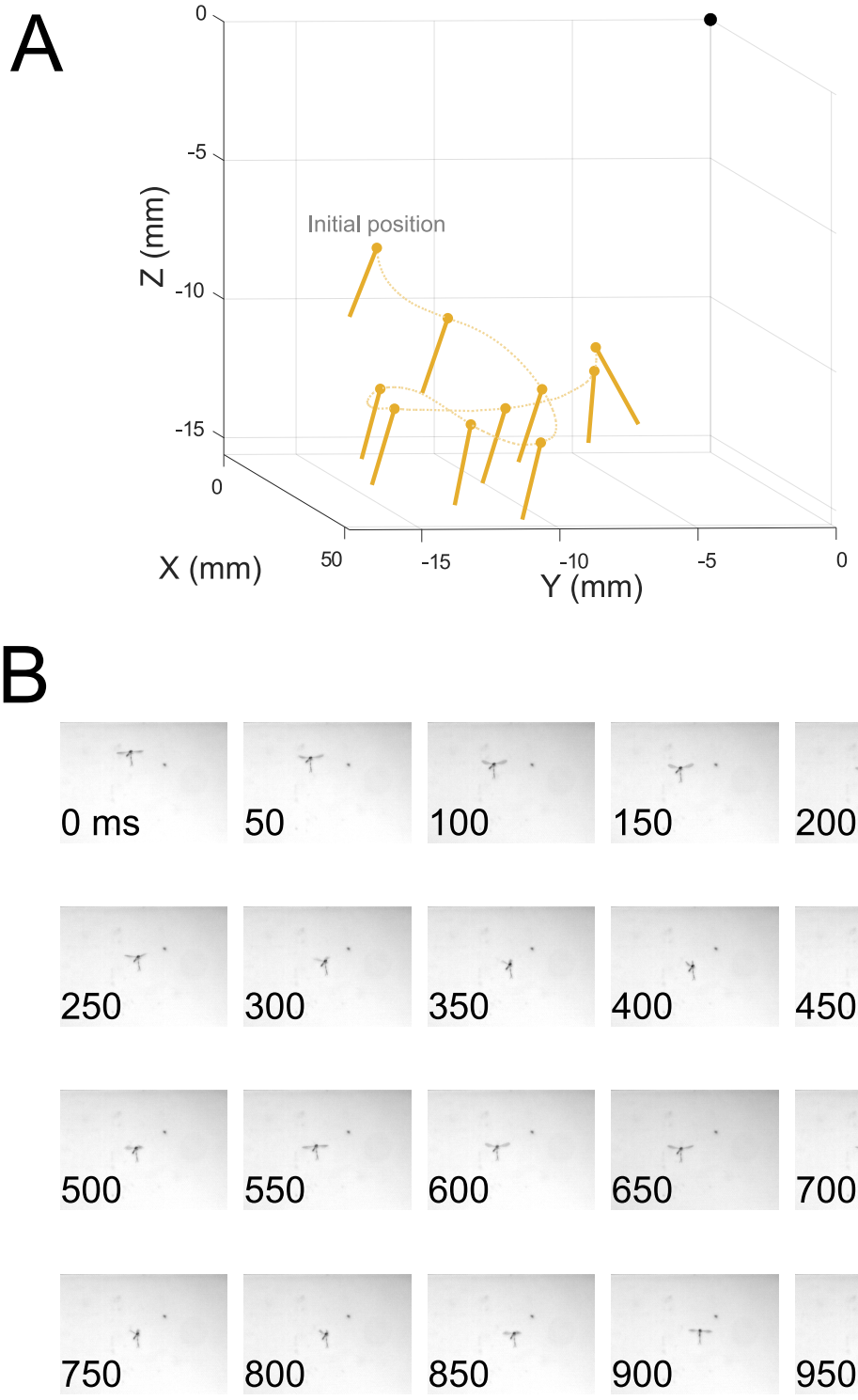

Fig. 3.S3. Darting robber flies can assess prey without performing an attack. The trajectory of a darting robber fly (dotted line) assessing a static fruit fly without surging. The position of the fly every 100 ms is shown as a point (thorax) and line (abdomen). The prey position is represented as a black point.

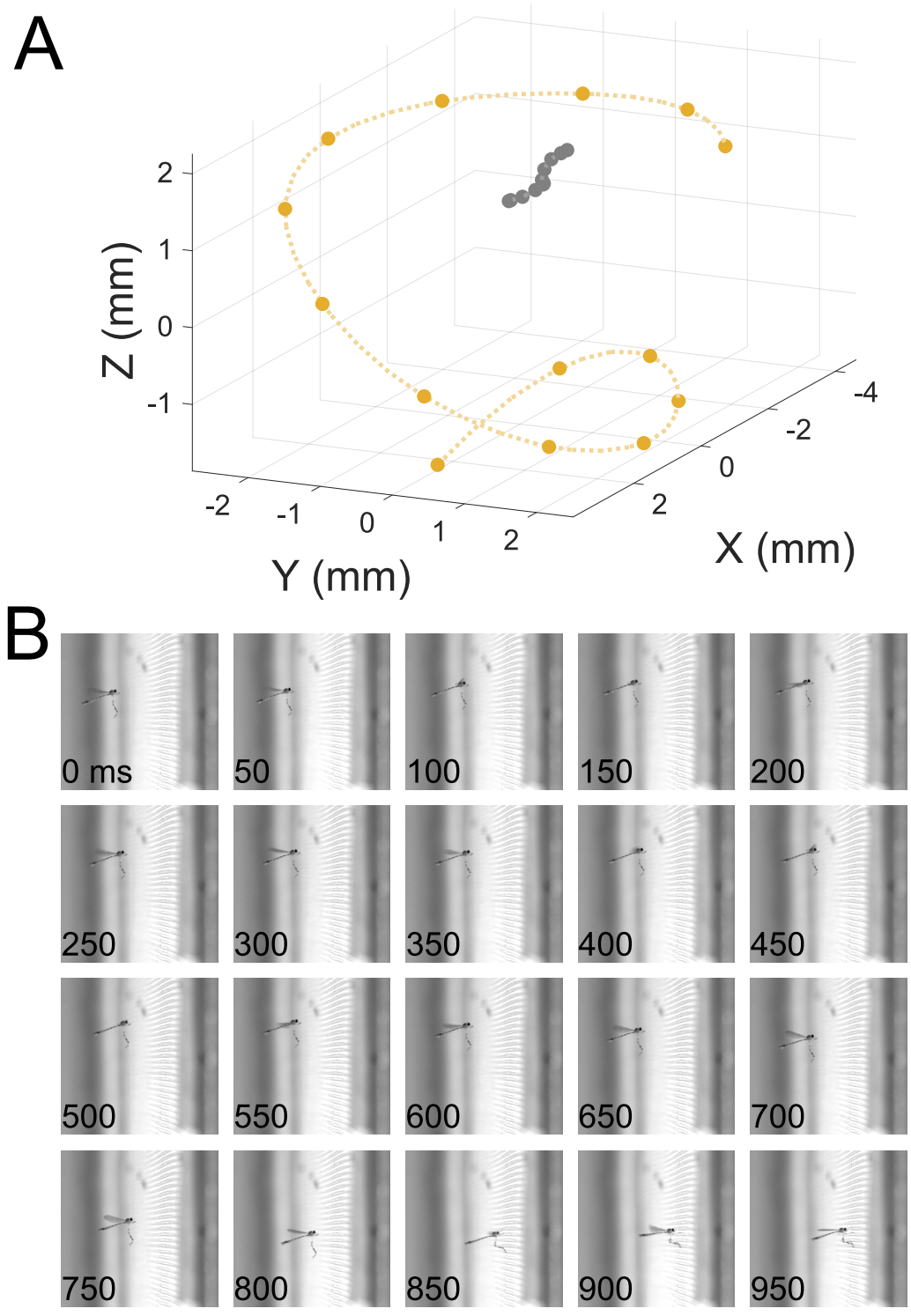

Fig. 3.S4. Darting robber flies are capable of flying at lower speed and with less translational movements than during assessments. A) The trajectory of a darting robber fly during an assessment (yellow dotted line), compared to a stationary flight (grey dotted line). The position of the thorax is shown every 30 ms (yellow and grey points). B) Sequential images of a darting robber fly performing a stationary flight over considerable time before landing.

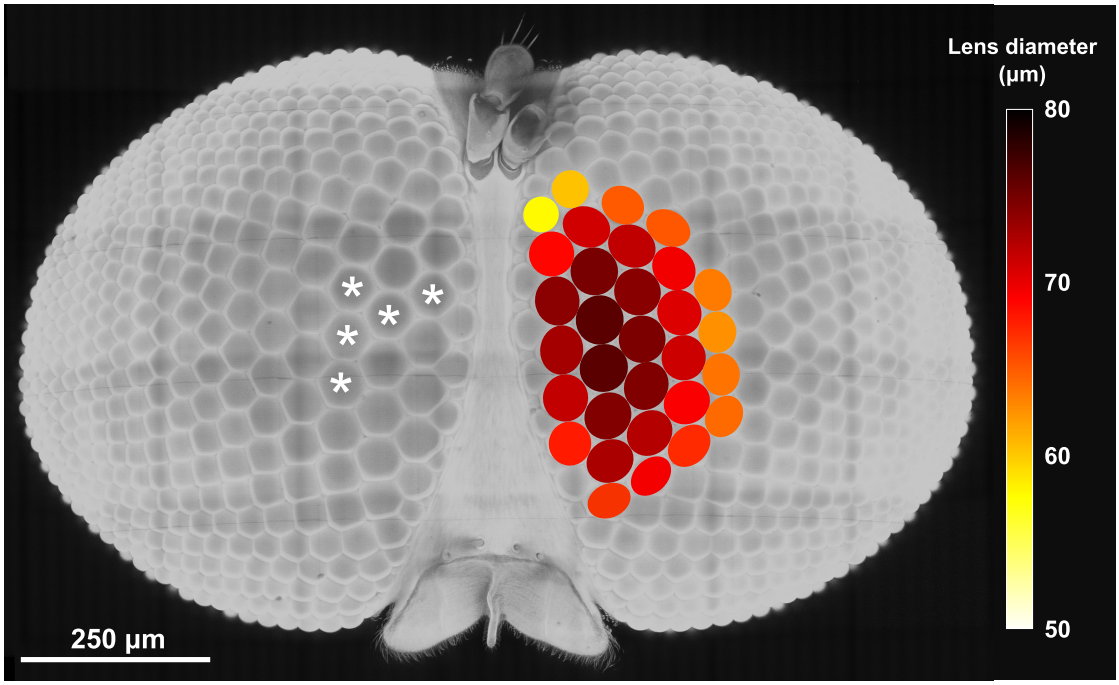

Fig. 3.S5. Transmission electron micrographs were centred in the acute zone of the darting robber fly's eye. The lenses of the darting robber fly's left eye are colour coded for their size (lighter colour indicate smaller lenses). On the right eye, asterisks indicate the locations where sections were centred for acquisition and measurement of electron micrographs.

Table 3.S1. A summary of the statistical tests comparing attacks to real fruit flies (size = 2.45 ± 0.19 mm, n = 16 flights) and fruit fly images shown on a computer screen (size= 2.81 mm, n = 8 flights).

Measurement	**Test**	**Statistic**	**Significance**
Initial distance	Wilcoxon rank sum test	$W = 55$	$p = 0.610$
Assessment duration	Wilcoxon rank sum test	$W = 91$	$p = 0.106$
Assessment straightness index	Wilcoxon rank sum test	$W = 49$	$p = 0.383$
Distance at the beginning of the attack	Wilcoxon rank sum test	$W = 47$	$p = 0.320$
Attack peak speed	Student's T-test	$t(13) = 0.293$	$p = 0.774$
Attack peak acceleration	Wilcoxon rank sum test	$W = 87$	$p = 0.172$

4. Gravity and Active Acceleration Limit the Steering Ability of an Active Predator When Attacking from Above

4.1. Introduction

Aerial predation is an intricate task, in which the predator's interaction with gravity changes according to the angle of its flight path. When flying upwards, predators need to overcome the force of gravity, but when chasing prey towards the ground, gravity will increase the total acceleration they achieve. Many birds of prey exploit gravity, using it to gain most of their velocity (Alerstam, 1987; Ponitz et al., 2014; Rudebeck, 1950; Tucker, 1998; Tucker and Parrott, 1970). The opposite hunting strategy consists of perching close to the ground and looking upwards, which makes targets easily detectable against a clearer background, the sky. This strategy is common among predators with limited visual resolution such as insects, like many dragonflies and some robber flies (Fabian et al., 2018; Olberg et al., 2000)

When attacking aerial prey, dragonflies (Olberg et al., 2000), hoverflies (Collett and Land, 1978) and robber flies (Fabian et al., 2018; Wardill et al., 2017) fly towards the future location of their prey, i.e. they employ interception. To intercept their target, predatory dipteran flies are thought to use a strategy called proportional navigation (PN) (Fabian et al., 2018). Under PN, the predator monitors the change in the bearing to the prey and uses this information to correct its own heading. This law allows an animal to intercept a target without knowledge of the target's absolute distance or velocity. Another strategy is to head towards where the target is currently perceived, which guarantees a capture only if the chaser is faster than its prey. This strategy, known as pursuit, is employed by tiger beetles (Haselsteiner et al., 2014), house flies (Land and Collett, 1974; Wagner,

1986), long legged flies (Land, 1993), and honey bees (Gries and Koeniger, 1996). Of all the predatory insects studied thus far, none has been reported to attack downwards, if not for a small portion of the chase.

The fact that most predatory insects have not evolved to hunt downwards suggests that the challenges posed on their visual system are not counterbalanced by substantial advantages. The potential contribution of the force of gravity to their speed is likely heavily counteracted by air resistance, i.e. drag, which scales with velocity square and therefore strongly reduces the advantage of increasing speed. Viscous drag also scales with the projected body area, as inertia does with mass. Thus, the movement of a flying insect is influenced by both inertia and viscous drag, unlike the heavier vertebrates, whose movement is mainly dominated by inertia. Quantitatively, the ratio of inertial to viscous forces is represented by the Reynolds number. Flying insects operate at intermediate Reynolds numbers (1 to 10^3), making them extremely useful investigative tools in biophysics (Combes et al., 2012; Klotsa, 2019).

As explained above, the large drag forces experienced by a downward-flying predatory insect likely reduce the relative contribution of gravity to its velocity. Meanwhile, the sensory complexity of detecting prey against the cluttered ground can be considerable. For these reasons, one may predict small predatory insects with low visual acuity to contrast prey against the sky and attack upwards. However, the killer fly *Coenosia attenuata*, a 4-mm long dipteran whose retina has a relatively poor spatial resolution of 2.2° (Gonzalez-Bellido et al., 2011), does not conform to such an expectation. Killer flies are fast and highly manoeuvrable dipteran predators, who hunt prey flying downwards as well as upwards (Wardill et al., 2015). In addition, in an enclosed arena, we observed killer flies positioning themselves on the arena ceiling and then attacking prey passing below them from such inverted position. Although not strictly typical of the killer fly's ecology in the wild, this behaviour provides a unique opportunity to investigate how aerial predators at intermediate Reynolds numbers are affected by gravity.

When hunting prey flying across from them or above them, the killer flies' trajectories are well explained by PN (Fabian et al., 2018). However, before the present study, the killer fly's control system during downward attacks and

whether killer flies account for gravity when generating vertical lift remained to be investigated. In this article, we compare attacks from the walls and floor of the behavioural arena to attacks from the arena ceiling, which we call dives. We analyse the dive kinematics and test the predictive power of PN and other steering models. After identifying a candidate navigational model, we test whether killer flies time their take-off to deploy an attack of minimal duration, or an attack that requires minimal power. Finally, we contextualise the killer fly's dive in the ecological relevance of it and its prey.

4.2. Materials and Methods

4.2.1. Animals

Female killer flies (*Coenosia attenuata*) (Stein and Becker, 1903) were taken from a laboratory colony, established from animals collected in Almeria (Spain). The colony was kept at 60-70% humidity and a 20-25°C temperature in a 12/12 hour light/dark cycle, and was fed live fruit flies (*Drosophila melanogaster*).

4.2.2. Animal preparation

Killer flies were individually placed in transparent vials with only wet filter paper provided for two to three days before testing, to ensure the animals were motivated to hunt (Wardill et al., 2015). After isolation, two flies were tested in the arena at a time, at room temperature of 20-22°C. The arena was a transparent 160 x 160 x 300 mm box made of 4 mm wide acrylic boards (Perspex®, Mitsubishi Chemical Lucite Group Ltd, Tokyo, Japan), placed with the long axis resting on a white table. The arena was illuminated with two artificial light sources (4Long-Studio, VelvetLight, Barcelona, Spain) each producing an output of 14,000 lx at 1m, corresponding to peak light levels of a moderately cloudy day (Thorington, 1985).

After placing the flies in the arena, a target was moved along the longitudinal dimension of the box, perpendicular to gravity, in either direction. The target was a black 2.1 mm bead, moved between 0.65 and 0.8 m/s (Wardill et al., 2015) on a transparent 0.15 mm thick fluorocarbon fishing line (Vanish, Berkley Fishing, IA, U.S.A.). The line ran along pulleys fixed at the corners of a transparent acrylic

support and was moved by a 23HS-108 MK.2 stepper motor controlled through computer software by a ST5-Q-NN DC motor controller (Applied Motion Products, Watsonville, CA, U.S.A.). The target always started moving outside the box. Flies were tested on repeated trials until they stopped responding to the target.

In order to measure the velocity of killer flies in free fall, female animals were taken from the colony and anaesthetised with carbon dioxide. Whilst unresponsive, each fly was dropped from a height of 160 mm, the same height of the behavioural arena.

To extract morphological measurements, female killer flies were also sedated with carbon dioxide. Whilst unresponsive, they were weighed (sensitivity: 0.1 mg), before having both their wings clipped and photographed in pairs for area measurements. Before clipping, a female killer fly was photographed, with its wings extended anteriorly and then posteriorly, to approximate the maximum stroke angle.

4.2.3. Photography, videography and data extraction

For filming, we used two SA2 Photron cameras (Photron Ltd., Tokyo, Japan), time synced via the inbuilt shaft encoders. The recording frame rate used to digitise trajectories was 1000 frames/second, whilst the frame rate to extract wingbeat frequency was 2500 frames/second. The system was calibrated using an altered version (Wardill et al., 2017) of the J.Y. Boguet's Laboratory's MATLAB toolbox (Caltech, http://www.vision.caltech.edu/bouguetj/calib_doc/), running on MATLAB R2014a (version 8.3, MathWorks Inc., Natick, MA, U.S.A.). The movements of the killer flies and target were digitised offline using custom MATLAB scripts for supervised automatic tracking (Wardill et al., 2017), and smoothed through a fitting algorithm combining trajectory generation using linear fitting with jerk minimisation (Dey and Krishnaprasad, 2012), run on MATLAB R2012a (version 7.14).

Wingbeat frequency was calculated directly from the videos recorded at 2500 frames/second, as the reciprocal of the time taken between two consecutive wing supinations (Wakeling and Ellington, 1997a). The photographs of clipped wings were analysed in ImageJ (version 2.1.0/1.53c, National Institutes of Health,

Bethesda, MD, U.S.A.). We fitted a polygonal shape to the wing in the pair with the sharpest edges, using the inbuilt tool, and then measured the wing area. We also used the inbuilt angle tool to measure the wing angle relative to the body when extended anteriorly and posteriorly (**Fig. 4.S1**). The angle difference approximated the maximal stroke amplitude.

4.2.4. Dynamic analysis

Kinematic measurements were performed from smoothed trajectories, analysed offline using MATLAB R2018a (version 9.4). First, we quantified the trajectory angle of the active hunts. To calculate this angle, we took the initial portion of the killer fly's trajectory, from take-off to the first point of minimal distance to the target's trajectory. The killer fly's trajectory was fitted with a line using the method of least squares. The trajectories were then projected on a plane orthogonal to the take-off surface and crossing the target trajectory. The trajectory angle was calculated as the angle between the fitted line and an axis orthogonal to the take-off surface. Therefore, more horizontal dives were assigned higher angles and more vertical dives were assigned lower angles.

For each recorded trajectory, we calculated the three-dimensional vectors of velocity and acceleration as the first and second derivative of object position. The acceleration of gravity (9.8 m/s^2) was then subtracted from the vertical component of the total acceleration. The remaining three-dimensional acceleration was multiplied by the average fly mass, to obtain the flight force. Power was then calculated as the dot product of the flight force and the fly's velocity at each timepoint. For comparison with previous literature, we divided the power by the fly's flight muscle, to calculate the power density. To do this, we assumed 30% of the fly's mass to be devoted to flight muscle, as found in other *Schizophora* (Lehmann, 2001; Lehmann and Dickinson, 1997). We also calculated the aerodynamic wing power densities (profile power, P_{pro}, and induced power, P_{ind}). To do this, we identified correlations in the literature (Lehmann and Dickinson, 1997) between aerodynamic power and flight force, normalised by body weight. We redigitised the data reported and fitted a linear regression for both profile power and induced power. We then used the killer flies' flight force

magnitude, divided by the value of their body weight, to find P_{pro} and P_{ind} through the fitted regressions. The aerodynamic power, P_{aero}, was then calculated as the sum of the two aerodynamic powers.

Also for comparison, we approximated the Reynolds number (*Re*) for diving killer flies' wings (Ellington, 1984):

$$Re = \frac{2S}{\upsilon} n\Phi \qquad \text{Equation 4.1}$$

where S is the mean wing surface area, υ is the kinematic viscosity of air at 20°C ($1.53 \cdot 10^{-5}$ m^2/s (Montgomery, 1947)), n is the mean stroke frequency during dives, and Φ is the maximum stroke amplitude.

4.2.5. Steering model selection *

All flight simulations were run in MATLAB R2018b (version 9.1). The initial 5% of each hunt was discarded from simulations to account for irregularities of flight accelerations linked to the animals getting airborne. At the first time point of the simulations, the models were fed the target's position and the killer fly's position and velocity. Subsequently, simulations were only fed the target's relative position, used to calculate the steering, and the killer fly's relative linear acceleration, so that both killer fly and simulation had identical speed. In this chapter, we compared the steering dictated by pursuit to the steering of proportional navigation. We excluded models that require absolute target size and speed (**Table 4.S1**), because killer flies do not appear to use such measures (Wardill et al., 2015).

A pure pursuit system minimises the error (δ) between its heading and the virtual line connecting it to its target, called the line-of-sight (LOS). The controller thus induces a steering $\dot{\gamma}$ which corrects this error δ by an intrinsic constant k, according to formula:

$$\dot{\gamma} = k \cdot \delta \qquad \text{Equation 4.2}$$

After testing for a range of biologically plausible values (1 s^{-1} – 100 s^{-1}, **Fig. 4.1**), the intrinsic constant k was fixed at 20 s^{-1} for comparative purposes, as used in

* All steering model simulations were performed by Dr. Samuel T. Fabian (Fabian, 2019)

previous work on the killer fly (Fabian et al., 2018) and similar to the value measured in the lesser house fly (Land and Collett, 1974).

Proportional navigation (PN) uses the rotation of the LOS to the target to proportionally rotate the pursuer's heading (Shneydor, 1998). The model takes the form:

$$\dot{\gamma} = N \cdot \dot{\lambda} \qquad \text{Equation 4.3}$$

in which $\dot{\gamma}$ is the rotation of the pursuer heading, $\dot{\lambda}$ is the rotation of the LOS and N is a fixed gain, termed the navigation constant. After testing for a range of values (see results, section b), the navigation constant for simulations was fixed at N = 1.3, with a 20 ms lag between stimulus and response, matching the best fitting values from constant value sweeps from diving trials.

To test the performance of pursuit and PN in replicating the trajectories of hunts from the ceiling, we compared the axis of the heading rotation required by each steering control to the heading of real flies. In planar situations, these axes are either aligned or directly opposed. However, during 3D chases, the axes required of PN and pursuit do not necessarily align. Comparing the heading rotation of the models to real flies has the advantage of revealing inconsistencies even in case of added modulators in the pursuit paradigm (Eq. 4.2), such as the derivative or integral of the error δ proposed in other systems (Land and Collett, 1974). The steering controller which could best predict the real animals' flightpaths, PN, was then used for the remainder of the computational work.

To check for trajectory optimality, we used the range vector correlation (Fabian et al., 2018; Mischiati et al., 2015). We first calculated the vectorial difference between consecutive LOS and then extracted the angle between this difference vector and the corresponding LOS (**Fig. 4.S2**). The angle was then converted to a correlation value, ranging from 1 (no angle difference) to -1 (180° angle difference). During interception, collision is guaranteed for vector range correlations of -1, which indicate that LOS are parallel and getting shorter; however, values below 0 can still lead to interception.

Steering was limited to reflect hypothesised biological limits. The steering limitation was generated by fixing the maximal amount of lateral acceleration, i.e. the component of acceleration orthogonal to velocity, that the model could apply

to the simulated fly. Lateral acceleration (a_{lat}) was calculated in the manner below:

$$\left|a_{tang}\right| = a \cdot \hat{v} \qquad \text{Equation 4.4}$$

$$a_{tang} = \hat{v}\left|a_{tang}\right| \qquad \text{Equation 4.5}$$

$$a_{lat} = a - a_{tang} \qquad \text{Equation 4.6}$$

where a is the fly acceleration, $\hat{v}$ is the unit velocity vector and a_{tang} is the tangential acceleration, i.e. the component of acceleration parallel to velocity. Lateral acceleration was used as it represents the closest approximation of steering limitation available from the data, and is in keeping with engineering navigational literature (Shneydor, 1998).

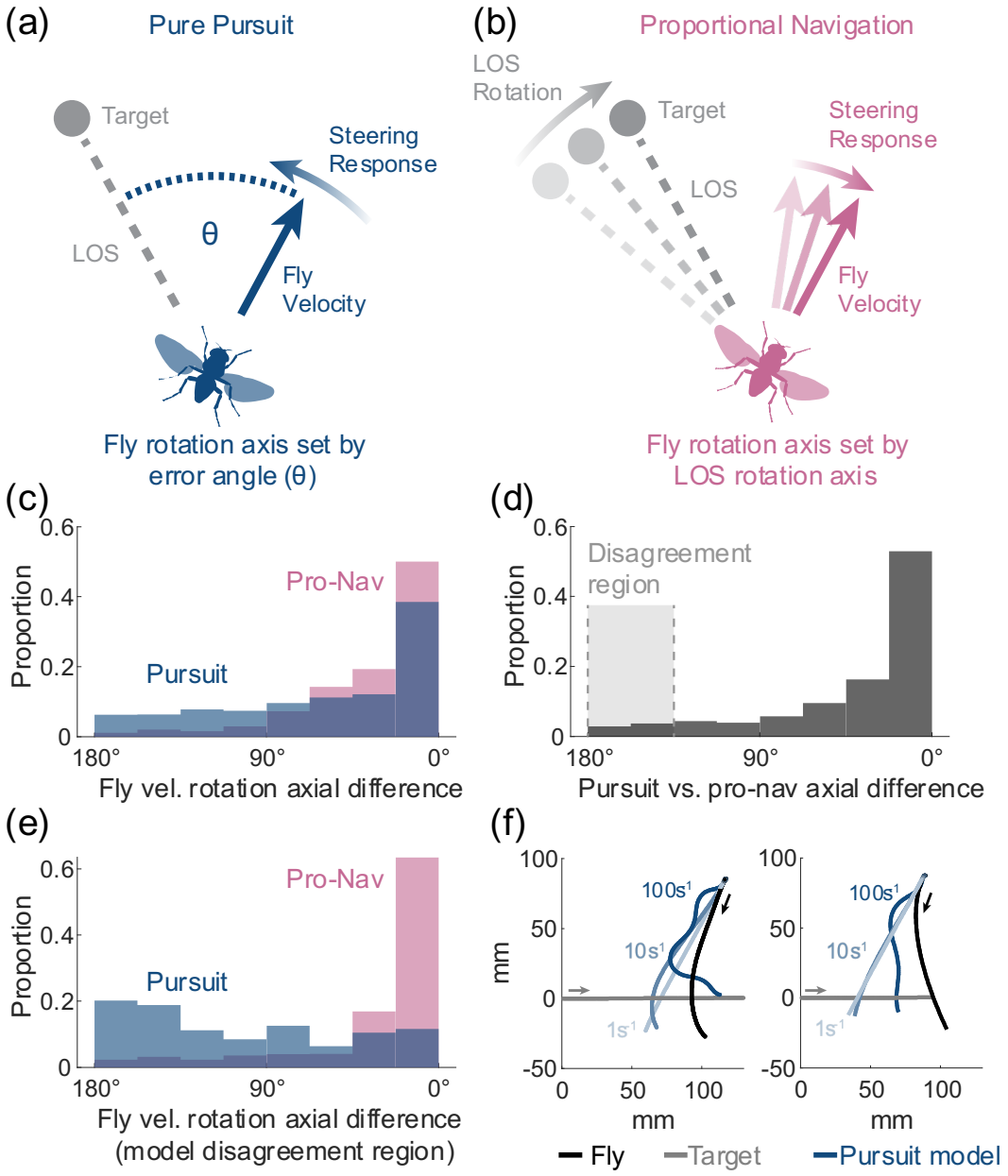

Figure 4.1. Axial comparison as a model selection criterion. Illustrations of (*a*) pursuit, and (*b*) proportional navigation steering toward a target. (*c*) The axial difference (angle between fly and model axes of turn) for pro-nav (*pink*) and pursuit (*blue*) (n = 7159). (*d*) The axial difference between pursuit and pro-nav. Shaded disagreement region shows where model axes of rotation are more than 130° opposed. (*e*) The axial difference between the fly and model axes of turn are given for the model disagreement region (n = 1057). (*f*) Example simulations of pure pursuit at varying gains encompassing biologically realistic values.

4.2.6. Mapping the outcome of the engagement geometry *

We questioned whether the variability in flightpath trajectories could be accounted for by the relative positions of the fly and target at the time of take-off, which we call the geometry of engagement. For this, we ran PN simulations, where the predator always initiated an attack from a ceiling 80 mm above a target that was travelling at 0.79 m/s from the origin, matching the conditions of real flights. The outcomes (according to metrics detailed in results) of simulated flights were then mapped across the 2D take off plane over an area encompassing all the recorded take offs: from 50 mm behind the target to 180 mm ahead and up to 110 mm on either side of it. Simulations were halted if the interceptor came within half a body length (2 mm) of the target. This threshold was arbitrarily chosen but reflects when the target would be within the grasp of the killer fly. Simulations were also halted if the killer fly height dropped 80 mm below the target, reflecting real flies that collided with the floor (**Movie 4.M1**).

Simulation maps were conducted under different kinematic regimes. Three alternative speed profiles were applied to the models, reflecting the mean speed profiles of killer flies taking off from the ceiling, wall, and floor of the arena. Steering limitations (see section above) were also applied to the relevant regime.

4.2.7. Data analysis and statistics

Statistical tests were run on R studio software, version 1.3.959, and R software, version 4.0.2 (R Core Team, 2017). In this chapter, mean ± standard error ($m \pm SE$) are used as descriptive statistics. Means, medians and standard deviations were calculated using the *pastecs* package. Variance homogeneity was tested using the Levene's test, within the *car* package. Significance value (p) was 0.05 for all tests, except where p values were adjusted; the circumstances of p value adjustment are specified below.

Correlations between variables were tested using Pearson's r tests, implemented in the *Hmisc* package. A linear regression model was fitted using the *stats* package to determine whether the initial LOS between killer fly and target

* All steering model simulations were performed by Dr. Samuel T. Fabian (Fabian, 2019)

(predictor variable) could explain the initial take-off angle of the killer fly (outcome variable). Comparisons between two datasets with heterogeneous variances were done using a Wilcoxon rank-sum test in the *stats* package. Multiple groups with heterogeneous variances were compared using a Kruskal-Wallis test, followed by post-hoc pairwise Wilcoxon comparisons with Hommel's adjusted p values, both in the *stats* package.

Steering model limitation was validated by a likelihood ratio test run in MATLAB R2018b (version 9.1), using the inbuilt function from the Econometrics toolbox.

4.3. Results

4.3.1. When attacking from the ceiling, killer flies accelerate with similar magnitudes in highly variable trajectories

When presented with targets, killer flies (*C. attenuata*) took off by extending the prothoracic legs, initiating wing flapping and detaching the pterothoracic legs from the arena surface, immediately aligning the body towards the target. The location killer flies took off from influenced the kinematics of the attack (**Fig. 4.2*a***). Killer flies performing a dive from the ceiling reached significantly higher accelerations (n = 44 flights, 17.9 ± 0.703 m/s^2) than killer flies taking off from the walls (n = 12 flights, 10.2 ± 0.332 m/s^2) or floor of the arena (n = 9 flights, 9.84 ± 1.01 m/s^2, Kruskal-Wallis test, $\chi^2(2) = 30.6$ $p < 0.001$), the latter two not having significantly different accelerations (p = 0.920). Interested in how and why such high accelerations are achieved, we analysed in more detail the angles (**Fig. 4.2*b***) and speeds (**Fig. 4.2*c***) of attacks initiated from the ceiling, which we termed dives.

When diving, all killer flies tested continuously flapped their wings at an average 303 Hz frequency (± 4.11, n = 15 flights), for the whole trajectory (**Fig. 4.S3**). The mean wing area of killer flies was 2.75 mm^2 (± 0.038, n = 20 animals) which, with a maximal stoke amplitude of 145°, means that killer flies' wings operate at an estimated Reynolds number of 276. Despite such a low Reynolds number, the impressive accelerations of diving killer flies led them to reach the height of the target's trajectory in 123 ± 3.96 ms. Although killer flies quickly

neared the target's trajectory, most of them (n = 41 flights) flew past it and failed to complete the capture (**Movie 4.M1**), meaning the success rate was 7%. We compared the diving flies to anaesthetised flies freely falling (**Fig. 4.2*d***). The peak accelerations of free falls (n = 12 flights, 9.01 ± 0.066 m/s^2) were significantly lower than the peak accelerations of the dives (Wilcoxon rank sum test; $W = 0$, $p < 0.001$). The peak accelerations across all dives (min: 11.4 m/s^2, max: 36.2 m/s^2) were higher than those from free falls (min: 8.61 m/s^2, max: 9.32 m/s^2), suggesting that gravity alone is insufficient to explain the killer fly's accelerations.

Observed dive trajectories were highly variable (**Fig. 4.2*b***). For example, some paths were profoundly curved, which placed the predator flying almost parallel to the target in the later stages of the attack (**Fig. 4.2*e***). At the other extreme, during some attacks killer flies flew almost perpendicularly to the target's trajectory (**Fig. 4.2*f***). We found that the take-off angle in the first 10 ms of the dive could be significantly predicted by the angle of the line-of-sight (LOS), the imaginary line between the fly and its target, at the moment of take-off (R^2 = 0.80, $F(1,42) = 165$, $p < 0.001$). The regression (**Fig. 4.S4**) had intercept -17° (SE = 3.01, $p < 0.001$) and slope 0.97°/s (SE = 0.076, $p < 0.001$). Therefore, although killer flies could manipulate the initial LOS by timing their take-off, they seemed to initiate the attack with a constant 17° lead over their target. The killer fly's dive angle relative to gravity (15.0 ± 1.87 °) was not however significantly correlated to the peak acceleration of the dive (Pearson's correlation, r = 0.12, p = 0.455).

The much higher accelerations recorded in dives from the ceiling compared to other attacks and free falls, together with sustained wingbeat frequencies throughout the dives, indicate that downward attacks were not powered by gravity alone. Killer flies could time their take-off to target position, thereby influencing the angle of their dive. However, dive angle was not correlated with the magnitude of the accelerations, meaning that flies accelerated independently of dive inclination.

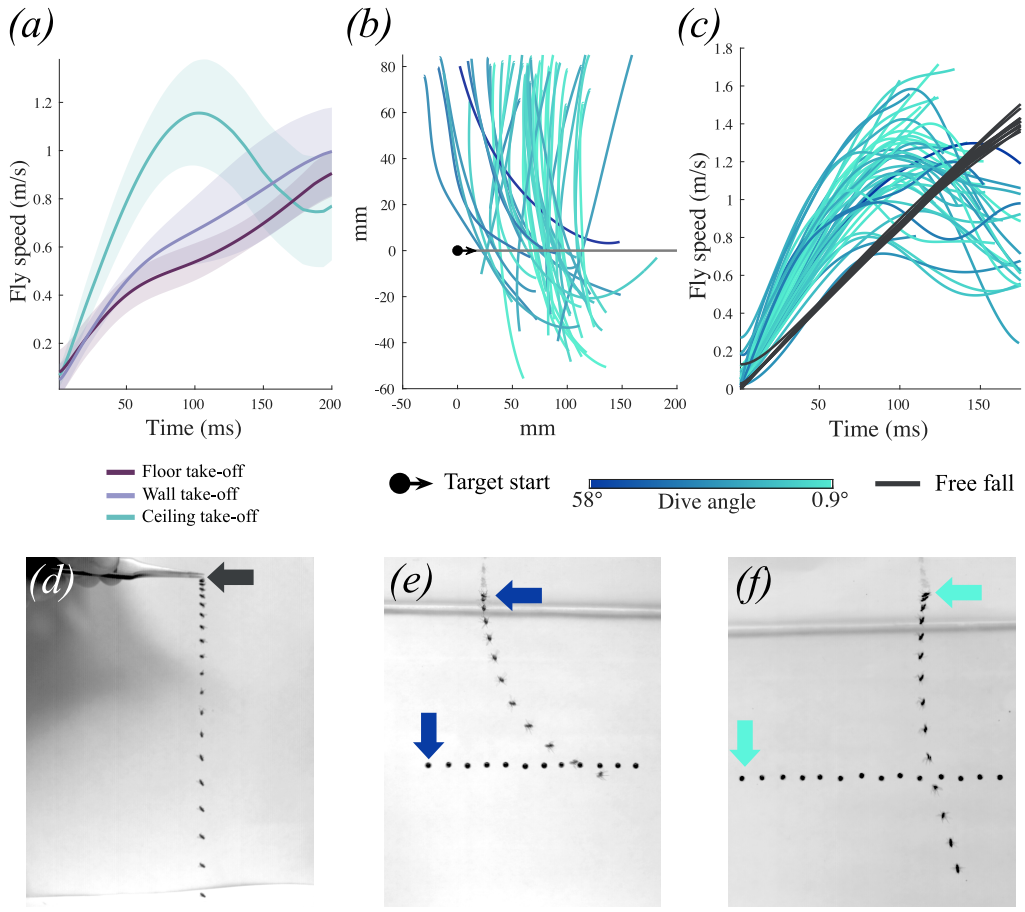

Fig. 4.2. Flies accelerate towards prey when diving downwards, with accelerations independent of dive angle. (*a*) Mean speed of killer flies taking off from the ceiling (*n* = 44, blue), wall (*n* = 12, lilac) or floor (*n* = 9, purple) of the arena. Shaded areas represent ± standard deviation. (*b*) Side view of the ceiling dives trajectories (blue lines) normalised for target position (black circle) and direction (arrow) at take-off. The intensity of the blue lines has been adjusted to dive angle, with lighter blues indicating more vertical dives, i.e. dives with lower angles. (*c*) Speed of individual killer flies diving towards prey (blue lines, colour-coded for trajectory angle) and anesthetised killer flies dropped from the same height (n = 12, black lines). (*d-f*) Superimposed fly and target positions (shown every 10 ms) during *(d)* a free fall of an anaesthetised fly, *(e)* a dive with a low angle and *(f)* a dive with a high angle. Arrows indicate initial positions in the sequence.

4.3.2. Dive kinematics can be replicated using lateral acceleration-limited proportional navigation

Differences between attacks from the arena ceiling and attacks from the walls and floor could be due to either a different navigational strategy employed during dives, or to a different interaction of the same navigational strategy with the environment. We implemented models of pure pursuit and proportional navigation (PN) to compare to the dives performed by real animals (**Fig. 4.1a-b**). Overall, PN was a better predictor of the steering response of real flies (PN axis alignment: 35.3 ± 0.425 °, pure pursuit: 57.4 ± 0.643 °, Wilcoxon rank sum test; W = 20.9 x 10^6, p < 0.001), but the rotation axes of PN and pursuit were predominantly aligned (**Fig. 4.1c**). We therefore repeated the analysis on the timepoints of the data where the two navigational model axes were directionally opposed by over 130° (**Fig. 4.1d**). In this region, PN greatly exceeded the explanatory capacity of pursuit (**Fig. 4.1e**). As found for other attacks, pursuit neither reproduces nor explains the kinematics of killer fly interception, with the simulated fly deviating early from the true flight course and failing to lead the target heading, irrespective of gain tuning (**Fig. 4.1f**). This is qualitatively evident from comparing our candidate models (pursuit and PN) to real flightpaths (**Fig. 4.3*a***), quantified in the angular difference between the models and recorded dives (**Fig. 4.3*a***).

If killer flies do follow PN even when diving from the ceiling, they should keep a collision course by having negative range vector correlations. We compared the range vector correlation between diving killer flies and flies taking off from the arena wall and floor (**Fig. 4.3*c***). Although all attacks started with negative range vector correlations, the range vector correlations of attacks from the ceiling turned positive as time progressed, suggesting a failure to maintain an interception course. This failure suggested that the flies either were unable to meet the steering requirements of interception or had lost interest in the target. To quantify the steering effort required, we used lateral acceleration. Using lateral acceleration as a limit of the heading rotation of the fly, we could factor in the effect of the speed at which the fly was travelling (an equivalent lateral acceleration at low speeds will generate greater turning response than at high speeds). We calculated the

lateral acceleration required to steer the bare minimum (N = 1, below which a collision course is not steered) course toward the target using model steering simulation and the speed of the fly, for flights taking off from the floor, wall, and ceiling (**Fig. 4.3*d***). We found that the required lateral acceleration differed depending on the take-off position (Kruskal-Wallis test, $\chi^2(2) = 20.6$, $p < 0.001$), with higher accelerations in attacks from the ceiling (21.9 ± 1.40 m/s^2) compared to attacks from the wall (13.5 ± 1.55 m/s^2, post-hoc comparisons, $p = 0.009$), whose acceleration was in turn higher than attacks from the floor (9.25 ± 1.00 m/s^2, $p = 0.049$). We then calculated the lateral acceleration output of the real flies throughout their trajectory and found that the type of surface that flies took off from affected the lateral accelerations they produced (**Fig. 4.3*e***, Kruskal-Wallis test, $\chi^2(2) = 2799$, $p < 0.001$). In flights from the ceiling, killer flies had higher lateral accelerations (12.1 ± 0.057 m/s^2) than their wall (8.31 ± 0.074 m/s^2, $p < 0.001$) and floor counterparts (6.70 ± 0.088 m/s^2, $p < 0.001$). The mean lateral acceleration requirements of PN with a low N = 1 (killer flies previously found to have N ≈ 1.5 (Fabian et al., 2018)) are frequently higher than the population of lateral accelerations generated by the fly. This suggests that this may be the limiting factor on the fly.

Parameter estimation (**Fig. 4.3*f-g***) was applied by sweeping biologically realistic values of lateral acceleration limit (from 0 to 40 m/s^2), N (from 0.1 to 5), and time delay (from 0 to 40 ms). The best fitting value for the lateral acceleration limit (15 m/s^2) was in keeping with the mean measured fly lateral acceleration of 12 m/s^2. We secondarily validated the limited model by testing the goodness-of-fit of the pure PN model and the limited PN model, which confirmed that the limited model was still the most probable, despite the additional term (likelihood ratio test, $\chi^2(1) = 12.4$, $p < 0.001$). The angular difference of PN and limited PN from real trajectories (**Fig. 4.3*a***) shows that the deviation in PN, predominantly occurring in the latter section of the flight, was reduced in the limited PN model. Similarly, simulations comparing limited PN to pure pursuit and PN (**Fig. 4.3*b***) show that, while pure PN simulations quickly compensate for their overshooting the trajectory, the limited model matches the fly in continuing to overshoot the target downwards.

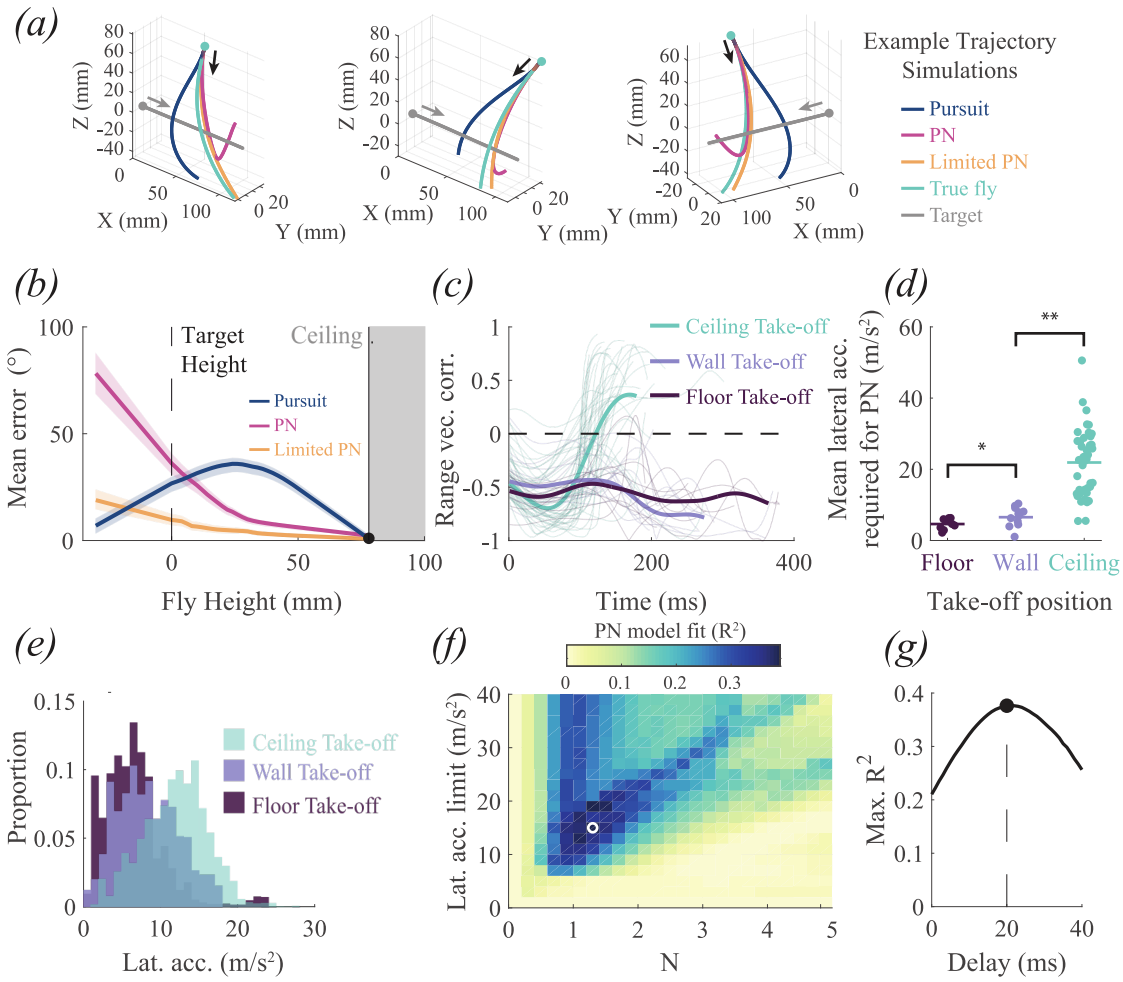

Fig. 4.3. (*a*) Three example simulations of the pure pursuit (dark blue), proportional navigation (pink), and limited proportional navigation (orange) models, compared to the trajectory of real flies (light blue). Arrows indicate direction of movement. (*b*) Angular error of the velocity vector between true flies and each of the model alternatives, plotted against the fly height, 0 being the target height and 80 being the ceiling height. (*c*) Range vector correlation of real killer fly attacks, colour-coded according to take-off positions. Mean lines are given in bold. (*d*) The mean lateral acceleration required to complete a minimal proportional navigation (PN with N = 1) toward the target for simulated flights, binned by take-off position. Significance values: * = $p < 0.05$, ** = $p < 0.01$. (*e*) Histograms of the lateral acceleration produced by flies starting in different positions. (*f*) The gain fitting map for proportional navigation gain (N) and the limit of lateral acceleration, coded by coefficient of determination. White circle denotes peak fit. (*g*) Peak fit of the PN model for time delay.

4.3.3. Killer flies take off in region that should lead to shortest trajectory, but are impaired by limited lateral acceleration

When performing dives, killer flies often missed their targets and overshot (**Fig. 4.4*a***). The modelled flights with different starting points along the virtual ceiling demonstrate that there is a virtual edge beyond which flies are unable to contact the target on a first pass (**Fig. 4.4*b***). After this edge, when the lateral acceleration is unlimited, the modelled flies turn a full tight loop and return to a near-collision course with the target. Simulations with limited lateral acceleration also have the same edge, beyond which flies are unable to loop as sharply. In this condition, the flies can only turn onto a collision course with the target once they are far below it.

We took the mean speed profiles of killer flies attacking from the different arena surfaces (ceiling, wall, and floor) and tested simulation models starting at the same positions as real killer flies taking off from the ceiling (n = 44 flights). We separately tested novel positions, with even spacing across the take-off plane, under the speed regimes of attacks from the ceiling, wall, and floor. We found that the trajectory angle (**Fig. 4.4*c***) was near equally well explained by both the PN models, unlimited (Pearson's correlation, $r = 0.63$, $p < 0.001$) and limited ($r = 0.64$, $p < 0.001$), when given the ceiling-launch speed profile ($R^2 = 0.40$, $R^2 = 0.42$ respectively). When given speed profiles of attacks from the walls or floor, the simulated dives were less steep than the real dives, with 93% and 95% of simulations respectively less steep than recorded dives. This demonstrates that speed is a key component of why killer flies' dives are so vertical.

We calculated the model's overshoot up to maximum 80 mm, as in the real arena, for the different conditions (**Fig. 4.4*d***). Using the unlimited model, minimal overshoot was generally a product of proximity to the target's start, and the flies' starting positions are generally within an area of small overshoot (< 20 mm). However, when the model has limited lateral acceleration, much of the area ahead of the target generates simulations that overshoot until they hit the floor (80 mm). This area encompasses most of the measured dives. This difference suggests that the modest overshoot of the unlimited model is a product of the model being able to use great lateral acceleration to steer out of the dive, which the limited model

and real flies are unable to do. When the models have the kinematic regime as flies taking off from either the walls or floor, the maximum overshoot area is largely absent, bar a much smaller region ahead of the target.

We quantified the point of 'first pass' by a minimum of distance between target and fly in the first 300 ms of the trajectory (**Fig. 4.4*e***). We mapped the time to first pass for each modelled starting position and found that the shortest times taken for first pass were close to the flies' mean take off location. The minimum time to first pass location and time taken varied between models, as minimal times for attacks from the wall and floor were longer and further forward. This is reflected by real killer flies, which first passed the target much sooner when taking off from the ceiling (112 ± 29 ms) than when taking off from the wall (286 ± 61ms) and floor (311 ± 71 ms). The starting position of real flies was in all cases close to the simulated area of minimal time to first pass.

We also calculated the time to contact in the whole trajectory with an upper limit of 2 s (**Fig. 4.4*f***). When using the unlimited model, this coincided with the area of minimal time to contact. However, in the limited simulation, a 'no-hit' region formed in which simulations inevitably overshot targets instead of making contact with them on first attempt. In the simulation with speed regimes of flies taking off from the walls and floors, the 'no-hit' region shrank, leaving a larger overlap between the areas of minimum time to contact and those of minimum time to first pass.

When attacking from the ceiling, killer flies seemed therefore to take off in the area of minimal time to first pass despite their limitations in lateral accelerations producing a large overshot, which severely affected the time taken to capture the target.

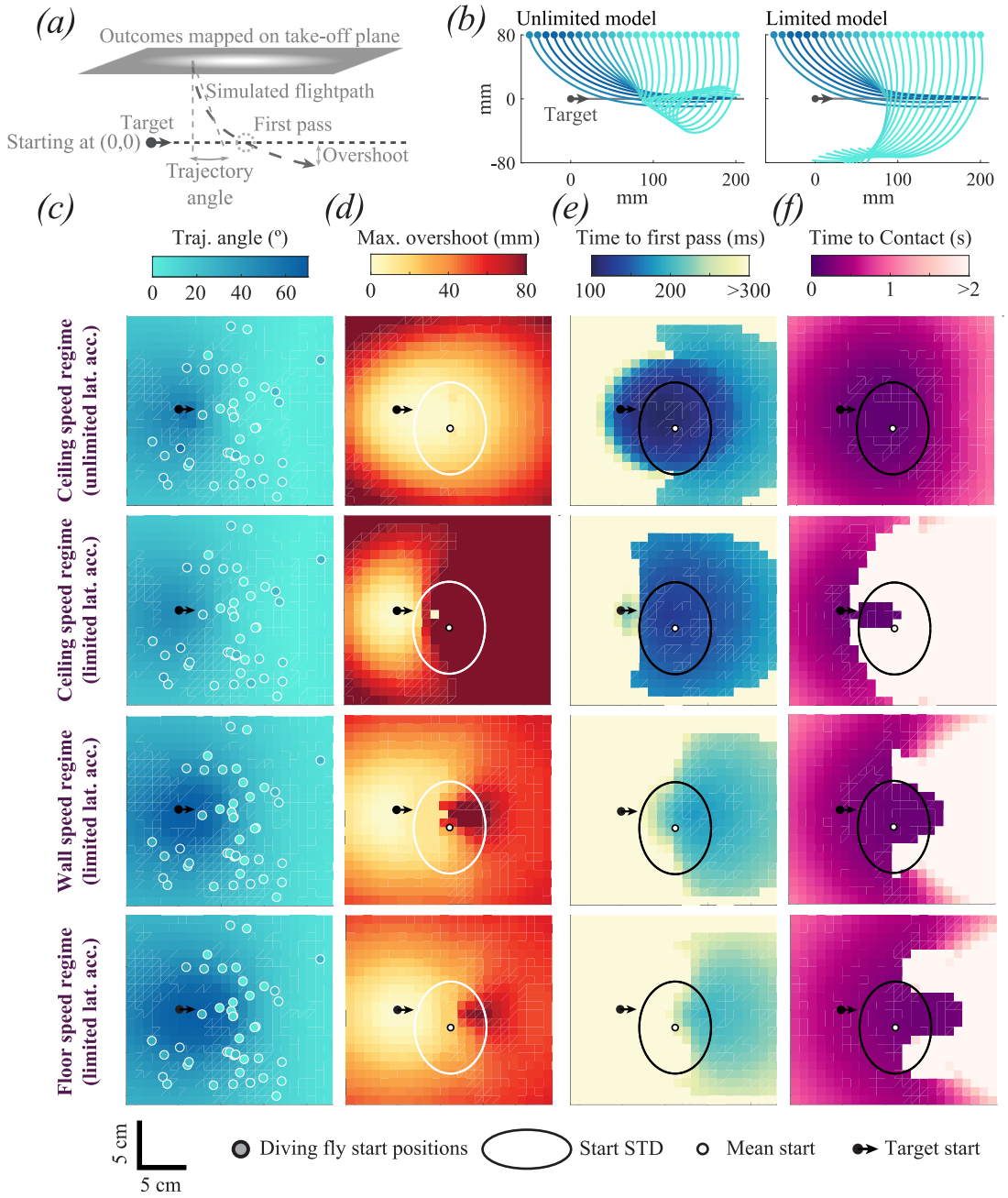

Fig. 4.4. (*a*) An illustration of key terminology for the figure. (*b*) Simulations (blue lines) dropping directly above the target (black dot) and displaced along the target-travel axis are shown for unlimited PN (*left*) and PN with limited lateral acceleration (*right*). (*c-f*) Maps of the flight outcomes, by different metrics (columns), of simulations under different lateral acceleration and speed regimes (rows). Coloured dots in (*c*) represent real killer fly take-off positions in ceiling dives (n = 44), white dots in (*d-f*) denote mean starting position of true flies, while ellipse denotes ± standard deviation of starting positions. Rows represent models with alternative kinematic regimes: unlimited lateral acceleration (*top row*) and limited lateral acceleration (*upper middle row*) models with simulated speed equal to the mean speed of killer flies attacking from the arena ceiling, limited lateral acceleration models with the speed of attacks from the wall (*lower middle row*), limited lateral acceleration models with speed of attacks from the floor (*bottom row*). Columns display metrics of simulation and real outcomes: (*c*) The resulting dive angle is mapped

across the starting plane. Markers give true fly starting positions of diving flies, and measured dive angles. (*d*) The maximum overshot distance of the simulation below the target is mapped across the starting plane. (*e*) The time to first pass is mapped across the starting plane. (*f*) The time taken to contact the target is mapped across the starting plane.

4.3.4. Killer flies maintain wing force magnitude during dives, producing higher aerodynamic power than attacks from the walls or floor of the arena.

The navigational model suggests that initiating a dive with some time delay leads to a reduced time to contact, although killer flies prefer to take off in the area of minimum time to first pass. We therefore tested if more vertical trajectories might be energetically more advantageous, requiring less force or power to be completed.

The acceleration of gravity was subtracted from the vertical component of the dive to isolate the acceleration produced by the fly. We multiplied the resulting acceleration by the killer flies' body mass (2.79 ± 0.056 mg, n = 45 animals), to calculate the force exerted during the dives. The mean force produced (38.1 ± 1.29 μN) was not significantly correlated with dive angle (Pearson's correlation, r = 0.23, p = 0.130, **Fig. 4.5*a***). The force produced initially decreased and subsequently increased during the dives. This further supports the proposition that flies try to maximise force production in the late stages of their attack to match the requirements of PN. This increase came mostly from a change in vertical dive force, which went from downwards, to zero, to upwards (**Fig. 4.5*b***). In contrast, the lateral flight force was more constant throughout the dive (**Fig. 4.5*c***), presumably near the fly's maximum capacity.

Wingbeat frequencies were relatively steady throughout the dive (**Fig. 4.S3**), suggesting that increases in force production might be achieved in other ways. Mean wingbeat frequencies (303 ± 4.11 Hz, n = 15 flights) were also not significantly correlated with dive angle (Pearson's correlation, r = -0.1, p = 0.731). At the beginning of the dive, killer flies directed their flight force directly downwards, but this vector was subsequently rotated to a horizontal orientation, and upwards in the later stages of the dive (**Fig. 4.5*d***). The dive angle was significantly correlated to the time at which the force vector change orientation

from downwards to upwards (Pearson's correlation, r = -0.61, p < 0.001), meaning that flies engaged in more vertical dives started directing force upwards later.

We calculated the power produced throughout each dive as the dot product of the flight force and the flight velocity (**Fig. 4.5*e***). The dive angle did not correlate with either the maximum positive power needed throughout the dive (13.9 ± 1.11 μW, Pearson's correlation, r = -0.12, p = 0.445), or with the maximum negative power needed to perform the total dive (-36.8 ± 3.05 μW, Pearson's correlation, r = -0.04, p = 0.801). Similar amounts of flight power were therefore required to perform dives in different directions, suggesting that dives with lower angles are as energetically expensive as dives with higher angles.

Although similar flight force and power are required for dives of different angles, the extreme accelerations produced in more vertical dives could have some advantages, such as the production of higher aerodynamic power. We compared the flight power of attacks starting from the ceiling, walls and floor of arena (**Fig. 4.5*f-h***). We used total flight power, minus the contribution of gravity, as an indication of the power that could be generated by the wings. We also calculated the profile (P_{pro}), and induced (P_{ind}) power density in dives from the ceiling, walls and floor, using the flight force (Lehmann and Dickinson, 1997). To compare flight and aerodynamic powers more easily, we recalculated the flight power from our attacks as power density, by dividing the flight power by the flight muscle mass, approximated as 30% (see methods) of the fly's average mass (2.79 mg).

The flight power density reached maximum absolute values of 43.4 ± 3.10 W/kg when flies took off from the ceiling (n = 44 flights), 19.2 ± 2.00 W/kg when taking off from the walls (n = 12 flights), and 28.9 ± 3.95 W/kg when taking off from the floor (n = 9 flights), a difference which was significant (Kruskal-Wallis test, $\chi^2(2)$ = 25.8 p < 0.001). Moreover, peak power was reached earlier in dives from the ceiling (121 ± 5.62 ms), than in dives from the walls (192 ± 22.9 ms) and floor (184 ± 26.9 ms) of the arena, also a significant difference (Kruskal-Wallis test, $\chi^2(2)$ = 17.4, p < 0.001). Peak power timing was significantly different between dives starting from the ceiling and attacks from the arena walls and floor, but the latter two did not have a significant difference (post-hoc comparisons, p = 0.002, p = 0.005, p = 0.804, respectively).

The peak aerodynamic wing power was also higher in dives from the ceiling (152 ± 7.68 W/kg) than in attacks taking off from the walls (120 ± 5.74 W/kg) and floor (115 ± 2.51 W/kg) of the arena. This difference was also significant (Kruskal-Wallis test, $\chi^2(2) = 11.1$, $p = 0.004$, post-hoc comparisons, $p = 0.026$ and $p = 0.019$, respectively). The peak power of attacks from the arena walls and floor was not however significantly different ($p = 0.546$).

Dives from the ceiling therefore reached higher absolute flight and aerodynamic power than attacks from the walls or floor of the arena. The absolute flight power was also reached sooner in dives from the ceiling.

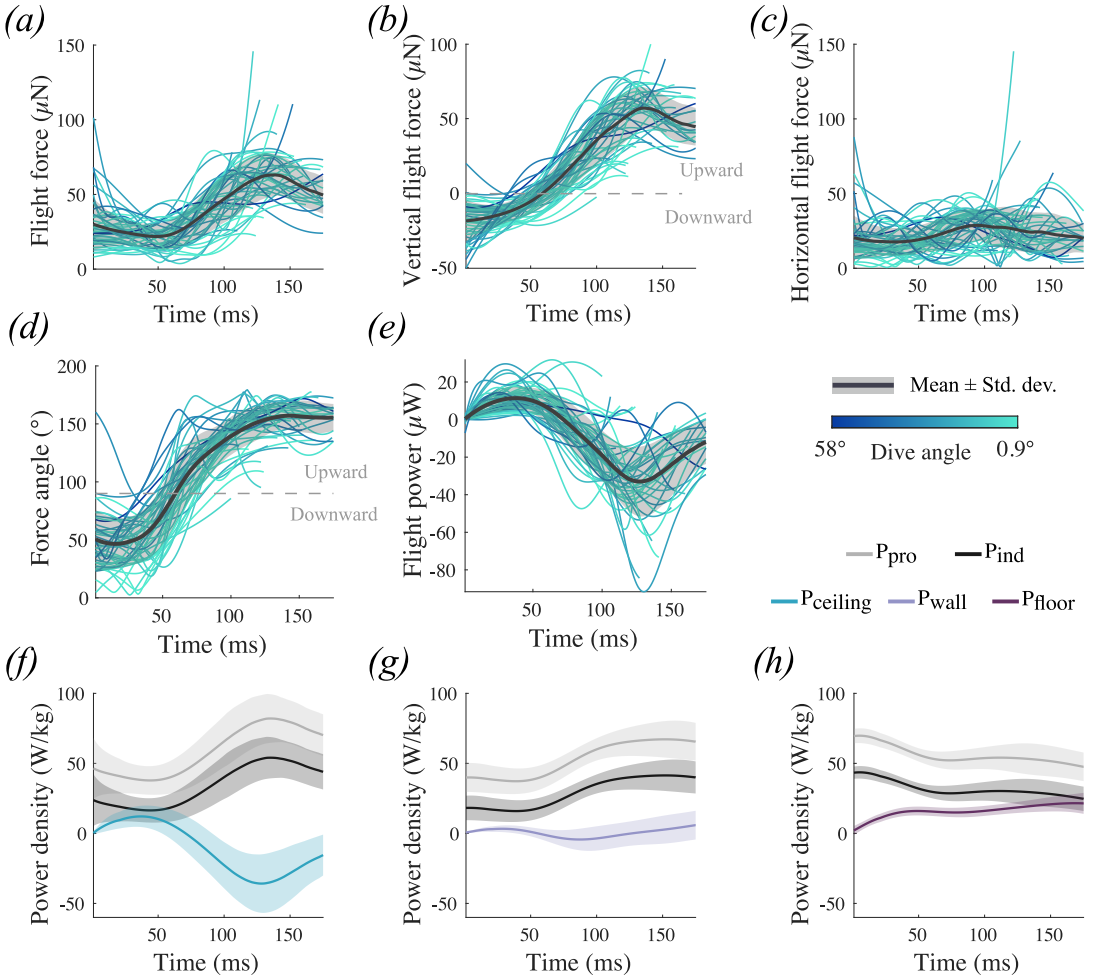

Fig. 4.5. (*a*) Flight force magnitude over time across all dives. (*b*) Vertical component of the flight force. Upward force is shown as positive, downward force as negative. (*c*) Lateral component of the flight force. (*d*) Orientation of the wing force vector over time for all dives. Angles below 90° indicate downward-oriented force vectors, 90° angles indicate horizontal forces, angles above 90° indicate upward-oriented vectors. (*e*) Flight power over time across all dives. (*f*) Flight power density (blue) and wing aerodynamic power densities (grey) of attacks from the ceiling. (*g*) Flight power density (lilac) and wing aerodynamic power densities (grey) of attacks from the wall. (*h*) Flight power density (purple) and wing aerodynamic power density (grey) of attacks from the floor. The aerodynamic power density in *f-h* has been decomposed into profile power (P_{pro}, light grey) and induced power (P_{ind}, black).

4.4. Discussion

Our results show that killer flies (*C. attenuata*) respond to targets presented below them by diving down towards them. When taking off from the ceiling of the arena, killer flies reached much higher accelerations than when taking off from the floor or walls, or indeed when in free fall (**Fig. 4.2**). Killer flies beat their wings at similar frequencies independently of dive angle, thereby producing flight forces of similar magnitudes; their speed is therefore determined by both gravity and wing power. During the downward hunts from the ceiling, killer flies averaged an acceleration of 18 m/s^2, with some individuals reaching accelerations that were larger than 30 m/s^2. Compared with diving raptors, which achieve accelerations of 6.8 m/s^2 (Ponitz et al., 2014), the killer fly demonstrates itself to be an impressive aerial predator. These accelerations are achieved even though killer flies' wings operate at intermediate Reynolds numbers ($\sim 3 \times 10^2$). This figure is just above that calculated for fruit flies (*D. virilis*, 200 (Vogel, 1967), *D. melanogaster*, 128 (Dickinson and Götz, 1993)) and considerably lower than the dragonfly (700-2400 (Wakeling and Ellington, 1997b)), highlighting the high viscous forces killer flies experience despite high success rates in the wild (Bonsignore, 2016).

4.4.1. Limited proportional navigation as steering controller

To understand how killer flies control their trajectories during these high acceleration dives, we tested and modelled the control algorithm that could steer killer flies during attacks. We implemented navigational models of proportional navigation (PN) and pure pursuit. By comparing the axis of the heading rotation for each model to the heading of real flies, we excluded the modified pursuit paradigms with added modulators. Another way of developing interception-type flightpaths is using the principle of deviated pursuit, when the pursuer attempts to steer ahead of the current target position by a set lead. The optimal lead is determined by the velocity of the target relative to the pursuer, and angles other than the optimum will lead to a first pass miss of the target (Shneydor, 1998). Deviated pursuit models have been put forward as the underlying algorithm driving the conspecific flights of hoverflies (Collett and Land, 1978), and blowflies

(in the elevation plane only) (Varennes et al., 2020), however in these cases the pursuer is able to rely on assumed knowledge of target size and speed, information which is unlikely to be available to a generalist predator which hunts a variety of different targets including conspecifics, like killer flies. A final possible interception model could be the forward models proposed for head stabilisation in dragonflies, able to correct not only their attitude adjustments (e.g. body roll), but also the parallax of relative translation (Mischiati et al., 2015). Such findings assume internal models of target speed and suggest that dragonflies may have a preconceived flight-plan. We find it unlikely that killer flies use a flight-plan to guide themselves. Killer flies have been demonstrated to rely on an angular size/speed ratio match to determine likely targets, resulting in them chasing after unsuitable targets that match the desired ratio (Wardill et al., 2015). This finding suggests that killer flies do not rely on target speed assumptions for predation, information that would be necessary to effectively compute the course to the target, therefore leaving only pursuit and PN as suitable models killer flies might use to control steering. Our findings agree with previously published conclusions (Fabian et al., 2018), that killer flies are unlike flies that only chase conspecifics, and do not use pursuit (Land and Collett, 1974; Wagner, 1986), but instead use proportional navigation with a gain (N) of ~1.3 and time delay of ~ 20 ms. Killer flies share this controller with other aerial predators, such as certain robber flies and raptors (Brighton and Taylor, 2019; Fabian et al., 2018).

Our results suggest that PN, combined with the speed of the target, the high speed of diving flies, and the initial geometry, frequently leads to near vertical attacks. While pure PN generally explains the initial steepness of the dive, it differs substantially as the fly approaches the height of the bead, curving back up after overshooting the target (**Fig. 4.3**). Performing this manoeuvre requires extremely large lateral acceleration. After limiting the lateral acceleration of the simulations, the model also overshoots the target in a similar fashion to that observed in the flies, and we find this lateral acceleration limit to be in the region of 15 m/s^2, although measured fly lateral accelerations do occasionally reach up to 20 m/s^2. Future work would benefit from closer examination of the flies' orientations during flights. This might give a clearer picture of steering limitations by

comparing potential planes of rotation and the limits of force generation. If a link is found between manoeuvre type and limitation, we might expect killer flies to adjust their flight posture to maximise their turning capabilities, e.g. rolling to increase pitch or yaw components during rotation. Lateral acceleration limits may also vary with flight speed, resulting in a more complex picture, beyond the scope of this work to illustrate.

4.4.2. Take-off timing

In our experiments, a trial was started whenever a killer fly was resting anywhere on a surface of the arena. Once the target was detected, killer flies could affect the distance to target at take off by choosing the timing of their take-off. We cannot know if the flies 'wait' for the target to approach a specific region, or if their visual target detection system matches a filter for objects passing through a specific region. Previous work (Fabian et al., 2018) has shown that killer flies predominantly take off while their target is coming toward them (as seen in dragonflies (Lin and Leonardo, 2017)), and in the position that would lead to minimal time to contact. Similarly, we found that killer flies take off within the region with minimal time to first pass. This behaviour puts them in the large overshoot region when travelling at the high dive speed, resulting in extremely long times until final contact (**Fig. 4.4**). Further experiments should test dives towards targets travelling at a range of speeds. Such data would allow us to determine whether killer flies adjust their take off timing according to the target's speed, and to what extent the target overshoot during dives is a product of the specific bead speed used in our experiments (0.79 m/s). In our experiments, killer flies took off with a constant 17° lead over the initial target position when attacking from the ceiling. Further analysis would also test whether this take-off angle is intrinsic to the killer fly or whether it depends on prey speed.

Killer flies could take off later and avoid the large overshoot region. This would lead to attacks which are energetically as expensive, but with reduced time to contact. Therefore, not accounting for the added acceleration of gravity when attacking from above could be seen as maladaptive. Steep dives may not occur in the wild, or at least not often enough to produce a selective pressure, as killer flies

have not been observed standing on the underside of leaves. However, killer flies often take off from a variety of elevations relative to their prey, attacking prey flying above as well as below them. Previous modelling of the killer fly's attack strategy has shown that it is highly successful (Fabian et al., 2018), but the effect of chasing prey flying lower than the killer fly was not investigated.

4.4.3. Potential advantages in early take-off

If it were to occur in the wild, a steep dive may not be a hindrance. Firstly, the high speeds and accelerations reached during a dive produce high aerodynamic power on the wings early in the dive, compared to attacks from the side or below the prey (**Fig. 4.5**). This power can be used to assist prey capture especially when chasing erratic prey. It is worth noting that we use a flight muscle ratio (Lehmann, 2001) and linear relationships with flight force (Lehmann and Dickinson, 1997) calculated in other *Schizophora* species to calculate aerodynamic power densities, meaning that the absolute values we present might be inaccurate. A thorough investigation of the wing kinematics in flight might confirm or correct the absolute values given in the present article. However, the pattern of the power profiles is unaffected by these inaccuracies, allowing a comparison of these contributions between attacks from different arena surfaces.

Even if the advantage given by high aerodynamic power was irrelevant, a steep dive provides the possibility of an extremely quick capture (**Movie 4.M2 and Fig. 4.S5**). In the 93% chance of a miss, the fast-approaching predator is likely to be detected by the prey as a big looming visual stimulus. Looming stimuli cause collision avoidance manoeuvres, which briefly reduce the horizontal velocity of the turning prey as the flight inertia is used to generate angular acceleration (Fry et al., 2003; Tammero and Dickinson, 2002). The prey therefore trades speed for increased path tortuosity. Killer flies seem to have adapted to catch such evasive prey; their low PN constant has been suggested as a way to optimise erratic target interception (Brighton and Taylor, 2019; Fabian et al., 2018). By accelerating towards their prey and creating a fast looming stimulus, killer flies might turn their target's escape manoeuvres to their own advantage (**Movie 4.M3 and Fig. 4.S6**), as some aerial (Jabłoński, 2001) and aquatic (Catania, 2009) vertebrate predators

do. This is because, after missing the target in their first dive, killer flies can launch a second attack, at a much reduced distance from the target.

This suggests that there might be another, more subtle reason for not taking into account the direction of gravity in downward attacks. Killer flies are unusual insect predators in that they can chase prey from above, whilst most other aerial insect hunters chase from below (Olberg et al., 2000; Wardill et al., 2017). The difficulty of hunting prey against the cluttered ground is exacerbated by the coarse resolution of the killer fly eyes (Gonzalez-Bellido et al., 2011), which is poor even relative to other predators with compound eyes (Horridge, 1978; Rossel, 1979; Sherk, 1978; Wardill et al., 2017). Under such conditions, diving towards prey at high speed could be beneficial, despite the associated drop in manoeuvrability: by reducing the distance to their targets, killer flies also increase the target's angular size on their retina, which would in turn make it less likely to lose track of it. Killer flies may therefore prioritise not losing sight of their prey, at the expense of flight duration. Thus, an apparently energy-inefficient attack strategy may still be adaptive when considering the need to keep visually tracking the prey.

4.5. Conclusions

Overall, our results show that PN is, in principle, an effective guidance law even when hunting from inverted positions, but not taking into account physical constraints in lateral accelerations decreases its effectiveness. Nevertheless, the effects of not accounting for the direction of gravity during downward dives may hypothetically be compensated by some advantages, such as the quick production of high aerodynamic power in the wings, forcing the potential prey to slow down and manoeuvre, and potentially improving visual tracking.

4.6. Supplementary Information

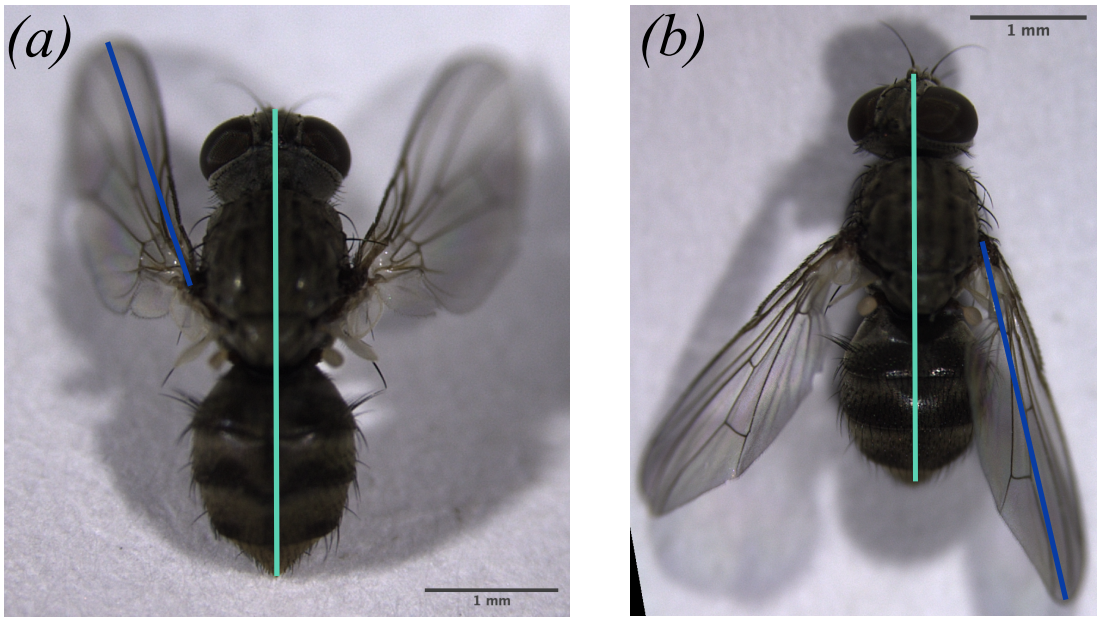

Fig. 4.S1. Illustrative examples of maximum stroke amplitude calculation. (*a*) Body (light blue) and wing (dark blue) axes when the wing was rotated anteriorly. (*b*) Body and wing axes when the wing was rotated posteriorly. The difference between the two angles was used as an approximation of maximal stroke amplitude.

Table 4.S1. Alternative candidate underlying models for killer fly navigation, with model inputs, axis of effect, and overall model evaluation.

Guidance Model	**Model input requirements**	**Axis of turn**	**Evaluation**
Pure Pursuit	LOS	Orthogonal to plane of LOS and current heading	Does not explain the killer fly's heading lead over the target. Does not match fly's axis of rotation.
Deviated Pursuit	LOS, lead	Orthogonal to plane of LOS and current heading	Fixed leads do not match measured trajectories. Does not match fly's axis of rotation.
Derivative/Integral Pursuit	LOS, egocentric LOS rate	Orthogonal to plane of LOS and current heading	Does not match fly's axis of rotation.
Proportional Navigation	Exocentric LOS rate	Orthogonal to plane of successive LOS	Previously published work demonstrates the model power in explaining killer fly interception. Most likely candidate.
Forward Prediction / Optimal Heading Computation	Assumed target velocity	Orthogonal to plane of optimal heading and current heading	Killer flies rely on external, not assumed, speed of their targets, lacking the information needed for such models.

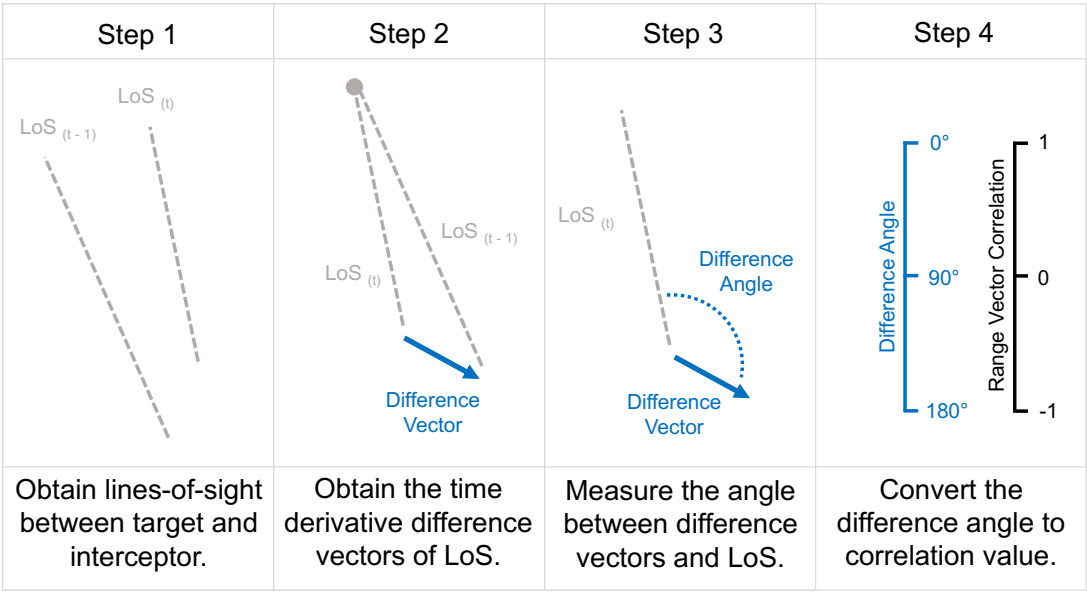

Figure 4.S2. Schematics explaining how to obtain range vector correlations from lines-of-sight between two animals. (Taken from Fabian et al., 2018.)

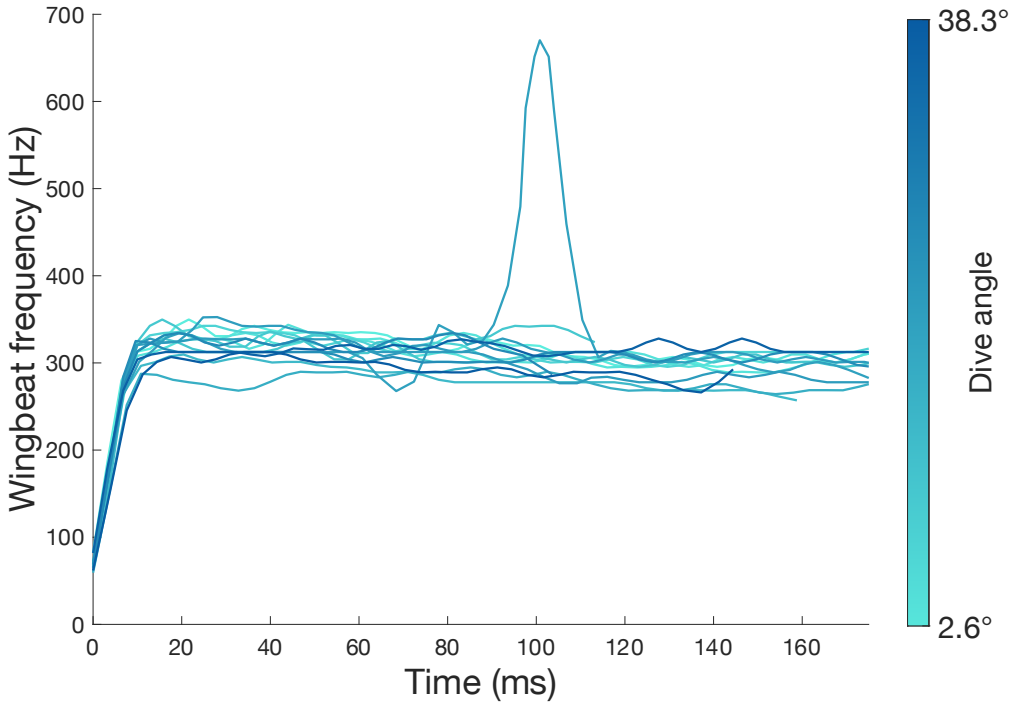

Figure 4.S3. Smoothed wingbeat frequency plotted over time shows that there is little difference between dives with different angles (n = 15).

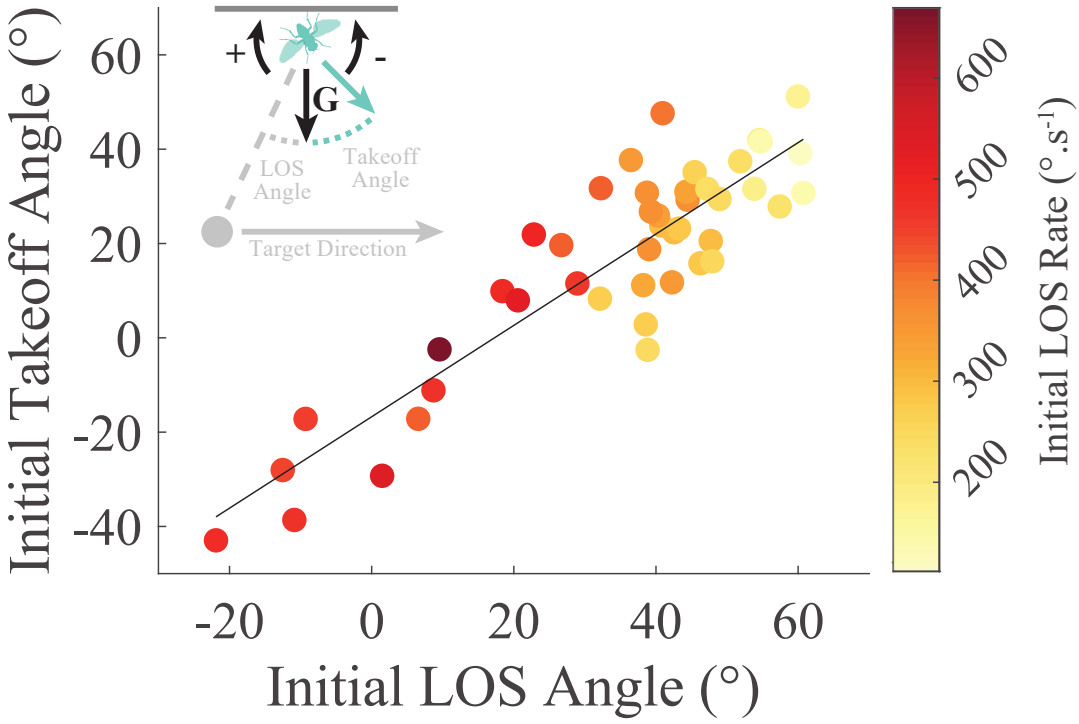

Figure 4.S4. Scatter diagram and best linear fit for the regression of the initial line of sight angle (from vertical) against initial take-off angle (first 10 ms, from vertical) for flights starting on the ceiling. Points are colour coded to initial (first 10 ms) rotation rates of the line-of-sight (LOS, exocentric).

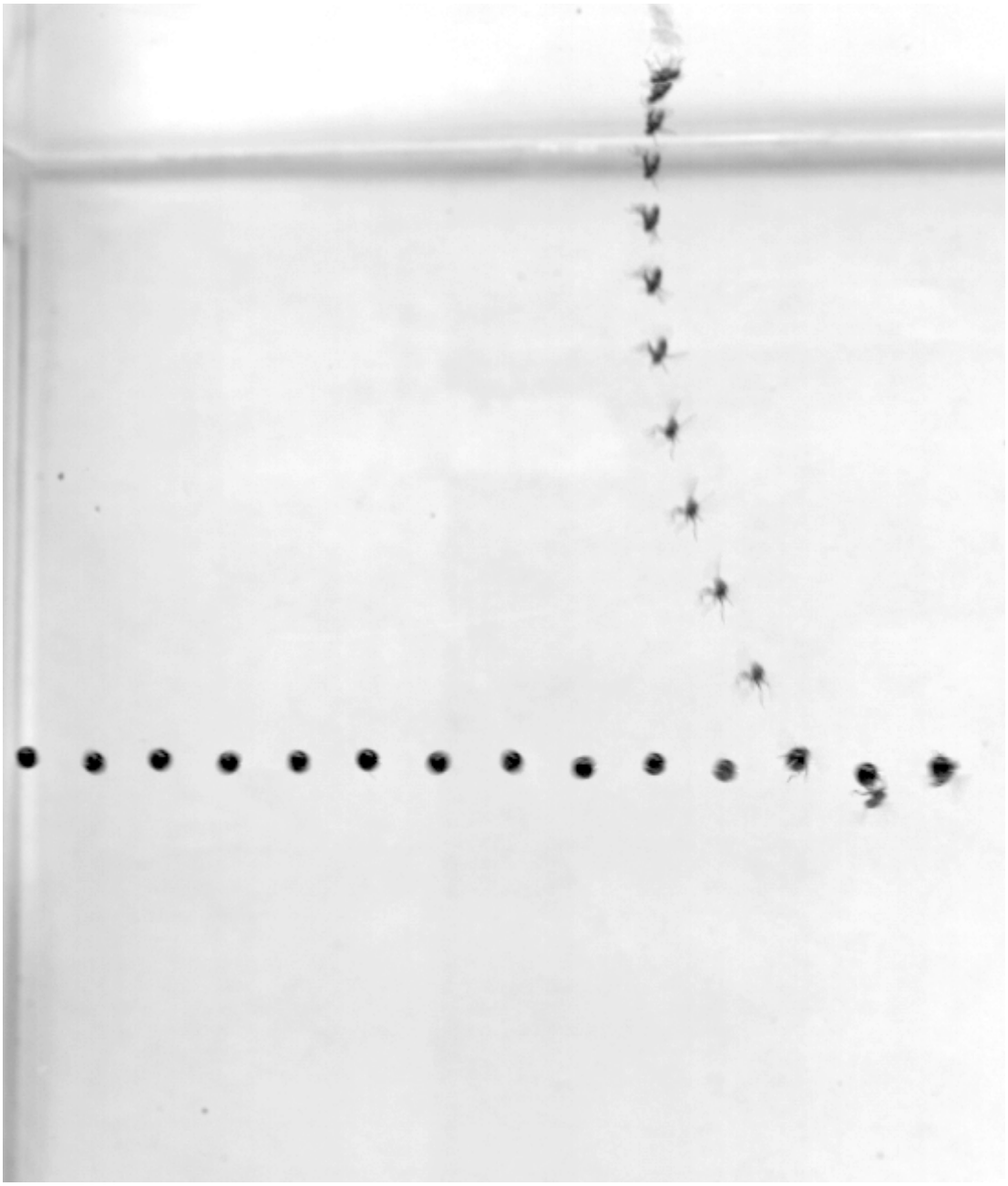

Figure 4.S5. A successful dive. Fly and target positions sequence, every 10 ms, during a dive from the arena ceiling shows that killer flies can catch their target mid-air during falcon dives, despite the high velocity they achieve.

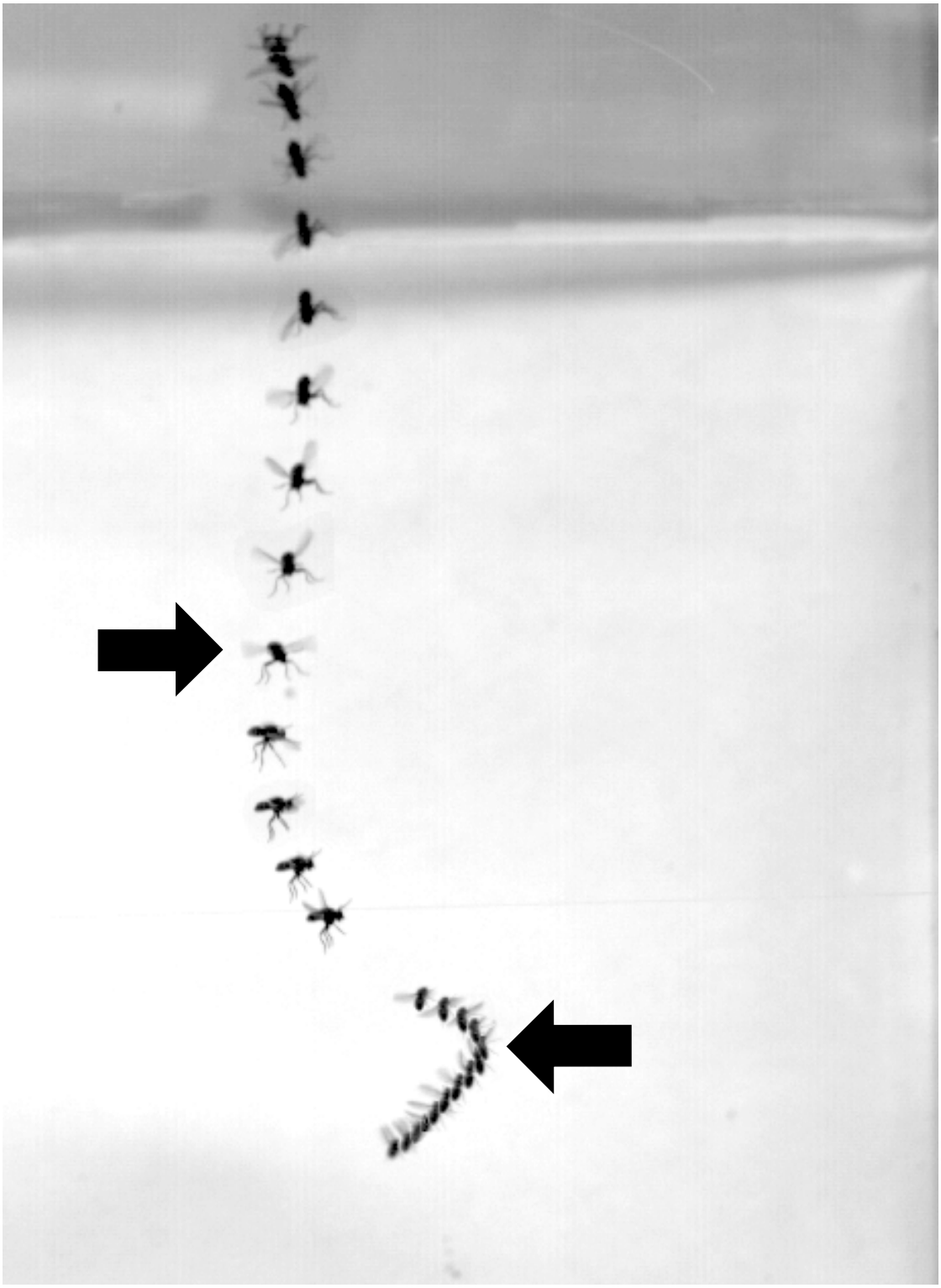

Figure 4.S6. Killer fly and fruit fly position, every 10 ms, during a dive from the arena ceiling shows that natural prey may respond to the killer fly's attack by deviating from its path. Arrows indicate the same time point in the killer fly and fruit fly's paths, at the moment when the fruit fly deviates from its initial trajectory.

5. Final Conclusions

This thesis presents a broad investigation of the role that active vision, defined as the movement of eyes aimed at improving visual processing, plays in predation. We identified a number of insect predators that use a range of behavioural tactics to capture prey, from sit-and-wait predators attacking moving prey (chapter 2), to ambush predators attacking static prey (chapter 3), to active predators attacking moving prey (chapter 4). In all the situations considered, we found evidence for at least some elements of active vision that likely contributes to the efficacy of the predator's behaviour.

Chapter 2 considered active vision in praying mantids. Praying mantids are sit-and-wait predators, famously catching their prey with specialised raptorial forelimbs (Copeland and Carlson, 1977; Corrette, 1990; Loxton and Nicholls, 1979; Prete, 1990). Their eyes have evolved to support a predatory lifestyle, with large frontal foveas and an extensive binocular overlap (Barros-Pita and Maldonado, 1970; Rossel, 1979) that they use for range finding (Nityananda et al., 2018; Rossel, 1983). While the visual system of the praying mantid has been studied in depth, few studies systematically investigate the behaviour of these animals. We found that the raptorial strikes of African praying mantids are influenced by a number of factors. Prey speed affected every aspect of the strike considered, from the likelihood of its initiation, to its completion, and even the chances of it being successful. Mantids had previously been shown to visually track prey at a variety of speeds (Rossel, 1980), which we also found, with slower prey speeds eliciting more and earlier head movements. We also reported strikes being initiated with no prior head movements, especially when prey speed greatly exceeded the angular speed of mantid head rotations (Lea and Mueller, 1977). We suggest that this may be done to reduce motion blur. The presence of a head movement did not significantly affect the likelihood of a strike being initiated; however, head movements performed before a strike greatly increased its chances of success. This demonstrates that active vision strategies can greatly enhance the fitness of predators even when their visual performance is already remarkable.

Chapter 3 investigated another ambush predator, the darting robber fly. Like mantids, darting robber flies are generalist predators. They predate by flying towards static prey at high speed, a strategy called gleaning. Despite the difference in head size of one order of magnitude, darting robber flies reach similar interommatidial angles in their foveas as that reported in some species of praying mantids (Horridge and Duelli, 1979). Contrary to praying mantids, however, the foveas of darting robber flies are very close to the head midline, greatly reducing their capacity to use stereopsis. Although darting robber flies attacked from distances correlated to prey's size, prey did not subtend the same angular size at the distance the attack was launched. We found that darting robber flies assessed prey with much more tortuous flights than a larger gleaner, the fragile forktail damselfly, suggesting that active vision might play a role in their attacks, too. Darting robber flies assess larger prey for longer, with more tortuous flight paths, and spanning a larger portion of space; however, they assessed all prey at similar flight velocities. These characteristics are similar to animals which approximate the width of a gap by motion parallax before jumping across it (Collett, 1978; Kral, 1998; Kral, 2003; Poteser and Kral, 1995). Consequently, we suggested that darting robber flies use active vision, specifically motion parallax, to compensate for the reduced stereopsis range determined by the small size of their head.

Chapter 4 investigated killer flies, small active predators that also possess a frontal fovea (Gonzalez-Bellido et al., 2011) but do not use it for stereopsis (Wardill et al., 2015). Killer flies capture moving prey by interception when attacking from below, likely following proportional navigation (Fabian et al., 2018). When positioned above prey, killer flies use both gravity and powered flight to achieve accelerations far greater than when hunting from below. Although they still follow proportional navigation to capture prey from above, the speed killer flies reach limits their lateral acceleration which causes them to produce suboptimal flight paths. Attack time could be reduced by either flying at lower speed or taking off later, yet killer flies have not evolved to do so. We suggest some reasons why this might not be the case. First, the elevated speed could produce higher aerodynamic power on the wing, thereby improving manoeuvrability when catching moving targets. Second, flying towards their prey at high speed might

trigger avoidance manoeuvres in prey, which would therefore slow down (Fry et al., 2003; Tammero and Dickinson, 2002). Third, the eye resolution of killer flies is poor (Gonzalez-Bellido et al., 2011), much poorer than other active insect predators (Horridge, 1978; Sherk, 1978; Wardill et al., 2017). We suggest that flying towards prey at high speed might help killer flies keep track of prey, especially when predating against a cluttered background. Greatly accelerating towards prey might therefore be maladaptive in terms of flight time, but could also be explained as being a strategy for active vision.

As the above examples show, active vision can have a considerable impact in a variety of predatory strategies. Whether predating upon static prey or moving prey, whether doing so by active or sit-and-wait predation, whether possessing high-resolution or low-resolution eyes, predators can greatly enhance their strategy via active vision. However, this is not to say that all active vision strategies are efficient. When faced with high prey speed, we showed praying mantids do not direct their gaze towards prey yet may attempt a strike, which is unlikely to be successful. Darting robber flies take very long times assessing prey via motion parallax, with the risk of being spotted by both prey itself and other predators. Killer flies fly at high speed in order to keep visual track of prey, yet this greatly reduces their ability to produce lateral acceleration. Some active vision strategies might sacrifice time, energy, or chance of success. Although suboptimal, at least from an engineering point of view, active vision strategies are not maladaptive. In fact, behaviours which may seem disadvantageous at first might reveal that other factors are momentarily being prioritised.

There are many examples of animal behaviour reflecting this. Foraging leaf cutter ants drop leaf pieces along a trail before reaching the nest, which causes them to head back towards the food source, prolonging the time spent foraging (Röschard and Roces, 2011). However, dropping leaf pieces at strategic nodes spreads information about food quality to the rest of the colony, which can improve energy intake. Although seemingly maladaptive, this behaviour prioritises food information over foraging time. Somewhat similarly, orcas prolong wave-washing attacks by allowing seals back on the ice (Visser et al., 2008). Seemingly counterintuitive, this behaviour might help orcas teach their young

necessary motor skills. These are only two examples where seemingly maladaptive behaviours may yet be advantageous.

Central to sensory ecology is the concept of information (Dusenbery, 1992), and how information is gathered and handled by animals. The three animals considered in this thesis have been shown to, at times, prioritise visual information gathering over uninformed attacks. Leaf cutter ants may prioritise chemosensory information acquisition in the colony over individual foraging time. Orcas may prioritise acquisition of motor information by young calves. To fully account for animal behaviour, neuroethology has to be complemented with sensory ecology and biomechanics. This thesis has tried to do so, by considering information gathered by predators, as well as their behavioural goal and their biomechanical conditions. The study of active sensing in animals is an excellent example of emerging field arising from the joint effort of multiple disciplines.

A knowledge gap exists in determining what neural circuitry implements active vision. Although some efforts have been made to understand the neurobiology of active vision in humans (Choi and Henderson, 2015; Hillen et al., 2013) and higher vertebrates (Hafed et al., 2021; Mazer and Gallant, 2003; Sparks, 1986), this problem could as well be tackled by more tractable invertebrates. There are fewer descending interneurons in the ventral nerve cord of insects than neurons in the optic lobe or in the ventral ganglia (Namiki et al., 2018). Some descending neurons are visually sensitive (Gonzalez-Bellido et al., 2013; Olberg, 1981a), but also their stimulation results in specific motor patterns, including changing wing angle and triggering head rotations (Olberg, 1979; Olberg, 1983). These neurons also respond to wind direction, head and body angles (Olberg, 1981b). As such, TSDNs seem the ideal candidate to investigate the neuronal circuitry of active vision in invertebrates. Similarly, neurons sensitive to small objects in the descending nerve cord of other animals (Gonka et al., 1999; Nicholas et al., 2018) may as well be part of neuronal circuitry of active vision.

As an emerging field, active vision brings challenges of incorporating vastly different methods, but also precious opportunities to gain deep insights into animal behaviour. Understanding how animals behave also means understanding what kind of information they gather from the environment through active and

passive sensing, what physical limitations they face and how active sensing is implemented by neural correlates. A fully integrated approach to animal behaviour arises not only from understanding how visual information affects motor outputs, but the many different ways in which motion feeds back into sensation.

Bibliography

Abrams, T. and Pearson, K. (1982). Effects of temperature on identified central neurons that control jumping in the grasshopper. *J. Neurosci.* **2**, 1538–1553.

Adams, M. D., Celniker, S. E., Holt, R. A., Evans, C. A., Gocayne, J. D., Amanatides, P. G., Scherer, S. E., Li, P. W., Hoskins, R. A., Galle, R. F., et al. (2000). The genome sequence of *Drosophila melanogaster*. *Science* **287**, 2185–95.

Agi, E., Langen, M., Altschuler, S. J., Wu, L. F., Zimmermann, T. and Hiesinger, P. R. (2014). The evolution and development of neural superposition. *J. Neurogenet.* **28**, 216–32.

Alcazar, J., Csapo, R., Ara, I. and Alegre, L. M. (2019). On the shape of the force-velocity relationship in skeletal muscles: the linear, the hyperbolic, and the double-hyperbolic. *Front. Physiol.* **10**, 769.

Alerstam, T. (1987). Radar observations of the stoop of the peregrine falcon *Falco peregrinus* and the goshawk *Accipiter gentilis*. *Ibis (Lond. 1859).* **129**, 267–273.

Aloimonos, J., Weiss, I. and Bandyopadhyay, A. (1988). Active vision. *Int. J. Comput. Vis.* **1**, 333–356.

Alonso, L. M. and Marder, E. (2020). Temperature compensation in a small rhythmic circuit. *Elife* **9**, e55470.

Andersson, K. I. (2004). Elbow-joint morphology as a guide to forearm function and foraging behaviour in mammalian carnivores. *Zool. J. Linn. Soc.* **142**, 91–104.

Arendt, D. (2003). Evolution of eyes and photoreceptor cell types. *Int. J. Dev. Biol.* **47**, 563–71.

Arendt, D. and Nübler-Jung, K. (1994). Inversion of dorsoventral axis? *Nature* **371**, 26–26.

Arendt, D. and Wittbrodt, J. (2001). Reconstructing the eyes of Urbilateria. *Philos. Trans. R. Soc. B Biol. Sci.* **356**, 1545–1563.

Arendt, D., Musser, J. M., Baker, C. V. H., Bergman, A., Cepko, C., Erwin, D. H., Pavlicev, M., Schlosser, G., Widder, S., Laubichler, M. D., et al. (2016). The origin and evolution of cell types. *Nat. Rev. Genet.* **17**, 744–757.

Atema, J. (1971). Structures and functions of the sense of taste in the catfish (*Ictalurus natalis*). *Brain. Behav. Evol.* **4**, 273–294.

Azevedo, F. A. C., Carvalho, L. R. B., Grinberg, L. T., Farfel, J. M., Ferretti, R. E.

L., Leite, R. E. P., Filho, W. J., Lent, R. and Herculano-Houzel, S. (2009). Equal numbers of neuronal and nonneuronal cells make the human brain an isometrically scaled-up primate brain. *J. Comp. Neurol.* **513**, 532–541.

Baker, L. J., Freed, L. L., Easson, C. G., Lopez, J. V, Fenolio, D., Sutton, T. T., Nyholm, S. V and Hendry, T. A. (2019). Diverse deep-sea anglerfishes share a genetically reduced luminous symbiont that is acquired from the environment. *Elife* **8**, e47606.

Barros-Pita, J. C. and Maldonado, H. (1970). A fovea in the praying mantis eye II. Some morphological characteristics. *Z. Vgl. Physiol.* **67**, 79–92.

Bates, D., Mächler, M., Bolker, B. and Walker, S. (2015). Fitting linear mixed-effects models using lme4. *J. Stat. Softw.* **67**, 1–48.

Bednarz, J. C. (1988). Cooperative hunting Harris' hawks (*Parabuteo unicinctus*). *Science* **239**, 1525–7.

Belanger, J. H. (2005). Contrasting tactics in motor control by vertebrates and arthropods. *Integr. Comp. Biol.* **45**, 672–678.

Bengtson, S. (2002). Origins and early evolution of predation. *Paleontol. Soc. Pap.* **8**, 289–318.

Bengtson, S. and Zhao, Y. (1992). Predatorial borings in late precambrian mineralized exoskeletons. *Science* **257**, 367–9.

Benhamou, S. (2004). How to reliably estimate the tortuosity of an animal's path: straightness, sinuosity, or fractal dimension? *J. Theor. Biol.* **229**, 209–220.

Bennet-Clark, H. C. (1975). The energetics of the jump of the locust *Schistocerca gregaria*. *J. Exp. Biol.* **63**, 53–83.

Bertsch, D. J., Martin, J. P., Svenson, G. J. and Ritzmann, R. E. (2019). Predatory behavior changes with satiety or increased insulin levels in the praying mantis (Tenodera sinensis). *J. Exp. Biol.* **222**, jeb197673.

Bianco, I. H., Kampff, A. R. and Engert, F. (2011). Prey capture behavior evoked by simple visual stimuli in larval zebrafish. *Front. Syst. Neurosci.* **5**, 101.

Billington, J., Webster, R. J., Sherratt, T. N., Wilkie, R. M. and Hassall, C. (2020). The (under)use of eye-tracking in evolutionary ecology. *Trends Ecol. Evol.* **35**, 495–502.

Birkhead, T. R., Lee, K. E. and Young, P. (1988). Sexual cannibalism in the praying mantis *Hierodula membranacea*. *Behaviour* **106**, 112–118.

Blest, A. D. and Land, M. F. (1977). The physiological optics of *Dinopis subrufus* L. Koch: A fish-lens in a spider. *Proc. R. Soc. London. Ser. B. Biol. Sci.* **196**, 197–222.

Bodznick, D. and Northcutt, R. G. (1981). Electroreception in lampreys: evidence

that the earliest vertebrates were electroreceptive. *Science* **212**, 465–7.

Bolker, J. (2012). There's more to life than rats and flies. *Nature* **491**, 31–33.

Bonsignore, C. P. (2016). Environmental factors affecting the behavior of *Coenosia attenuata*, a predator of *Trialeurodes vaporariorum* in tomato greenhouses. *Entomol. Exp. Appl.* **158**, 87–96.

Borst, A. and Egelhaaf, M. (1989). Principles of visual motion detection. *Trends Neurosci.* **12**, 297–306.

Brännström, P. A. (1999). Visual Ecology of Insect Superposition Eyes.

Brighton, C. H. and Taylor, G. K. (2019). Hawks steer attacks using a guidance system tuned for close pursuit of erratically manoeuvring targets. *Nat. Commun.* **10**, 2462.

Brighton, C. H., Thomas, A. L. R. and Taylor, G. K. (2017). Terminal attack trajectories of peregrine falcons are described by the proportional navigation guidance law of missiles. *Proc. Natl. Acad. Sci.* **114**, 13495–13500.

Brito, J. C., Martínez-Freiría, F., Sierra, P., Sillero, N. and Tarroso, P. (2011). Crocodiles in the Sahara desert: An update of distribution, habitats and population status for conservation planning in Mauritania. *PLoS One* **6**, e14734.

Buatois, A., Flumian, C., Schultheiss, P., Avarguès-Weber, A. and Giurfa, M. (2018). Transfer of visual learning between a virtual and a real environment in honey bees: The role of active vision. *Front. Behav. Neurosci.* **12**, 139.

Bullock, T. H. and Diecke, F. P. J. (1956). Properties of an infra-red receptor. *J. Physiol.* **134**, 47–87.

Bullock, T. H., Bodznick, D. A. and Northcutt, R. G. (1983). The phylogenetic distribution of electroreception: Evidence for convergent evolution of a primitive vertebrate sense modality. *Brain Res. Rev.* **6**, 25–46.

Burkhardt, D., Darnhofer-Demar, B. and Fischer, K. (1973). Zum binokularen Entfernungssehen der Insekten. *J. Comp. Physiol.* **87**, 165–188.

Burmeister, H. (1838). *Handbuch der Entomologie 2: Kaukerfe. Gymnognatha. (Erste Hälfte, Vulgo Orthoptera)*. Berlin: Reimer.

Burrows, M. (1969). The mechanics and neural control of the prey capture strike in the mantid shrimps *Squilla* and *Hemisquilla*. *Z. Vgl. Physiol.* **62**, 361–381.

Burrows, M. (1989). Effects of temperature on a central synapse between identified motor neurons in the locust. *J. Comp. Physiol. A* **165**, 687–695.

Burrows, M. (2003). Froghopper insects leap to new heights. *Nature* **424**, 509–509.

Burrows, M. and Hoyle, G. (1972). Neuromuscular physiology of the strike

mechanism of the mantis shrimp, *Hemisquilla*. *J. Exp. Zool.* **179**, 379–393.

Burrows, M. and Morris, O. (2003). Jumping and kicking in bush crickets. *J. Exp. Biol.* **206**, 1035–49.

Buschbeck, E. K., Sbita, S. J. and Morgan, R. C. (2007). Scanning behavior by larvae of the predacious diving beetle, *Thermonectus marmoratus* (Coleoptera: Dytiscidae) enlarges visual field prior to prey capture. *J. Comp. Physiol. A* **193**, 973–982.

Bybee, S. M., Taylor, S. D., Riley Nelson, C. and Whiting, M. F. (2004). A phylogeny of robber flies (Diptera: Asilidae) at the subfamilial level: molecular evidence. *Mol. Phylogenet. Evol.* **30**, 789–797.

Cartmill, M. (1974). Rethinking primate origins. *Science* **184**, 436–43.

Catania, K. C. (2000). Epidermal sensory organs of moles, shrew moles, and desmans: A atudy of the family Talpidae with comments on the function and evolution of Eimer's organ. *Brain. Behav. Evol.* **56**, 146–174.

Catania, K. C. (2009). Tentacled snakes turn C-starts to their advantage and predict future prey behavior. *Proc. Natl. Acad. Sci.* **106**, 11183–7.

Catania, K. C. and Remple, F. E. (2005). Asymptotic prey profitability drives star-nosed moles to the foraging speed limit. *Nature* **433**, 519–522.

Catania, K. C., Leitch, D. B. and Gauthier, D. (2010). Function of the appendages in tentacled snakes (*Erpeton tentaculatus*). *J. Exp. Biol.* **213**, 359–67.

Caveney, S. and McIntyre, P. (1981). Design of graded-index lenses in the superposition eyes of scarab beetles. *Philos. Trans. R. Soc. B Biol. Sci.* **294**, 589–632.

Cellini, B. and Mongeau, J.-M. (2020). Active vision shapes and coordinates flight motor responses in flies. *Proc. Natl. Acad. Sci.* **117**, 23085–23095.

Chittka, L. and Niven, J. (2009). Are bigger brains better? *Curr. Biol.* **19**, R995–R1008.

Choi, W. and Henderson, J. M. (2015). Neural correlates of active vision: An fMRI comparison of natural reading and scene viewing. *Neuropsychologia* **75**, 109–118.

Cisne, J. L. (1974). Trilobites and the origin of arthropods. *Science* **186**, 13–8.

Cleal, K. S. and Prete, F. R. (1996). The predatory strike of free ranging praying mantises, *Sphodromantis lineola* (Burmeister). II: Strikes in the horizontal plane. *Brain. Behav. Evol.* **48**, 191–204.

Coddington, J. and Sobrevilla, C. (1987). Web manipulation and two stereotyped attack behaviors in the ogre-faced spider *Deinopis spinosus* Marx (Araneae, Deinopidae). *J. Arachnol.* **15**, 213–225.

Cohen, B. L. (2005). Not armour, but biomechanics, ecological opportunity and increased fecundity as keys to the origin and expansion of the mineralized benthic metazoan fauna. *Biol. J. Linn. Soc.* **85**, 483–490.

Collett, T. S. (1978). Peering - A locust behaviour pattern for obtaining motion parallax information. *J. Exp. Biol.* **76**, 237–241.

Collett, T. S. and Land, M. F. (1978). How hoverflies compute interception courses. *J. Comp. Physiol. A* **125**, 191–204.

Collett, T. S. and Paterson, C. J. (1991). Relative motion parallax and target localisation in the locust, *Schistocerca gregaria*. *J. Comp. Physiol. A* **169**, 615–621.

Combes, S. A., Rundle, D. E., Iwasaki, J. M. and Crall, J. D. (2012). Linking biomechanics and ecology through predator–prey interactions: flight performance of dragonflies and their prey. *J. Exp. Biol.* **215**, 903–913.

Comer, C. M. and Robertson, R. M. (2001). Identified nerve cells and insect behavior. *Prog. Neurobiol.* **63**, 409–439.

Copeland, J. and Carlson, A. D. (1977). Prey capture in mantids: Prothoracic tibial flexion reflex. *J. Insect Physiol.* **23**, 1151–1156.

Corbet, P. S. (1999). *Dragonflies: Behaviour and Ecology of Odonata*. Colchester, UK: Harley Books.

Corcoran, A. J., Barber, J. R. and Conner, W. E. (2009). Tiger moth jams bat sonar. *Science* **325**, 325–7.

Corey, D. P. and Hudspeth, A. J. (1983). Kinetics of the receptor current in bullfrog saccular hair cells. *J. Neurosci.* **3**, 962–76.

Corrette, B. J. (1990). Prey capture in the praying mantis *Tenodera aridifolia sinensis*: coordination of the capture sequence and strike movements. *J. Exp. Biol.* **148**, 147–180.

Creel, S. and Creel, N. M. (1995). Communal hunting and pack size in African wild dogs, *Lycaon pictus*. *Anim. Behav.* **50**, 1325–1339.

Crisp, D. J. and Southward, A. J. (1961). Different types of cirral activity of barnacles. *Philos. Trans. R. Soc. B Biol. Sci.* **243**, 271–307.

Dalquest, W. W. and Orcutt, D. R. (1942). The biology of the least shrew-mole, *Neurotrichus gibbsii minor*. *Am. Midl. Nat.* **27**, 387.

Davies, M. N. O. and Green, P. R. (1988). Head-bobbing during walking, running and flying: Relative motion perception in the pigeon. *J. Exp. Biol.* **138**, 71–91.

Dawkins, M. S. and Woodington, A. (2000). Pattern recognition and active vision in chickens. *Nature* **403**, 652–655.

de Vries, S. E. J. and Clandinin, T. R. (2012). Loom-sensitive neurons link

computation to action in the *Drosophila* visual system. *Curr. Biol.* **22**, 353–362.

de Margerie, E., Simonneau, M., Caudal, J.-P., Houdelier, C. and Lumineau, S. (2015). 3D tracking of animals in the field using rotational stereo videography. *J. Exp. Biol.* **218**, 2496–504.

DeAngelis, B. D., Zavatone-Veth, J. A. and Clark, D. A. (2019). The manifold structure of limb coordination in walking *Drosophila*. *Elife* **8**, e46409.

Dearing, M. D., Mangione, A. M. and Karasov, W. H. (2000). Diet breadth of mammalian herbivores: nutrient versus detoxification constraints. *Oecologia* **123**, 397–405.

Deban, S. M., Wake, D. B. and Roth, G. (1997). Salamander with a ballistic tongue. *Nature* **389**, 27–28.

Denton, E. J. and Nicol, J. A. C. (1966). A survey of reflectivity in silvery teleosts. *J. Mar. Biol. Assoc. United Kingdom* **46**, 685–722.

Derby, C. D., Steullet, P., Horner, A. J. and Cate, H. S. (2001). The sensory basis of feeding behaviour in the Caribbean spiny lobster, *Panulirus argus*. *Mar. Freshw. Res.* **52**, 1339–1350.

DeVoe, R. D. (1980). Movement sensitivities of cells in the fly's medulla. *J. Comp. Physiol. A* **138**, 93–119.

deVries, M. S., Murphy, E. A. K. and Patek, S. N. (2012). Strike mechanics of an ambush predator: the spearing mantis shrimp. *J. Exp. Biol.* **215**, 4374–84.

Dey, B. and Krishnaprasad, P. S. (2012). Trajectory smoothing as a linear optimal control problem. In *2012 50th Annual Allerton Conference on Communication, Control, and Computing (Allerton)*, pp. 1490–1497. IEEE.

Dickinson, M. H. and Götz, K. G. (1993). Unsteady aerodynamic performance of model wings at low Reynolds numbers. *J. Exp. Biol.* **174**, 45–64.

Domenici, P., Blagburn, J. M. and Bacon, J. P. (2011). Animal escapology II: escape trajectory case studies. *J. Exp. Biol.* **214**, 2474–94.

Douglass, J. K. and Strausfeld, N. J. (1995). Visual motion detection circuits in flies: Peripheral motion computation by identified small-field retinotopic neurons. *J. Neurosci.* **15**, 5596–611.

Douglass, J. K. and Strausfeld, N. J. (1996). Visual motion-detection circuits in flies: Parallel direction- and non-direction-sensitive pathways between the medulla and lobula plate. *J. Neurosci.* **16**, 4551–62.

Dusenbery, D. B. (1992). *Sensory Ecology: How Organisms Acquire and Respond to Information*. New York, NY: W.H. Freeman.

Dzik, J. (2007). The Verdun Syndrome: simultaneous origin of protective armour and infaunal shelters at the Precambrian–Cambrian transition. *Geol. Soc. Publ.*

286, 405–414.

Dzimirski, I. (2010). Untersuchungen über Bewegungssehen und Optomotorik bei Springspinnen (Salticidae).1. *Z. Tierpsychol.* **16**, 385–402.

Edgecombe, G. D. (2020). Arthropod origins: Integrating paleontological and molecular evidence. *Annu. Rev. Ecol. Evol. Syst.* **51**, 1–25.

Egelhaaf, M. (1985). On the neuronal basis of figure-ground discrimination by relative motion in the visual system of the fly I. Behavioural constraints imposed on the neuronal network and the role of the optomotor system. *Biol. Cybern.* **52**, 123–140.

Egelhaaf, M., Kern, R., Lindemann, J. P., Braun, E. and Geurten, B. (2009). Active Vision in Blowflies: Strategies and Mechanisms of Spatial Orientation. In *Flying Insects and Robots* (ed. Floreano, D.), Zufferey, J.-C.), Srinivasan, M. V.), and Ellington, C.), pp. 51–61. Berlin, Heidelberg: Springer Berlin Heidelberg.

El Jundi, B., Huetteroth, W., Kurylas, A. E. and Schachtner, J. (2009). Anisometric brain dimorphism revisited: Implementation of a volumetric 3D standard brain in *Manduca sexta*. *J. Comp. Neurol.* **517**, 210–225.

Ellard, C. G., Goodale, M. A. and Timney, B. (1984). Distance estimation in the mongolian gerbil: The role of dynamic depth cues. *Behav. Brain Res.* **14**, 29–39.

Ellington, C. (1984). The aerodynamics of hovering insect flight. VI. Lift and power requirements. *Philos. Trans. R. Soc. B Biol. Sci.* **305**, 145–181.

Elner, R. W. and Campbell, A. (2009). Force, function and mechanical advantage in the chelae of the American lobster *Homarus americanus* (Decapoda: Crustacea). *J. Zool.* **193**, 269–286.

Erickson, G. M., Kirk, S. D. Van, Su, J., Levenston, M. E., Caler, W. E. and Carter, D. R. (1996). Bite-force estimation for *Tyrannosaurus rex* from tooth-marked bones. *Nature* **382**, 706–708.

Evans, M. E. G. and Forsythe, T. G. (2009). A comparison of adaptations to running, pushing and burrowing in some adult Coleoptera: especially Carabidae. *J. Zool.* **202**, 513–534.

Ewert, J.-P. (1987). Neuroethology of releasing mechanisms: Prey-catching in toads. *Behav. Brain Sci.* **10**, 337–368.

Ewert, J.-P. and Hock, F. (1972). Movement-sensitive neurones in the toad's retina. *Exp. Brain Res.* **16**, 41–59.

Exner, S. (1891). *Die Physiologie der facettirten Augen von Krebsen und Insecten: eine Studie*. (ed. Deuticke, F.) Liepzig.

Fabian, S. T. (2019). *Visual Adaptations and Behavioural Strategies to Detect and Catch Small Targets*, PhD thesis, University of Cambridge, UK.

Fabian, S. T., Sumner, M. E., Wardill, T. J., Rossoni, S. and Gonzalez-Bellido, P. T. (2018). Interception by two predatory fly species is explained by a proportional navigation feedback controller. *J. R. Soc. Interface* **15**, 20180466.

Fabian, J. M., el Jundi, B., Wiederman, S. D. and O'Carroll, D. C. (2020). The complex optic lobe of dragonflies. *bioRxiv* 2020.05.10.087437.

Feller, K. D., Sharkey, C. R., McDuffee-Altekruse, A., Bracken-Grissom, H. D., Lord, N. P., Porter, M. L. and Schweikert, L. E. (2021). Surf and turf vision: Patterns and predictors of visual acuity in compound eye evolution. *Arthropod Struct. Dev.* **60**, 101002.

Ferguson, G. P. and Benjamin, P. R. (1991). The whole-body withdrawal response of *Lymnaea stagnalis*. I. Identification of central motoneurones and muscles. *J. Exp. Biol.* **158**, 63–95.

Fertin, A. and Casas, J. (2006). Efficiency of antlion trap construction. *J. Exp. Biol.* **209**, 3510–5.

Fischbach, K.-F. and Dittrich, A. P. M. (1989). The optic lobe of *Drosophila melanogaster*. I. A Golgi analysis of wild-type structure. *Cell Tissue Res.* **258**, 441–475.

Fisher, A. M., Holwell, G. I. and Price, T. A. R. (2020). Behavioural correlations and aggression in praying mantids. *Behav. Ecol. Sociobiol.* **74**, 61.

Flood, P. R. (1970). The connection between spinal cord and notochord in Amphioxus (*Branchiostoma lanceolatum*). *Zeitschrift für Zellforsch. und Mikroskopische Anat.* **103**, 115–128.

Fox, R., Lehmkuhle, S. W. and Westendorf, D. H. (1976). Falcon visual acuity. *Science* **192**, 263–5.

Freed, L. L., Easson, C., Baker, L. J., Fenolio, D., Sutton, T. T., Khan, Y., Blackwelder, P., Hendry, T. A. and Lopez, J. V (2019). Characterization of the microbiome and bioluminescent symbionts across life stages of Ceratioid anglerfishes of the Gulf of Mexico. *FEMS Microbiol. Ecol.* **95**, fiz146.

Fry, S. N., Sayaman, R., Dickinson, M. H. and Dickinson, M. H. (2003). The aerodynamics of free-flight maneuvers in Drosophila. *Science* **300**, 495–498.

Frye, M. A. and Olberg, R. M. (1995). Visual receptive field properties of feature detecting neurons in the dragonfly. *J. Comp. Physiol. A* **177**, 569–576.

Gahtan, E., Tanger, P. and Baier, H. (2005). Visual prey capture in larval zebrafish is controlled by identified reticulospinal neurons downstream of the tectum. *J. Neurosci.* **25**, 9294–303.

Galloway, J. A. M., Green, S. D., Stevens, M. and Kelley, L. A. (2020). Finding a signal hidden among noise: How can predators overcome camouflage strategies? *Philos. Trans. R. Soc. B Biol. Sci.* **375**, 20190478.

Gans, C. and Northcutt, R. G. (1983). Neural crest and the origin of vertebrates: A new head. *Science* **220**, 268–73.

Gardiner, J. M. and Atema, J. (2010). The function of bilateral odor arrival time differences in olfactory orientation of sharks. *Curr. Biol.* **20**, 1187–1191.

Gårding, J., Porrill, J., Mayhew, J. E. W. and Frisby, J. P. (1995). Stereopsis, vertical disparity and relief transformations. *Vision Res.* **35**, 703–722.

Gazda, S. K., Connor, R. C., Edgar, R. K. and Cox, F. (2005). A division of labour with role specialization in group–hunting bottlenose dolphins (*Tursiops truncatus*) off Cedar Key, Florida. *Proc. R. Soc. B Biol. Sci.* **272**, 135–140.

Gibson, J. J. (1950). *The Perception of the Visual World*. Boston, MA: Houghton Mifflin.

Gilbert, C. (1997). Visual control of cursorial prey pursuit by tiger beetles (Cicindelidae). *J. Comp. Physiol. A* **181**, 217–230.

Gilbert, C., Penisten, D. and DeVoe, R. (1991). Discrimination of visual motion from flicker by identified neurons in the medulla of the fleshfly *Sarcophaga bullata*. *J. Comp. Physiol. A* **168**, 653–673.

Gonka, M. D., Laurie, T. J. and Prete, F. R. (1999). Responses of movement-sensitive visual interneurons to prey-like stimuli in the praying mantis *Sphodromantis lineola* (Burmeister). *Brain. Behav. Evol.* **54**, 243–262.

Gonzalez-Bellido, P. T. and Wardill, T. J. (2012). Labeling and confocal imaging of neurons in thick invertebrate tissue samples. *Cold Spring Harb. Protoc.* **2012**, 969–83.

Gonzalez-Bellido, P. T., Wardill, T. J. and Juusola, M. (2011). Compound eyes and retinal information processing in miniature dipteran species match their specific ecological demands. *Proc. Natl. Acad. Sci.* **108**, 4224–9.

Gonzalez-Bellido, P. T., Peng, H., Yang, J., Georgopoulos, A. P. and Olberg, R. M. (2013). Eight pairs of descending visual neurons in the dragonfly give wing motor centers accurate population vector of prey direction. *Proc. Natl. Acad. Sci.* **110**, 696–701.

Goulet, M., Campan, R. and Lambin, M. (1981). The visual perception of relative distances in the wood-cricket, *Nemobius sylvestris*. *Physiol. Entomol.* **6**, 357–367.

Gray, P. T. and Mill, P. J. (1983). The mechanics of the predatory strike of the praying mantid *Heirodula Membranacea*. *J. Exp. Biol.* **107**, 245–275.

Gries, M. and Koeniger, N. (1996). Straight forward to the queen: pursuing honeybee drones (Apis mellifera L.) adjust their body axis to the direction of the queen. *J. Comp. Physiol. A* **179**, 539–544.

Griffiths, D. (1980). Foraging costs and relative prey size. *Am. Nat.* **116**, 743–752.

Grimaldi, D. and Engel, M. S. (2005). *Evolution of the Insects*. Cambridge: Cambridge University Press.

Grobecker, D. B. and Pietsch, T. W. (1979). High-Speed Cinematographic Evidence for Ultrafast Feeding in Antennariid Anglerfishes. *Science* **205**, 1161–1162.

Gronenberg, W., Tautz, J. and Hölldobler, B. (1993). Fast trap jaws and giant neurons in the ant Odontomachus. *Science* **262**, 561–563.

Gwynne, D. T. (2008). Sexual conflict over nuptial gifts in insects. *Annu. Rev. Entomol.* **53**, 83–101.

Hafed, Z. M., Chen, C.-Y., Tian, X., Baumann, M. and Zhang, T. (2021). Active vision at the foveal scale in the primate superior colliculus. *J. Neurophysiol.* jn.00724.2020.

Hagen, H. (1861). *Synopsis of the Neuroptera of North America: With a List of the South American Species*. Washington, DC: Smithsonian Institution.

Hales, K. G., Korey, C. A., Larracuente, A. M. and Roberts, D. M. (2015). Genetics on the fly: A primer on the *Drosophila* model system. *Genetics* **201**, 815–842.

Hamner, W. M., Hamner, P. P., Strand, S. W. and Gilmer, R. W. (1983). Behavior of antarctic krill, Euphausia superba: Chemoreception, feeding, schooling, and molting. *Science* **220**, 433–435.

Harkness, L. (1977). Chameleons use accommodation cues to judge distance. *Nature* **267**, 346–349.

Harris, V. A. (1990). *Sessile Animals of the Sea Shore*. London: Chapman and Hall.

Haselsteiner, A. F., Gilbert, C. and Wang, Z. J. (2014). Tiger beetles pursue prey using a proportional control law with a delay of one half-stride. *J. R. Soc. Interface* **11**, 20140216.

Hayward, M. W., Hofmeyr, M., O'Brien, J. and Kerley, G. I. H. (2006). Prey preferences of the cheetah (*Acinonyx jubatus*) (Felidae: Carnivora): Morphological limitations or the need to capture rapidly consumable prey before kleptoparasites arrive? *J. Zool.* **270**, 615–627.

Heiligenberg, W. (1989). Coding and processing of electrosensory information in gymnotiform fish. *J. Exp. Biol.* **146**, 255–75.

Heiligenberg, W. (1991). The neural basis of behavior: A neuroethological view. *Annu. Rev. Neurosci.* **14**, 247–267.

Heiling, A. M., Cheng, K. and Herberstein, M. E. (2004). Exploitation of floral signals by crab spiders (*Thomisus spectabilis*, Thomisidae). *Behav. Ecol.* **15**, 321–326.

Heiling, A. M., Chittka, L., Cheng, K. and Herberstein, M. E. (2005). Colouration

in crab spiders: substrate choice and prey attraction. *J. Exp. Biol.* **208**, 1785–92.

Heinrich, B. (1993). Cold Jumpers. In *The Hot-Blooded Insects*, pp. 422–446. Berlin: Springer-Verlag.

Heitler, W. J., Goodman, C. S. and Rowell, C. H. F. (1977). The effects of temperature on the threshold of identified neurons in the locust. *J. Comp. Physiol. A* **117**, 163–182.

Hendrie, C. A., Weiss, S. M. and Eilam, D. (1998). Behavioural response of wild rodents to the calls of an owl: A comparative study. *J. Zool.* **245**, 439–446.

Higham, T. E., Rogers, S. M., Langerhans, R. B., Jamniczky, H. A., Lauder, G. V., Stewart, W. J., Martin, C. H. and Reznick, D. N. (2016). Speciation through the lens of biomechanics: locomotion, prey capture and reproductive isolation. *Proc. R. Soc. B Biol. Sci.* **283**, 20161294.

Hildebrand, M. and Hurley, J. P. (1985). Energy of the oscillating legs of a fast-moving cheetah, pronghorn, jackrabbit, and elephant. *J. Morphol.* **184**, 23–31.

Hillen, R., Günther, T., Kohlen, C., Eckers, C., van Ermingen-Marbach, M., Sass, K., Scharke, W., Vollmar, J., Radach, R. and Heim, S. (2013). Identifying brain systems for gaze orienting during reading: fMRI investigation of the Landolt paradigm. *Front. Hum. Neurosci.* **7**, 384.

Holling, C. S. (1966). The functional response of invertebrate predators to prey density. *Mem. Entomol. Soc. Canada* **98**, 1–86.

Horn, M. M. (1989). Biology of marine herbivorous fishes. In *Oceanography and Marine Biology: An Annual Review. Vol. 27*, pp. 167–272. Aberdeen: Aberdeen University Press.

Horridge, G. A. (1978). The separation of visual axes in apposition compound eyes. *Philos. Trans. R. Soc. B Biol. Sci.* **285**, 1–59.

Horridge, G. A. (1980). Review lecture: Apposition eyes of large diurnal insects as organs adapted to seeing. *Proc. R. Soc. B Biol. Sci.* **207**, 287–309.

Horridge, G. A. and Duelli, P. (1979). Anatomy of the regional differences in the eye of the mantis *Ciulfina*. *J. Exp. Biol.* **80**, 165–190.

Howe, K., Clark, M. D., Torroja, C. F., Torrance, J., Berthelot, C., Muffato, M., Collins, J. E., Humphray, S., McLaren, K., Matthews, L., et al. (2013). The zebrafish reference genome sequence and its relationship to the human genome. *Nature* **496**, 498–503.

Hume, I. D. (2002). Digestive strategies of mammals. *Acta Zool. Sin.* **48**, 1–19.

Immonen, E.-V., Dacke, M., Heinze, S. and el Jundi, B. (2017). Anatomical organization of the brain of a diurnal and a nocturnal dung beetle. *J. Comp. Neurol.* **525**, 1879–1908.

Jabłoński, P. G. (1999). A rare predator exploits prey escape behavior: the role of tail-fanning and plumage contrast in foraging of the painted redstart (Myioborus pictus). *Behav. Ecol.* **10**, 7–14.

Jabłoński, P. G. (2001). Sensory exploitation of prey: Manipulation of the initial direction of prey escapes by a conspicuous "rare enemy." *Proc. R. Soc. B Biol. Sci.* **268**, 1017–1022.

Jenkin, P. M. (1957). The filter-feeding and food of flamingoes (Phoenicopteri). *Philos. Trans. R. Soc. B Biol. Sci.* **240**, 401–493.

Johnson, C. R. (1973). Behaviour of the Australian crocodiles, *Crocodylus johnstoni* and *C. porosus*. *Zool. J. Linn. Soc.* **52**, 315–336.

Jollie, M. (1973). The origin of the Chordates. *Acta Zool.* **54**, 81–100.

Kagaya, K. and Patek, S. N. (2016). Feed-forward motor control of ultrafast, ballistic movements. *J. Exp. Biol.* **219**, 319–33.

Kalmijn, A. J. (1971). The electric sense of sharks and rays. *J. Exp. Biol.* **55**, 371–83.

Kane, S. A., Fulton, A. H. and Rosenthal, L. J. (2015). When hawks attack: animal-borne video studies of goshawk pursuit and prey-evasion strategies. *J. Exp. Biol.* **218**, 212–22.

Karanth, K. U. and Sunquist, M. E. (2000). Behavioural correlates of predation by tiger (*Panthera tigris*), leopard (*Panthera pardus*) and dhole (*Cuon alpinus*) in Nagarahole, India. *J. Zool.* **250**, 255–265.

Karashchuk, P., Rupp, K. L., Dickinson, E. S., Sanders, E., Azim, E., Brunton, B. W. and Tuthill, J. C. (2020). Anipose: A toolkit for robust markerless 3D pose estimation. *bioRxiv* 2020.05.26.117325.

Karban, R. and Agrawal, A. A. (2002). Herbivore offense. *Annu. Rev. Ecol. Syst.* **33**, 641–664.

Keleş, M. F. and Frye, M. A. (2017). Object-detecting neurons in *Drosophila*. *Curr. Biol.* **27**, 680–687.

Kirkegaard, J. B. and Goldstein, R. E. (2016). Filter-feeding, near-field flows, and the morphologies of colonial choanoflagellates. *Phys. Rev. E* **94**, 052401.

Kirschfeld, K. (1966). Die Projektion der optischen Umwelt auf das Raster der Rhabdomere im Komplexauge von Musca. *Exp. Brain Res.* **3**, 248–270.

Klotsa, D. (2019). As above, so below, and also in between: mesoscale active matter in fluids. *Soft Matter* **15**, 8946–8950.

Knudsen, E. I. and Konishi, M. (1979). Mechanisms of Sound Localization in the Barn Owl (*Tyto alba*). *J. Comp. Physiol. A* **133**, 13–21.

Kral, K. (1998). Side-to-side head movements to obtain motion depth cues: A short

review of research on the praying mantis. *Behav. Processes* **43**, 71–77.

Kral, K. (2003). Behavioural–analytical studies of the role of head movements in depth perception in insects, birds and mammals. *Behav. Processes* **64**, 1–12.

Kral, K. (2013). Vision in the mantispid: a sit-and-wait and stalking predatory insect. *Physiol. Entomol.* **38**, 1–12.

Kral, K., Vernik, M. and Devetak, D. (2000). The visually controlled prey-capture behaviour of the European mantispid *Mantispa styriaca*. *J. Exp. Biol.* **203**, 2117–2123.

Krapp, H. G., Hengstenberg, B. and Hengstenberg, R. (1998). Dendritic structure and receptive-field organization of optic flow processing interneurons in the fly. *J. Neurophysiol.* **79**, 1902–1917.

Krebs, H. A. (1975). The August Krogh principle: "For many problems there is an animal on which it can be most conveniently studied." *J. Exp. Zool.* **194**, 221–226.

Krogh, A. (1929). The progress of physiology. *Am. J. Physiol.* **90**, 243–251.

Kynaston, S. E., McErlain-Ward, P. and Mill, P. J. (1994). Courtship, mating behaviour and sexual cannibalism in the praying mantis, *Sphodromantis lineola*. *Anim. Behav.* **47**, 739–741.

Land, M. F. (1969). Movements of the retinae of jumping spiders (Salticidae: Dendryphantinae) in response to visual stimuli. *J. Exp. Biol.* **51**, 471–493.

Land, M. F. (1982). Scanning eye movements in a heteropod mollusc. *J. Exp. Biol.* **96**, 427–430.

Land, M. F. (1993). Chasing and pursuit in the dolichopodid fly *Poecilobothrus nobilitatus*. *J. Comp. Physiol. A* **173**, 605–613.

Land, M. F. (1999). Motion and vision: why animals move their eyes. *J. Comp. Physiol. A* **185**, 341–352.

Land, M. F. (2003). Visual acuity in insects. *Annu. Rev. Entomol.* **42**, 147–177.

Land, M. (2019). Eye movements in man and other animals. *Vision Res.* **162**, 1–7.

Land, M. F. and Collett, T. S. (1974). Chasing behaviour of houseflies (*Fannia canicularis*). *J. Comp. Physiol.* **89**, 331–357.

Land, M. F. and Nilsson, D.-E. (2002). *Animal Eyes*. Oxford: Oxford University Press.

Land, M. F., Marshall, J. N., Brownless, D. and Cronin, T. W. (1990). The eye-movements of the mantis shrimp Odontodactylus scyllarus (Crustacea: Stomatopoda). *J. Comp. Physiol. A* **167**, 155–166.

Lappin, A. K., Monroy, J. A., Pilarski, J. Q., Zepnewski, E. D., Pierotti, D. J. and

Nishikawa, K. C. (2006). Storage and recovery of elastic potential energy powers ballistic prey capture in toads. *J. Exp. Biol.* **209**, 2535–53.

Laughlin, S. B. and Hardie, R. C. (1978). Common strategies for light adaptation in the peripheral visual systems of fly and dragonfly. *J. Comp. Physiol. A* **128**, 319–340.

Laughlin, S. and McGinness, S. (1978). The structures of dorsal and ventral regions of a dragonfly retina. *Cell Tissue Res.* **188**, 427–447.

Laughlin, S. B. and Weckström, M. (1993). Fast and slow photoreceptors - a comparative study of the functional diversity of coding and conductances in the Diptera. *J. Comp. Physiol. A* **172**, 593–609.

Lawrence, S. E. (1992). Sexual cannibalism in the praying mantid, *Mantis religiosa*: a field study. *Anim. Behav.* **43**, 569–583.

Lea, J. Y. and Mueller, C. G. (1977). Saccadic head movements in mantids. *J. Comp. Physiol. A* **114**, 115–128.

Lehmann, F.-O. (2001). The efficiency of aerodynamic force production in *Drosophila*. *Comp. Biochem. Physiol. Part A Mol. Integr. Physiol.* **131**, 77–88.

Lehmann, F. O. and Dickinson, M. H. (1997). The changes in power requirements and muscle efficiency during elevated force production in the fruit fly *Drosophila melanogaster*. *J. Exp. Biol.* **200**, 1133–1143.

Lehrer, M. and Collett, T. S. (1994). Approaching and departing bees learn different cues to the distance of a landmark. *J. Comp. Physiol. A* **175**, 171–177.

Lehrer, M. and Srinivasan, M. V. (1994). Active vision in honeybees: Task-oriented suppression of an innate behaviour. *Vision Res.* **34**, 511–516.

Lehrer, M., Srinivasan, M. V., Zhang, S. W. and Horridge, G. A. (1988). Motion cues provide the bee's visual world with a third dimension. *Nature* **332**, 356–357.

Leonelli, S. and Ankeny, R. A. (2013). What makes a model organism? *Endeavour* **37**, 209–212.

Levín, L. and Maldonado, H. (1970). A fovea in the praying mantis eye III. The centring of the prey. *Z. Vgl. Physiol.* **67**, 93–101.

Lin, H.-T. and Leonardo, A. (2017). Heuristic rules underlying dragonfly prey selection and interception. *Curr. Biol.* **27**, 1124–1137.

Lissman, H. W. (1958). On the function and evolution of electric organs in fish. *J. Exp. Biol.* **35**, 156–191.

Lissman, H. W. and Machin, K. E. (1958). The mechanism of object location in *Gymnarchus Niloticus* and similar fish. *J. Exp. Biol.* **35**, 451–86.

Long, J. H., Koob-Emunds, M., Sinwell, B. and Koob, T. J. (2002). The notochord

of hagfish *Myxine glutinosa* : visco-elastic properties and mechanical functions during steady swimming. *J. Exp. Biol.* **205**, 3819–3831.

Longden, K. D., Wicklein, M., Hardcastle, B. J., Huston, S. J. and Krapp, H. G. (2017). Spike burst coding of translatory optic flow and depth from motion in the fly visual system. *Curr. Biol.* **27**, 3225-3236.e3.

Longo, S. J., Cox, S. M., Azizi, E., Ilton, M., Olberding, J. P., St Pierre, R. and Patek, S. N. (2019). Beyond power amplification: latch-mediated spring actuation is an emerging framework for the study of diverse elastic systems. *J. Exp. Biol.* **222**,.

Loxton, R. G. and Nicholls, I. (1979). The functional morphology of the praying mantis forelimb (Dictyoptera: Mantodea). *Zool. J. Linn. Soc.* **66**, 185–203.

Lucas, J. R. (1982). The biophysics of pit construction by antlion larvae (*Myrmeleon*, Neuroptera). *Anim. Behav.* **30**, 651–664.

Lutz, G. J. and Rome, L. C. (1994). Built for jumping: The design of the frog muscular system. *Science* **263**, 370–372.

MaBouDi, H., Roper, M., Guiraud, M., Marshall, J. A. R. and Chittka, L. (2021). Automated video tracking and flight analysis show how bumblebees solve a pattern discrimination task using active vision. *bioRxiv* 2021.03.09.434580.

Machin, K. E., Sutton Pringle, J. W. and Tamasige, M. (1962). The physiology of insect fibrillar muscle - IV. The effect of temperature on a beetle flight muscle. *Proc. R. Soc. B Biol. Sci.* **155**, 493–499.

Maeno, K. O., Ould Ely, S., Ould Mohamed, S., Jaavar, M. E. H., Nakamura, S. and Ould Babah Ebbe, M. A. (2019). Defence tactics cycle with diel microhabitat choice and body temperature in the desert locust, *Schistocerca gregaria*. *Ethology* **125**, 250–261.

Maldonado, H. (1972). A learning process in the praying mantis. *Physiol. Behav.* **9**, 435–445.

Marshall, C. R. (2006). Explaining the Cambridan “explosion” of animals. *Annu. Rev. Earth Planet. Sci.* **34**, 355–384.

Martin, C. H. (1968). The new family Leptogastridae (the grass flies) compared with the Asilidae (robber flies) (Diptera). *J. Kansas Entomol. Soc.* **41**, 70–100.

Mathis, A., Mamidanna, P., Cury, K. M., Abe, T., Murthy, V. N., Mathis, M. W. and Bethge, M. (2018). DeepLabCut: Markerless pose estimation of user-defined body parts with deep learning. *Nat. Neurosci.* **21**, 1281–1289.

Mauseth, J. D. (2014). *Botany: An Introduction to Plant Biology*. 5th ed. Burlington, MA: Jones & Bartlett Learning.

Mazer, J. A. and Gallant, J. L. (2003). Goal-related activity in V4 during free viewing visual search: evidence for a ventral stream visual salience map.

Neuron **40**, 1241–1250.

McElligott, M. B. and O'Malley, D. M. (2005). Prey tracking by larval zebrafish: Axial kinematics and visual control. *Brain. Behav. Evol.* **66**, 177–196.

McGowan, C. P. and Collins, C. E. (2018). Why do mammals hop? Understanding the ecology, biomechanics and evolution of bipedal hopping. *J. Exp. Biol.* **221**, jeb161661.

McMenamin, M. A. and Schulte McMenamin, D. L. (1990). *The Emergence of Animals: The Cambrian Breakthrough*. New York, NY: Columbia University Press.

Meijering, E. (2008). MTrackJ (ImageJ plugin). *Biomed. Imaging Gr. Rotterdam, Erasmus MC—University Med. Center, Rotterdam, Netherlands*.

Meinertzhagen, I. A. (1996). Ultrastructure and quantification of synapses in the insect nervous system. *J. Neurosci. Methods* **69**, 59–73.

Meinertzhagen, I. A. (2016). Morphology of invertebrate neurons and synapses. In *The Oxford Handbook of Invertebrate Neurobiology* (ed. Byrne, J. H.), pp. 247–84. Oxford: Oxford University Press.

Meinertzhagen, I. A. and O'Neil, S. D. (1991). Synaptic organization of columnar elements in the lamina of the wild type in Drosophila melanogaster. *J. Comp. Neurol.* **305**, 232–263.

Meinertzhagen, I. A. and Sorra, K. E. (2001). Synaptic organization in the fly's optic lamina: few cells, many synapses and divergent microcircuits. In *Progress in Brain Research* (ed. Kolb, H.), Ripps, H.), and Wu, S.), pp. 53–69. Amsterdam: Elsevier.

Meinertzhagen, I. A., Takemura, S., Meinertzhagen, I. A., Takemura, S., Lu, Z., Huang, S., Gao, S., Ting, C.-Y. and Lee, C.-H. (2009). From form to function: the ways to know a neuron. *J. Neurogenet.* **23**, 68–77.

Menzel, R. and Giurfa, M. (2001). Cognitive architecture of a mini-brain: the honeybee. *Trends Cogn. Sci.* **5**, 62–71.

Merron, G. S. (1993). Pack-hunting in two species of catfish, *Clavias gariepinus* and *C. ngamensis*, in the Okavango Delta, Botswana. *J. Fish Biol.* **43**, 575–584.

Milledge, G. (1990). Revision of the genus *Nesoxypilus* Beier (Mantodea: Amorphoscelidae: Paraoxypilinae). *Mem. Museum Victoria* **50**, 347–355.

Miller, W. H., Bernard, G. D. and Allen, J. L. (1968). The optics of insect compound eyes. *Science* **162**, 760–7.

Mischiati, M., Lin, H.-T., Herold, P., Imler, E., Olberg, R. and Leonardo, A. (2015). Internal models direct dragonfly interception steering. *Nature* **517**, 333–338.

Misof, B., Liu, S., Meusemann, K., Peters, R. S., Donath, A., Mayer, C., Frandsen, P. B., Ware, J., Flouri, T., Beutel, R. G., et al. (2014). Phylogenomics resolves the timing and pattern of insect evolution. *Science* **346**, 763–7.

Mitchell, J. F., Reynolds, J. H. and Miller, C. T. (2014). Active vision in marmosets: A model system for visual neuroscience. *J. Neurosci.* **34**, 1183–94.

Mizuno, T., Yamaguchi, S., Yamamoto, I., Yamaoka, R. and Akino, T. (2014). "Double-trick" visual and chemical mimicry by the juvenile orchid mantis *Hymenopus coronatus* used in predation of the oriental honeybee *Apis cerana*. *Zoolog. Sci.* **31**, 795–801.

Montgomery, R. B. (1947). Viscosity and Thermal Conductivity of Air and Diffusivity of Water Vapor in Air. *J. Meteorol.* **4**, 193–196.

Moore, T. Y. and Biewener, A. A. (2015). Outrun or outmaneuver: Predator–prey interactions as a model system for integrating biomechanical studies in a broader ecological and evolutionary context. *Integr. Comp. Biol.* **55**, icv074.

Mørup Jørgensen, J., Flock, Å. and Wersäll, J. (1972). The lorenzinian ampullae of *Polyodon spathula*. *Zeitschrift für Zellforsch. und Mikroskopische Anat.* **130**, 362–377.

Motta, P. J., Maslanka, M., Hueter, R. E., Davis, R. L., de la Parra, R., Mulvany, S. L., Habegger, M. L., Strother, J. A., Mara, K. R., Gardiner, J. M., et al. (2010). Feeding anatomy, filter-feeding rate, and diet of whale sharks *Rhincodon typus* during surface ram filter feeding off the Yucatan Peninsula, Mexico. *Zoology* **113**, 199–212.

Munk, O. (1999). The escal photophore of ceratioids (Pisces; Ceratioidei) - a review of structure and function. *Acta Zool.* **80**, 265–284.

Namiki, S., Dickinson, M. H., Wong, A. M., Korff, W. and Card, G. M. (2018). The functional organization of descending sensory-motor pathways in Drosophila. *Elife* **7**, e34272.

Nelson, T. C. (1923). The mechanism of feeding in the oyster. *Proc. Soc. Exp. Biol. Med.* **21**, 166–168.

Nevitt, G. A., Veit, R. R. and Kareiva, P. (1995). Dimethyl sulphide as a foraging cue for Antarctic Procellariiform seabirds. *Nature* **376**, 680–682.

Nevitt, G. A., Losekoot, M. and Weimerskirch, H. (2008). Evidence for olfactory search in wandering albatross, *Diomedea exulans*. *Proc. Natl. Acad. Sci.* **105**, 4576–81.

Newkirk, M. R. (1963). The feeding and mating of *Leptogaster annulatus* (Diptera: Asilidae). *Ann. Entomol. Soc. Am.* **56**, 234–236.

Nicholas, S., Supple, J., Leibbrandt, R., Gonzalez-Bellido, P. T. and Nordström, K. (2018). Integration of small- and wide-field visual features in target-selective descending neurons of both predatory and nonpredatory dipterans.

J. Neurosci. **38**, 10725–10733.

Nicol, J. A. C. (1950). Responses of *Branchiomma vesiculosum* (Montagu) to photic stimulation. *J. Mar. Biol. Assoc. United Kingdom* **29**, 303–320.

Nilsson, D.-E. (1996). Eye ancestry: Old genes for new eyes. *Curr. Biol.* **6**, 39–42.

Nilsson, D.-E. (2009). The evolution of eyes and visually guided behaviour. *Philos. Trans. R. Soc. B Biol. Sci.* **364**, 2833–2847.

Nishida, R. (2002). Sequestration of defensive substances from plants by Lepidoptera. *Annu. Rev. Entomol.* **47**, 57–92.

Nityananda, V. and Read, J. C. A. (2017). Stereopsis in animals: Evolution, function and mechanisms. *J. Exp. Biol.* **220**, 2502–2512.

Nityananda, V., Tarawneh, G., Rosner, R., Nicolas, J., Crichton, S. and Read, J. (2016a). Insect stereopsis demonstrated using a 3D insect cinema. *Sci. Rep.* **6**, 18718.

Nityananda, V., Bissianna, G., Tarawneh, G. and Read, J. (2016b). Small or far away? Size and distance perception in the praying mantis. *Philos. Trans. R. Soc. B Biol. Sci.* **371**, 20150262.

Nityananda, V., Tarawneh, G., Henriksen, S., Umeton, D., Simmons, A. and Read, J. C. A. (2018). A novel form of stereo vision in the praying mantis. *Curr. Biol.* **28**, 588-593.e4.

Niven, J. E., Anderson, J. C. and Laughlin, S. B. (2007). Fly photoreceptors demonstrate energy-information trade-offs in neural coding. *PLoS Biol.* **5**, e116.

Nordström, K. and O'Carroll, D. C. (2006). Small object detection neurons in female hoverflies. *Proc. R. Soc. B Biol. Sci.* **273**, 1211–1216.

Northcutt, R. G. and Gans, C. (1983). The genesis of neural crest and epidermal placodes: A reinterpretation of vertebrate origins. *Q. Rev. Biol.* **58**, 1–28.

O'Carroll, D. (1993). Feature-detecting neurons in dragonflies. *Nature* **362**, 541–543.

O'Hanlon, J. C., Holwell, G. I. and Herberstein, M. E. (2014). Pollinator deception in the orchid mantis. *Am. Nat.* **183**, 126–132.

O'Shea, M. and Williams, J. L. D. (1974). The anatomy and output connection of a locust visual interneurone; the lobular giant movement detector (LGMD) neurone. *J. Comp. Physiol.* **91**, 257–266.

Olberg, R. (1979). Visual and Multimodal Interneurosn in Dragonflies.

Olberg, R. M. (1981a). Object- and self-movement detectors in the ventral nerve cord of the dragonfly. *J. Comp. Physiol. A* **141**, 327–334.

Olberg, R. M. (1981b). Parallel encoding of direction of wind, head, abdomen, and visual pattern movement by single interneurons in the dragonfly. *J. Comp. Physiol. A* **142**, 27–41.

Olberg, R. M. (1983). Identified interneurons steer flight in the dragonfly. In *Society for Neuroscience Abstracts*, p. 326.

Olberg, R. M. (2012). Visual control of prey-capture flight in dragonflies. *Curr. Opin. Neurobiol.* **22**, 267–271.

Olberg, R. M., Worthington, A. H. and Venator, K. R. (2000). Prey pursuit and interception in dragonflies. *J. Comp. Physiol. A* **186**, 155–162.

Olberg, R. M., Seaman, R. C., Coats, M. I. and Henry, A. F. (2007). Eye movements and target fixation during dragonfly prey-interception flights. *J. Comp. Physiol. A* **193**, 685–693.

Otsuna, H. and Ito, K. (2006). Systematic analysis of the visual projection neurons of *Drosophila melanogaster*. I. Lobula-specific pathways. *J. Comp. Neurol.* **497**, 928–958.

Oufiero, C. E. (2020). Evolutionary diversification in the raptorial forelegs of Mantodea: Relations to body size and depth perception. *J. Morphol.* **281**, 513–522.

Packer, C., Scheel, D. and Pusey, A. E. (1990). Why lions form groups: food is not enough. *Am. Nat.* **136**, 1–19.

Parker, A. R. (1998). Colour in Burgess Shale animals and the effect of light on evolution in the Cambrian. *Proc. R. Soc. B Biol. Sci.* **265**, 967–972.

Patek, S. N., Korff, W. L. and Caldwell, R. L. (2004). Deadly strike mechanism of a mantis shrimp. *Nature* **428**, 819–820.

Patek, S. N., Rosario, M. V and Taylor, J. R. A. (2013). Comparative spring mechanics in mantis shrimp. *J. Exp. Biol.* **216**, 1317–29.

Paterson, J. R., García-Bellido, D. C., Lee, M. S. Y., Brock, G. A., Jago, J. B. and Edgecombe, G. D. (2011). Acute vision in the giant Cambrian predator *Anomalocaris* and the origin of compound eyes. *Nature* **480**, 237–240.

Pembury Smith, M. Q. R. and Ruxton, G. D. (2020). Camouflage in predators. *Biol. Rev.* **95**, 1325–1340.

Pérez-de la Fuente, R. and Peñalver, E. (2019). A mantidfly in Cretaceous Spanish amber provides insights into the evolution of integumentary specialisations on the raptorial foreleg. *Sci. Rep.* **9**, 13248.

Perl, C. D. and Niven, J. E. (2016). Differential scaling within an insect compound eye. *Biol. Lett.* **12**, 20160042.

Perl, C. D., Rossoni, S. and Niven, J. E. (2017). Conservative whole-organ scaling

contrasts with highly labile suborgan scaling differences among compound eyes of closely related Formica ants. *Ecol. Evol.* **7**, 1663–1673.

Pick, B. (1977). Specific misalignments of rhabdomere visual axes in the neural superposition eye of dipteran flies. *Biol. Cybern.* **26**, 215–224.

Pietsch, T. W. and Grobecker, D. B. (1978). The compleat angler: Aggressive mimicry in an antennariid anglerfish. *Science* **201**, 369–370.

Ponitz, B., Schmitz, A., Fischer, D., Bleckmann, H. and Brücker, C. (2014). Diving-flight aerodynamics of a peregrine falcon (*Falco peregrinus*). *PLoS One* **9**, e86506.

Poteser, M. and Kral, K. (1995). Visual distance discrimination between stationary targets in praying mantis: An index of the use of motion parallax. *J. Exp. Biol.* **198**, 2127–2137.

Prete, F. R. (1990). Prey capture in mantids: The role of the prothoracic tibial flexion reflex. *J. Insect Physiol.* **36**, 335–338.

Prete, F. R., Placek, P. J., Wilson, M. A., Mahaffey, R. J. and Nemcek, R. R. (1993). Stimulus speed and order of presentation effect the visually released predatory behaviors of the praying mantis *Sphodromantis lineola* (Burr.). *Brain. Behav. Evol.* **42**, 281–294.

Prete, F. R., Hurd, L. E., Branstrator, D. and Johnson, A. (2002). Responses to computer-generated visual stimuli by the male praying mantis, *Sphodromantis lineola* (Burmeister). *Anim. Behav.* **63**, 503–510.

R Core Team (2017). R: A language and environment for statistical computing. R Foundation for Statistical Computing, Vienna, Austria. 2016.

Ravi, S., Bertrand, O., Siesenop, T., Manz, L.-S., Doussot, C., Fisher, A. and Egelhaaf, M. (2019). Gap perception in bumblebees. *J. Exp. Biol.* **222**, jeb184135.

Rayer, B., Naynert, M. and Stieve, H. (1990). Phototransduction: different mechanisms in vertebrates and invertebrates. *J. Photochem. Photobiol. B Biol.* **7**, 107–48.

Rilling, S., Mittelstaedt, H. and Roeder, K. D. (1959). Prey recognition in the praying mantis. *Behaviour* **14**, 164–184.

Rind, F. C. and Simmons, P. J. (1992). Orthopteran DCMD neuron: a reevaluation of responses to moving objects. I. Selective responses to approaching objects. *J. Neurophysiol.* **68**, 1654–66.

Ritzmann, R. E. (1973). Snapping behavior of the shrimp Alpheus californiensis. *Science* **181**, 459–60.

Robinson, M. H. and Robinson, B. (1971). The predatory behavior of the ogre-faced spider *Dinopis longipes* F. Cambridge (Araneae: Dinopidae). *Am. Midl.*

Nat. **85**, 85.

Roche, B. E., Schulte-Hostedde, A. I. and Brooks, R. J. (1999). Route choice by deer mice (*Peromyscus maniculatus*): Reducing the risk of auditory detection by predators. *Am. Midl. Nat.* **142**, 194–197.

Roeder, K. D. (1937). The control of tonus and locomotor activity in the praying mantis (*Mantis religiosa* L.). *J. Exp. Zool.* **76**, 353–374.

Roeder, K. D. (1998). *Nerve Cells and Insect Behavior*. Cambridge, MA: Harvard University Press.

Roeder, K. D., Tozian, L. and Weiant, E. A. (1960). Endogenous nerve activity and behaviour in the mantis and cockroach. *J. Insect Physiol.* **4**, 45–62.

Rogers, B. and Graham, M. (1979). Motion parallax as an independent cue for depth perception. *Perception* **8**, 125–34.

Rogers, B. and Graham, M. (1982). Similarities between motion parallax and stereopsis in human depth perception. *Vision Res.* **22**, 261–270.

Röschard, J. and Roces, F. (2011). Sequential load transport in grass-cutting ants (*Atta vollenweideri*): maximization of plant delivery rate or improved information transfer? *Psyche A J. Entomol.* **2011**, 1–10.

Rosner, R., von Hadeln, J., Salden, T. and Homberg, U. (2017). Anatomy of the lobula complex in the brain of the praying mantis compared to the lobula complexes of the locust and cockroach. *J. Comp. Neurol.* **525**, 2343–2357.

Rosner, R., von Hadeln, J., Tarawneh, G. and Read, J. C. A. (2019). A neuronal correlate of insect stereopsis. *Nat. Commun.* **10**, 2845.

Rossel, S. (1979). Regional differences in photoreceptor performance in the eye of the praying mantis. *J. Comp. Physiol. A* **131**, 95–112.

Rossel, S. (1980). Foveal fixation and tracking in the praying mantis. *J. Comp. Physiol. A* **139**, 307–331.

Rossel, S. (1983). Binocular stereopsis in an insect. *Nature* **302**, 821–822.

Rossoni, S. and Niven, J. E. (2020). Prey speed influences the speed and structure of the raptorial strike of a 'sit-and-wait' predator. *Biol. Lett.* **16**, 20200098.

Rowell, C. H. F. (1989). The taxonomy of invertebrate neurons: a plea for a new field. *Trends Neurosci.* **12**, 169–174.

Rudebeck, G. (1950). The choice of prey and modes of hunting of predatory birds with special reference to their selective effect. *Oikos* **2**, 65.

Ruiz, C. and Theobald, J. C. (2020). Ventral motion parallax enhances fruit fly steering to visual sideslip. *Biol. Lett.* **16**, 20200046.

Sabrosky, C. W. (1989). Family Chloropidae. In *Catalog of the Diptera of the*

Australasian and Oceanian Regions (ed. Evenhuis, N.), pp. 650–665. Honolulu, HI: Bishop Museum Special Publication.

Sanderson, S. L. and Wassersug, R. (1993). Convergent and alternative designs for vertebrate suspension feeding. In *The Skull, Volume 3: Functional and Evolutionary Mechanisms* (ed. Hanken, J.) and Hall, B. K.), pp. 37–112. London: University of Chicago Press.

Sato, K. and Yamawaki, Y. (2014). Role of a looming-sensitive neuron in triggering the defense behavior of the praying mantis *Tenodera aridifolia*. *J. Neurophysiol.* **112**, 671–682.

Savitzky, A. and Golay, M. J. E. (1964). Smoothing and differentiation of data by simplified least squares procedures. *Anal. Chem.* **36**, 1627–1639.

Savoca, M. S., Wohlfeil, M. E., Ebeler, S. E. and Nevitt, G. A. (2016). Marine plastic debris emits a keystone infochemical for olfactory foraging seabirds. *Sci. Adv.* **2**, e1600395.

Say, T. (1859). *The Complete Writings of Thomas Say on the Entomology of North America*. New York, NY: Bailliere Brothers.

Schiff, H., Abbott, B. C. and Manning, R. B. (1985). Possible monocular range-finding mechanisms in stomatopods from different environmental light conditions. *Comp. Biochem. Physiol. Part A Physiol.* **80**, 271–280.

Schlosser, G. (2018). A short history of nearly every sense—The evolutionary history of vertebrate sensory cell types. *Integr. Comp. Biol.* **58**, 301–316.

Schneirla, T. C. (1934). Raiding and other outstanding phenomena in the behavior of army ants. *Proc. Natl. Acad. Sci.* **20**, 316–21.

Seidensticker, J. and McDougal, C. (1993). Tiger predatory behaviour, ecology and conservation. *Symp. Zool. Soc. London* 105–125.

Seitz, G. (1968). Der strahlengang im appositionsauge von Calliphora erythrocephala (Meig.). *Z. Vgl. Physiol.* **59**, 205–231.

Sharp, N. C. C. (1997). Timed running speed of a cheetah (*Acinonyx jubatus*). *J. Zool.* **241**, 493–494.

Shashar, N. and Cronin, T. W. (1996). Polarization contrast vision in Octopus. *J. Exp. Biol.* **199**, 999–1004.

Shashar, N., Hanlon, R. T. and Petz, A. deM. (1998). Polarization vision helps detect transparent prey. *Nature* **393**, 222–223.

Shashar, N., Hagan, R., Boal, J. G. and Hanlon, R. T. (2000). Cuttlefish use polarization sensitivity in predation on silvery fish. *Vision Res.* **40**, 71–75.

Shaw, S. R., Fröhlich, A. and Meinertzhagen, I. A. (1989). Direct connections between the R7/8 and R1?6 photoreceptor subsystems in the dipteran visual

system. *Cell Tissue Res.* **257**, 295–302.

Sherk, T. E. (1978). Development of the compound eyes of dragonflies (odonata). III. Adult compound eyes. *J. Exp. Zool.* **203**, 61–79.

Shlaer, R. (1972). An eagle's eye: quality of the retinal image. *Science* **176**, 920–2.

Shneydor, N. A. (1998). *Missile Guidance and Pursuit: Kinematics, Dynamics and Control*. Amsterdam: Elsevier.

Shu, D.-G., Luo, H.-L., Conway Morris, S., Zhang, X.-L., Hu, S.-X., Chen, L., Han, J., Zhu, M., Li, Y. and Chen, L.-Z. (1999). Lower Cambrian vertebrates from south China. *Nature* **402**, 42–46.

Sillar, K. T., Picton, L. D. and Heitler, W. J. (2016). *The Neuroethology of Predation and Escape*. Chichester: John Wiley & Sons, Ltd.

Smolla, M., Ruchty, M., Nagel, M. and Kleineidam, C. J. (2014). Clearing pigmented insect cuticle to investigate small insects' organs in situ using confocal laser-scanning microscopy (CLSM). *Arthropod Struct. Dev.* **43**, 175–181.

Snelling, E. P., Becker, C. L. and Seymour, R. S. (2013). The effects of temperature and body mass on jump performance of the locust *Locusta migratoria*. *PLoS One* **8**, e72471.

Snyder, A. W. (1977). Acuity of compound eyes: Physical limitations and design. *J. Comp. Physiol. A* **116**, 161–182.

Sobel, E. C. (1990). The locust's use of motion parallax to measure distance. *J. Comp. Physiol. A* **167**, 579–588.

Soto, A. P. and McHenry, M. J. (2020). Pursuit predation with intermittent locomotion in zebrafish. *J. Exp. Biol.* **223**, jeb230623.

Sparks, D. L. (1986). Translation of sensory signals into commands for control of saccadic eye movements: role of primate superior colliculus. *Physiol. Rev.* **66**, 118–71.

Spence, R., Fatema, M. K., Ellis, S., Ahmed, Z. F. and Smith, C. (2007a). Diet, growth and recruitment of wild zebrafish in Bangladesh. *J. Fish Biol.* **71**, 304–309.

Spence, R., Gerlach, G., Lawrence, C. and Smith, C. (2007b). The behaviour and ecology of the zebrafish, *Danio rerio*. *Biol. Rev.* **83**, 13–34.

Srinivasan, M. V. and Davey, M. (1995). Strategies for active camouflage of motion. *Proc. R. Soc. B Biol. Sci.* **259**, 19–25.

Srinivasan, M. V., Lehrer, M., Zhang, S. W. and Horridge, G. A. (1989). How honeybees measure their distance from objects of unknown size. *J. Comp. Physiol. A* **165**, 605–613.

Stafstrom, J. A. and Hebets, E. A. (2016). Nocturnal foraging enhanced by enlarged secondary eyes in a net-casting spider. *Biol. Lett.* **12**, 20160152.

Stander, P. E. (1992). Cooperative hunting in lions: the role of the individual. *Behav. Ecol. Sociobiol.* **29**, 445–454.

Stavenga, D. G. (1975). The neural superposition eye and its optical demands. *J. Comp. Physiol. A* **102**, 297–304.

Stavenga, D. G. (1979). Pseudopupils of compound eyes. In *Comparative physiology and evolution of vision in invertebrates. Handbook of Sensory Physiology.*, pp. 357–439. Berlin, Heidelberg: Springer.

Stavenga, D. G. (2003). Angular and spectral sensitivity of fly photoreceptors. II. Dependence on facet lens F-number and rhabdomere type in Drosophila. *J. Comp. Physiol. A* **189**, 189–202.

Stavenga, D. G., Kruizinga, R. and Leertouwer, H. L. (1990). Dioptrics of the facet lenses of male blowflies *Calliphora* and *Chrysomyia*. *J. Comp. Physiol. A* **166**, 365–371.

Stein, P. and Becker, T. (1903). Aegyptische Dipteren. *Mitteilungen aus dem Zool. Museum Berlin* **2**, 67–195.

Stevens, M. (2013). *Sensory Ecology, Behaviour, and Evolution*. Oxford: Oxford University Press.

Stevenson, R. D., Hill, M. F. and Bryant, P. J. (1995). Organ and cell allometry in Hawaiian *Drosophila* : how to make a big fly. *Proc. R. Soc. B Biol. Sci.* **259**, 105–110.

Stork, N. E. (2018). How many species of insects and other terrestrial arthropods are there on Earth? *Annu. Rev. Entomol.* **63**, 31–45.

Strübin, C., Steinegger, M. and Bshary, R. (2011). On group living and collaborative hunting in the yellow saddle goatfish (*Parupeneus cyclostomus*). *Ethology* **117**, 961–969.

Supple, J. A. (2019). *Descending Premotor Target Tracking Systems in Flying Insects*, PhD thesis, University of Cambridge, UK.

Supple, J. A., Pinto-Benito, D., Khoo, C., Wardill, T. J., Fabian, S. T., Liu, M., Pusdekar, S., Galeano, D., Pan, J., Jiang, S., et al. (2020). Binocular encoding in the damselfly pre-motor target tracking system. *Curr. Biol.* **30**, 645-656.e4.

Svenson, G. J., Hardy, N. B., Cahill Wightman, H. M. and Wieland, F. (2015). Of flowers and twigs: Phylogenetic revision of the plant-mimicking praying mantises (Mantodea: Empusidae and Hymenopodidae) with a new suprageneric classification. *Syst. Entomol.* **40**, 789–834.

Swallow, J. G., Wilkinson, G. S. and Marden, J. H. (2000). Aerial performance of stalk-eyed flies that differ in eye span. *J. Comp. Physiol. B* **170**, 481–7.

Tammero, L. F. and Dickinson, M. H. (2002). The influence of visual landscape on the free flight behavior of the fruit fly Drosophila melanogaster. *J. Exp. Biol.* **205**, 327–343.

Tang, L. S., Goeritz, M. L., Caplan, J. S., Taylor, A. L., Fisek, M. and Marder, E. (2010). Precise temperature compensation of phase in a rhythmic motor pattern. *PLoS Biol.* **8**, e1000469.

Thomas, J. A., Moss, C. F. and Vater, M. (2004). *Echolocation in Bats and Dolphins*. Chicago, IL: University of Chicago Press.

Thorington, L. (1985). Spectral, irradiance, and temporal aspects of natural and artificial light. *Ann. N. Y. Acad. Sci.* **453**, 28–54.

Tucker, V. (1998). Gliding flight: speed and acceleration of ideal falcons during diving and pull out. *J. Exp. Biol.* **201**, 403–414.

Tucker, V. A. and Parrott, G. C. (1970). Aerodynamics of gliding flight in a falcon and other birds. *J. Exp. Biol.* **52**, 345–367.

Tuthill, J. C., Nern, A., Holtz, S. L., Rubin, G. M. and Reiser, M. B. (2013). Contributions of the 12 neuron classes in the fly lamina to motion vision. *Neuron* **79**, 128–140.

Usherwood, J. R., Sparkes, E. L. and Weller, R. (2014). Leap and strike kinetics of an acoustically "hunting" barn owl (*Tyto alba*). *J. Exp. Biol.* **217**, 3002–5.

Van Buskirk, R. W. and Nevitt, G. A. (2008). The influence of developmental environment on the evolution of olfactory foraging behaviour in procellariiform seabirds. *J. Evol. Biol.* **21**, 67–76.

van der Willigen, R., Frost, B. and Wagner, H. (2002). Depth generalization from stereo to motion parallax in the owl. *J. Comp. Physiol. A* **187**, 997–1007.

Varennes, L., Krapp, H. G. and Viollet, S. (2020). Two pursuit strategies for a single sensorimotor control task in blowfly. *Sci. Rep.* **10**, 20762.

Vasas, V. and Chittka, L. (2019). Insect-inspired sequential inspection strategy enables an artificial network of four neurons to estimate numerosity. *iScience* **11**, 85–92.

Vermeij, G. J. (1989). The origin of skeletons. *Palaios* **4**, 585–589.

Vermeij, G. J. (1993). *Evolution and Escalation: An Ecological History of Life*. Princeton, NJ: Princeton University Press.

Vermeij, G. J. (2004). *Nature: An Economic History*. Princeton, NJ: Princeton University Press.

Vinnikov, Y. A. (1982). Evolution of receptor cells: Cytological, membranous and molecular levels. *Mol. Biol. Biochem. Biophys.* **34**, 1–141.

Visser, I. N., Smith, T. G., Bullock, I. D., Green, G. D., Carlsson, O. G. L. and

Imberti, S. (2008). Antarctic peninsula killer whales (*Orcinus orca*) hunt seals and a penguin on floating ice. *Mar. Mammal Sci.* **24**, 225–234.

Vogel, S. (1967). Flight in *Drosophila*: III. Aerodynamic characteristics of fly wing sand wing models. *J. Exp. Biol.* **46**, 431–443.

von Reyn, C. R., Breads, P., Peek, M. Y., Zheng, G. Z., Williamson, W. R., Yee, A. L., Leonardo, A. and Card, G. M. (2014). A spike-timing mechanism for action selection. *Nat. Neurosci.* **17**, 962–970.

Wagner, H. (1986). Flight performance and visual control of flight of the free-flying housefly (*Musca domestica* L.) II. Pursuit of targets. *Philos. Trans. R. Soc. B Biol. Sci.* **312**, 553–579.

Wainwright, P. C. and Bennett, A. F. (1992). The mechanism of tongue projection in chameleons: I. Electromyographic tests of functional hypotheses. *J. Exp. Biol.* **168**, 1–21.

Wakeling, J. and Ellington, C. (1997a). Dragonfly flight. II. Velocities, accelerations and kinematics of flapping flight. *J. Exp. Biol.* **200**, 557–582.

Wakeling, J. and Ellington, C. (1997b). Dragonfly flight. I. Gliding flight and steady-state aerodynamic forces. *J. Exp. Biol.* **200**, 543–556.

Walcher, F. and Kral, K. (1994). Visual deprivation and distance estimation in the praying mantis larva. *Physiol. Entomol.* **19**, 230–240.

Wallace, G. K. (1959). Visual scanning in the desert locust *Schistocerca Gregaria* Forskål. *J. Exp. Biol.* **36**, 512–525.

Wardill, T. J., Knowles, K., Barlow, L., Tapia, G., Nordström, K., Olberg, R. M. and Gonzalez-Bellido, P. T. (2015). The killer fly hunger games: Target size and speed predict decision to pursuit. *Brain. Behav. Evol.* **86**, 28–37.

Wardill, T. J., Fabian, S. T., Pettigrew, A. C., Stavenga, D. G., Nordström, K. and Gonzalez-Bellido, P. T. (2017). A novel interception strategy in a miniature robber fly with extreme visual acuity. *Curr. Biol.* **27**, 854–859.

Warrant, E. J. and McIntyre, P. D. (1990). Limitations to resolution in superposition eyes. *J. Comp. Physiol. A* **167**, 785–803.

Waterston, R. H., Lindblad-Toh, K., Birney, E., Rogers, J., Abril, J. F., Agarwal, P., Agarwala, R., Ainscough, R., Alexandersson, M., An, P., et al. (2002). Initial sequencing and comparative analysis of the mouse genome. *Nature* **420**, 520–562.

Webb, J. E. (2009). The role of the notochord in forward and reverse swimming and burrowing in the amphioxus Branchiostoma lanceolatum. *J. Zool.* **170**, 325–338.

Wehner, R. (1987). “Matched filters” - neural models of the external world. *J. Comp. Physiol. A* **161**, 511–531.

Westneat, M. W. (2004). Evolution of levers and linkages in the feeding mechanisms of fishes. *Integr. Comp. Biol.* **44**, 378–389.

Wiederman, S. D. and O'Carroll, D. C. (2013). Selective attention in an insect visual neuron. *Curr. Biol.* **23**, 156–61.

Wiederman, S. D., Shoemaker, P. A. and O'Carroll, D. C. (2008). A model for the detection of moving targets in visual clutter inspired by insect physiology. *PLoS One* **3**, e2784.

Wijngaard, W. and Stavenga, D. G. (1975). On optical crosstalk between fly rhabdomeres. *Biol. Cybern.* **18**, 61–67.

Wilson, A. M., Lowe, J. C., Roskilly, K., Hudson, P. E., Golabek, K. A. and McNutt, J. W. (2013). Locomotion dynamics of hunting in wild cheetahs. *Nature* **498**, 185–189.

Wilson, A. M., Hubel, T. Y., Wilshin, S. D., Lowe, J. C., Lorenc, M., Dewhirst, O. P., Bartlam-Brooks, H. L. A., Diack, R., Bennitt, E., Golabek, K. A., et al. (2018). Biomechanics of predator–prey arms race in lion, zebra, cheetah and impala. *Nature* **554**, 183–188.

Wu, M., Nern, A., Williamson, W. R., Morimoto, M. M., Reiser, M. B., Card, G. M. and Rubin, G. M. (2016). Visual projection neurons in the Drosophila lobula link feature detection to distinct behavioral programs. *Elife* **5**, e21022.

Yager, D. D., May, M. L. and Fenton, M. B. (1990). Ultrasound-triggered, flight-gated evasive maneuvers in the praying mantis *Parasphendale agrionina*. I. Free flight. *J. Exp. Biol.* **152**, 17–39.

Yamawaki, Y. (2000a). Saccadic tracking of a light grey target in the mantis, *Tenodera aridifolia*. *J. Insect Physiol.* **46**, 203–210.

Yamawaki, Y. (2000b). Effects of luminance, size, and angular velocity on the recognition of nonlocomotive prey models by the praying mantis. *J. Ethol.* **18**, 85–90.

Yamawaki, Y. (2003). Responses to worm-like-wriggling models by the praying mantis: effects of amount of motion on prey recognition. *J. Ethol.* **21**, 123–129.

Yamawaki, Y. (2018). Unravelling the functional organization of lobula complex in the mantis brain by identification of visual interneurons. *J. Comp. Neurol.* **527**, cne.24603.

Yamawaki, Y. and Toh, Y. (2009a). Responses of descending neurons to looming stimuli in the praying mantis *Tenodera aridifolia*. *J. Comp. Physiol. A* **195**, 253–264.

Yamawaki, Y. and Toh, Y. (2009b). A descending contralateral directionally selective movement detector in the praying mantis *Tenodera aridifolia*. *J. Comp. Physiol. A* **195**, 1131–1139.

Yau, K.-W. and Hardie, R. C. (2009). Phototransduction motifs and variations. *Cell* **139**, 246–264.

Yurkiewicz, W. J. and Smyth, T. (1966). Effect of temperature on flight speed of the sheep blowfly. *J. Insect Physiol.* **12**, 189–194.

Zeil, J. (1993). Orientation flights of solitary wasps (*Cerceris*; Sphecidae; Hymenoptera). *J. Comp. Physiol. A* **172**, 207–222.

Zheng, Z., Lauritzen, J. S., Perlman, E., Robinson, C. G., Nichols, M., Milkie, D., Torrens, O., Price, J., Fisher, C. B., Sharifi, N., et al. (2018). A complete electron microscopy volume of the brain of adult Drosophila melanogaster. *Cell* **174**, 730–743.